


12-2010

Characterization of the *Agrobacterium tumefaciens* VirB2 pilin of the VirB/D4 Type IV Secretion System

Jennifer Kerr

Follow this and additional works at: http://digitalcommons.library.tmc.edu/utgsbs_dissertations

 Part of the [Molecular Genetics Commons](#), and the [Pathogenic Microbiology Commons](#)

Recommended Citation

Kerr, Jennifer, "Characterization of the *Agrobacterium tumefaciens* VirB2 pilin of the VirB/D4 Type IV Secretion System" (2010). *UT GSBS Dissertations and Theses (Open Access)*. Paper 97.

This Dissertation (PhD) is brought to you for free and open access by the Graduate School of Biomedical Sciences at DigitalCommons@The Texas Medical Center. It has been accepted for inclusion in UT GSBS Dissertations and Theses (Open Access) by an authorized administrator of DigitalCommons@The Texas Medical Center. For more information, please contact laurel.sanders@library.tmc.edu.

**CHARACTERIZATION OF THE AGROBACTERIUM TUMEFACIENS VIRB2 PILIN
OF THE VIRB/D4 TYPE IV SECRETION SYSTEM**

by

Jennifer Evangeline Kerr, B.A.

APPROVED:

Supervisory Professor - Peter J. Christie, Ph.D.

William Margolin, Ph.D.

Ambro van Hoof, Ph.D.

Renhao Li, Ph.D.

Mikhail Bogdanov, Ph.D.

APPROVED:

George M. Stancel, Ph.D. - Dean, The University of Texas
Graduate School of Biomedical Sciences at Houston

**CHARACTERIZATION OF THE AGROBACTERIUM TUMEFACIENS VIRB2 PILIN OF
THE VIRB/D4 TYPE IV SECRETION SYSTEM**

A

DISSERTATION

Presented to the Faculty of
The University of Texas
Health Science Center at Houston

and

The University of Texas
M. D. Anderson Cancer Center
Graduate School of Biomedical Sciences

in Partial Fulfillment
of the Requirements
for the Degree of

DOCTOR OF PHILOSOPHY

By

Jennifer Evangeline Kerr, B.A.

Houston, Texas

December 2010

ACKNOWLEDGEMENTS

I would like to acknowledge my advisor Dr. Peter Christie for his guidance in my growth as a writer, speaker, and independent scientific researcher. His dedication and knowledge for his subject has provided an excellent resource for me to turn to during my time here. He always pushed me to try and achieve excellence and for that I am thankful.

I would like to acknowledge the faculty members that served on my Advisory, Exam, and Supervisory Committees consisting of Dr. William Margolin, Dr. Heidi Kaplan, Dr. Kevin Ridge, Dr. Thomas Vida, Dr. Ambro van Hoof, Dr. Renhao Li, Dr. William Dowhan and Dr. Mikhail Bogdanov who have been gracious with their support, advice, and suggestions. I would especially like to thank Dr. Mikhail Bogdanov and Dr. William Dowhan for their help with the Scanning Cysteine Accessibility Method and Dr. William Margolin for use of his microscope facility.

I would like to thank the past and present members of the Christie lab for their collegiality and support. Mrs. Vidyha Krishnamorthy and Dr. Krishnamohan Atmakuri both played an important role in welcoming me to the lab and provided invaluable assistance in my training. I would especially like to thank Dr. Cristina Martinez, Dr. Simon Jakubowski and Mr. Isaac Garza for their technical assistance and most importantly friendship.

I would also like to thank my teaching mentors Dr. Lisa Morano and Dr. Thomas Goka for their guidance, support, and advice. Their enthusiasm for teaching has been infectious. I am privileged to have worked with such passionate educators.

I would like to thank the faculty, staff, and students of the Department of Microbiology and Molecular Genetics. I would especially like to acknowledge Kristina Fox and Karen Gomez not only for the lunch breaks, sanity checks, and conversations but for your constant support and friendship.

In my time here, I was fortunate to be selected for a number of awards/fellowships, and I would like to thank the people that continually support graduate student education: Molecular Basis of Infections Disease Training Grant (Dr. Steve Norris) financial support for my 2008-2010 school terms and travel assistance to scientific meetings, the Ralph H. and Ruth J. McCullough Foundation fellowship, and the Dean's Award of the University of Texas Medical School at Houston (Dr. Giuseppe N. Colasurdo, M.D.).

I would like to thank my family. My aunts (Robin, Rhonda, Angie, and Sallie) and uncles (Dick, David, and Tommy) have always supported me by showing an interest in my life and career path. My parents, Mary and Bill, have always encouraged my independence and curiosity and afforded me the freedom to pursue my own interests. I would also like to

thank our close family friend Mrs. Ruth Sanders who has been an inspiration and shown a keen interest in my life.

Finally, I would like to thank my wonderful group of friends that have truly become my family and supported me in more ways than I can count: Kelly Howard, Carrie Grin, Kristina Brown, Bill Wibker, Matt Givens, Zach Keane, Emelyn Berg, Phil Philkington, Ben and Michelle Kvanli, April Abbott, Amy Monier, and Marge Daly. I could not have done this without you.

**Characterization of the *Agrobacterium tumefaciens* VirB2 pilin
of the VirB/D4 Type IV Secretion System**

Publication No. _____

Jennifer Evangeline Kerr

Supervisory Professor: Peter J. Christie, Ph.D.

The *Agrobacterium tumefaciens* VirB/D4 type IV secretion system (T4SS) delivers oncogenic T-DNA and effector proteins to susceptible plant cells. This leads to the formation of tumors termed Crown Galls. The VirB/D4 T4SS is comprised of 12 subunits (VirB1 to VirB11 and VirD4), which assemble to form two structures, a secretion channel spanning the cell envelope and a T-pilus extending from the cell surface. In *A. tumefaciens*, the VirB2 pilin subunit is required for assembly of the secretion channel and is the main subunit of the T-pilus. The focus of this thesis is to define key reactions associated with the T4SS biogenesis pathway involving the VirB2 pilin. Topology studies demonstrated that VirB2 integrates into the inner membrane with two transmembrane regions, a small cytoplasmic loop, and a long periplasmic loop comprised of covalently linked N and C termini. VirB2 was shown by the substituted cysteine accessibility method (SCAM) to adopt distinct structural states when integrated into the inner membrane and when assembled as a component of the secretion channel and the T-pilus. The VirB4 and VirB11 ATPases were shown by SCAM to modulate the structural state of membrane-integrated VirB2 pilin, and evidence was also obtained that VirB4 mediates extraction of pilin from the membrane. A model that VirB4 functions as a pilin dislocase by an energy-dependent mechanism was further supported by coimmunoprecipitation and osmotic shock studies. Mutational studies identified two regions of VirB10, an N-terminal transmembrane domain and an outer membrane-associated domain termed the antennae projection, that contribute selectively to T-pilus biogenesis. Lastly, characterization of a VirB10 mutant that confers a 'leaky' channel phenotype further highlighted the role of VirB10 in gating substrate translocation across the outer membrane as well as T-pilus biogenesis. Results of my studies support a working model in which the VirB4 ATPase catalyzes dislocation of membrane-integrated pilin, and distinct domains of VirB10 coordinate pilin incorporation into the secretion channel and the extracellular T-pilus.

TABLE OF CONTENTS

Approval Sheet	i
Title Page.....	ii
Acknowledgements.....	iii
Abstract.....	v
Table of Contents.....	vii
List of Illustrations	x
List of Tables.....	xii
Abbreviations	xiii
Chapter 1: Introduction	1
I) Type IV Secretion Systems (T4SS).....	2
II) <i>Agrobacterium tumefaciens</i> T4SS.....	2
III) Infection Process	4
IV) Substrates Transferred by the Secretion Channel	8
V) General Architectural Features of VirB/D4 T4SS	9
VI) Structure - Function Analysis of T4SS	9
Core Components	9
Outer Membrane Core Complex Structure.....	10
Structure of Inner Membrane Complex	13
Inner Membrane-Associated ATPases.....	13
VII) VirB2 Pilin and T-Pilus Biogenesis Pathway	15
‘Uncoupling’ Mutations	20
VIII) Significance of This Work.....	20
IX) Dissertation Focus and Specific Aims	21

Chapter 2: Material and Methods	22
Strains, plasmids, and induction conditions	23
VirE2-FLAG tag construction.....	23
VirB2-FIAsH tag construction	23
VirB2-FLAG tag construction.....	29
Virulence assays	29
Conjugation assays	29
Protein analysis and immunoblotting.....	29
T-pilus isolation and extracellular blot assay.....	30
Analytical gel filtration.....	30
Chemical labeling of cysteine residues	30
Detection of labeled cysteine residues.....	31
Growth Curves	32
Flag-VirE2 release screen.....	32
Assays for vancomycin and SDS sensitivity.....	32
Assays for outer membrane integrity.....	32
Co-immunoprecipitation	33
Osmotic shock.....	33
Electron microscopy.....	34
Disulfide crosslinking.....	34
Immunofluorescence microscopy.....	34
Chapter 3: T-Pilus Maturation as Monitored by Cysteine Accessibility	36
Introduction.....	37
Results	39
Discussion	49

Chapter 4: VirB4 and VirB11 ATPases Modulate the Structural State of Membrane-Integrated VirB2 Pilin During Biogenesis of the VirB/D4 Type IV Secretion System.....	58
Introduction.....	59
Results	60
Discussion	77
Chapter 5: The Role of VirB10 Domains in T-Pilus Biogenesis and Type IV Substrate Secretion.....	82
Introduction.....	83
Results	86
Discussion	99
Chapter 6: Characterization of a <i>virB10</i> Mutant Conferring Release of VirE2 to the Extracellular Milieu While Selectively Blocking T-Pilus Biogenesis.....	104
Introduction.....	105
Results	107
Discussion	118
Chapter 7: Summary, Future Directions, and Perspectives	123
Summary	124
Future Directions	127
Perspectives.....	145
References.....	146
Vita	168

LIST OF ILLUSTRATIONS

Figure 1.1: Schematic of the role of type IV secretion systems in bacteria	4
Figure 1.2: Schematic of the localization of the <i>Agrobacterium tumefaciens</i> VirB/D4 type IV secretion components and the T-DNA secretion pathway	6
Figure 1.3: Structure of the 'core' type IV secretion system	12
Figure 1.4: Sequence alignment of VirB2 pro-pilin homologues.....	17
Figure 1.5: Schematic of the pilin processing and proposed T-pilus biogenesis pathway of the <i>Agrobacterium tumefaciens</i> VirB/D4 secretion system.....	19
Figure 3.1: Phenotypes of VirB2 Cys substitution mutations.	41
Figure 3.2: MPB accessibility of Cys substitutions.....	43
Figure 3.3: Disposition of VirB2 in VirB-producing cells and T-pili.....	47
Figure 3.4: Mutations in domains of related pilin subunits have similar effects on function	51
Figure 3.5: Helical wheel representations of VirB2 transmembrane helices, regions II and IV.....	56
Figure 4.1: Effects of VirB4 ATPase on MPB-labeling patterns of pilins.....	62
Figure 4.2: Effects of VirB11 ATPase on MPB-labeling patterns.....	65
Figure 4.3: VirB protein complexes.....	68
Figure 4.4: MPB-labeling of VirB4.....	71
Figure 4.5: VirB4-mediated release of VirB2 upon osmotic shock treatment	73
Figure 4.6: Schematic summarizing effects of VirB4, VirB11, and other VirB subunits on MPB-labeling patterns.....	76
Figure 4.7: Model of T-pilus biogenesis pathway.....	81
Figure 5.1: Schematic of VirB10 domains and mutations	88
Figure 5.2: Phenotypes of VirB10 N-terminal insertions and deletion mutations.....	90
Figure 5.3: Phenotypes of VirB10 PRR deletions and substitution mutations	93

Figure 5.4: Phenotypes of β -barrel deletions and substitution mutations	96
Figure 5.5: Effects of VirB10 helix projection mutations on T-pilus assembly	98
Figure 5.6: Models of VirB10 TM and AP domain involvement during T4SS T-pilus assembly.....	103
Figure 6.1: Effects of the VirB10 G272R mutation on VirE2 release and growth	109
Figure 6.2: Effects of VirB10 G272R on membrane integrity, as monitored by vancomycin and SDS sensitivity, and release of periplasmic proteins	111
Figure 6.3: Effects of G272R mutation on DNA transfer, surface display of VirB2 pilin and the pilin-associated protein VirB5	115
Figure 6.4: Effects of the Δ AP mutation on VirE2 release, cell growth, and OM integrity	117
Figure 6.5: Modeling of G272R in pKM101 crystal structure	120
Figure 7.1: Schematic of FIAsH tag cassette and effects of tag introduction into VirB2 on surface display of VirB2 and virulence.....	130
Figure 7.2: Effects of flagella minus mutant on surface display of VirB2 and observed T-pili	133
Figure 7.3: Disulfide cross-linking of Cys-substituted VirB2 in the T-pilus.....	136
Figure 7.4: Effects of <i>virB</i> deletion mutations on surface display of VirB2 and VirB5.....	141
Figure 7.4: Immunofluorescence assays showing localization VirB2 and VirB5 in the wild-type strain and nonpolar <i>virB1</i> , <i>virB2</i> , and <i>virB5</i> deletion mutants	143

LIST OF TABLES

Table 2.1: Strains	24
Table 2.2: Plasmids and Vectors.....	25
Table 2.3: Oligonucleotide primers used for epitope tag construction and insertion.....	28

ABBREVIATIONS

ABIM: AB buffered induction media
AMS: 4-acetamido-4'-maleimidylstilbene-2,2'-disulfonic acid
AP: Antennae projection
AS: Acetosyringone
A.t.: *Agrobacterium tumefaciens*
ATP: Adenosine triphosphate
BD: Bridging domain
 β -ME: Beta-mercaptoethanol
CP: Cell pellet
Cys: Cysteine
DNA: Deoxyribonucleic acid
DSP: Dithiobis[succinimidyl propionate]
EM: Electron microscope/-scopy
FIAsH: Fluorescein arsenical hairpin binder
IFM: Immunofluorescence microscopy
IM: Inner membrane
IP: Immunoprecipitation
IPTG: Isopropyl β -D-1-thiogalactopyranoside
MPB: 3-(N-maleimidylpropionyl) biocytin
NTP: Nucleoside triphosphate
OM: Outer membrane
PAGE: Poly-acrylamide gel electrophoresis
PCR: Polymerase chain reaction
Per: Periplasm
PRR: Proline rich region

RO: Reverse osmosis

SCAM: Scanning cysteine accessibility method

SDS: Sodium dodecyl sulfate

SSB: Single-stranded DNA-binding protein

STEM: Scanning transmission electron microscope

T4SS: Type IV secretion systems

T-DNA: Oncogenic transfer DNA

TM: Transmembrane

TrIP: Transfer DNA immunoprecipitation

Chapter 1: Introduction

*NOTE: Crystal structure images were modeled in PyMOL. An educational-use program copy of PyMOL was obtained from <http://pymol.org/ep>, which states that images may be used for thesis/dissertation projects. All structural coordinates were obtained from the RCSB protein data base <http://www.rcsb.org/pdb> and individual identification numbers and specific references are included in the figure legends. Figure 1.1 was modified from figure 1 in a previously published review article: "The versatile bacterial type IV secretion systems." *Nature Reviews Microbiology* 1, 137-14; November 2003, (doi:10.1038/nrmicro753). I have been given permission by the publisher of *Nature Reviews Microbiology*, Nature Publishing Group, to reproduce this figure in print or electronically for the purposes of my dissertation (License Number 2544420868323). Figure 1.4 was modified from Figure 3 in "The T-pilus of *Agrobacterium tumefaciens*." *Trends Microbiol.* 8, 361-69. (doi:10.1016/S0966-842X(00)01802-3). I have been given permission by the publisher of *Trends in Microbiology*, Elsevier, to reproduce this figure in print or electronically for the purposes of my dissertation (License Number 2551440934372).*

I) **Type IV Secretion Systems**

Bacterial Type IV secretion systems (T4SSs) represent a functionally diverse group of transporters dedicated to the movement of DNA or protein substrates across the cell envelope (1-3). They are linked to many important processes, such as the spread of antibiotic resistance (4-6), genomic plasticity (7), bacterial colonization, and the introduction of virulence factors into eukaryotic host cells (1, 8-14). T4SSs are widely distributed among both Gram-negative and Gram-positive bacteria (1, 4, 15), and they play a key role in the virulence of many bacterial pathogens (16-22). These systems stimulate changes in basic host cellular processes that aid in the establishment of pathogenic or symbiotic relationships with the host (1, 16, 23, 24). All T4SSs identified assemble as multi-subunit machines that form a secretion channel spanning the cell envelope, and many T4SSs also encode a pilus or other surface protein(s) that mediates direct contact with target cells (15, 16, 25-28). These systems have been grouped into three different 'types' based on function: 1) conjugation machines, systems that translocate DNA to recipient cells through direct cell-cell contact, 2) DNA uptake/release machines that translocate DNA to or from the milieu, and 3) effector translocation machines, which transport proteins and sometimes DNA to eukaryotic recipient cells (Fig. 1.1) (2, 15).

II) ***Agrobacterium tumefaciens* Type IV Secretion System**

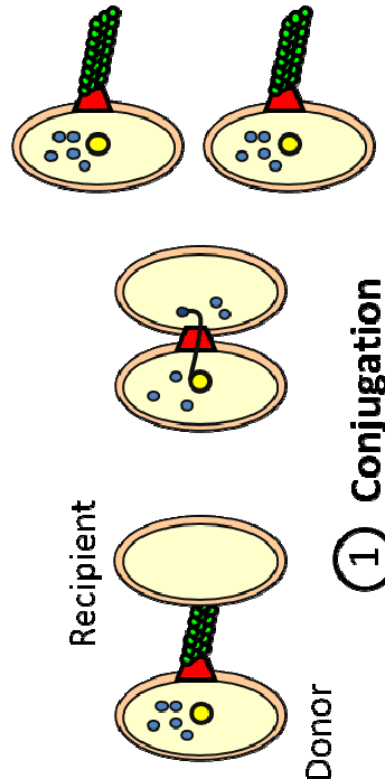
The prototypical T4SS, the *Agrobacterium tumefaciens* VirB/D4 system, serves as an excellent model for defining substrates and substrate translocation signals, assembly pathways and architectures, and the dynamics of substrate movement through the T4SSs. The *A. tumefaciens* VirB/D4 T4SS is comprised of a secretion channel and an extracellular pilus called the T-pilus (2, 3, 29, 30) (Fig. 1.2). The secretion channel mediates the transfer of effector proteins and DNA across the cell envelope. The T-pilus functions mainly or exclusively as an attachment organelle to enable formation of productive contacts between *A. tumefaciens* and target cells. Though not required for substrate translocation, the T-pilus increases substrate transfer efficiencies (31, 32).

III) **Infection Process**

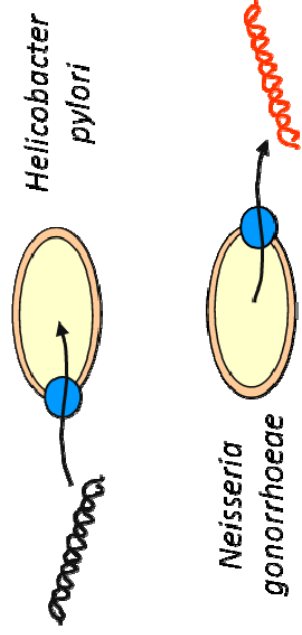
As with many bacterial pathogens, *A. tumefaciens* infects only at wound sites in a cell-cell contact dependent fashion (33, 34). Infection is initiated when bacteria sense an array of signals, including various plant cell wall precursors and acidic pH, that are present at a plant wound site (35). Signal perception is mediated by the VirA/VirG signal

Figure 1.1 Schematic of the role of type IV secretion systems in bacteria

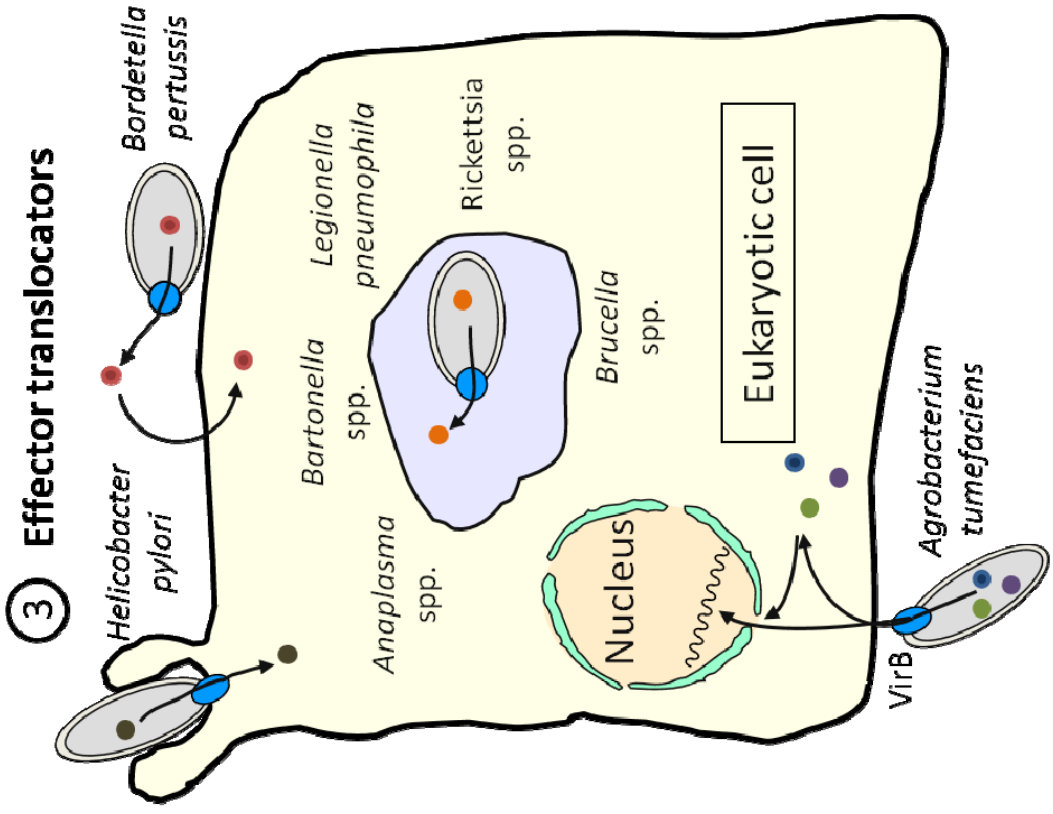
Three groups of type IV secretion systems depicted: 1) Conjugation, deliver plasmids or integrative and conjugative elements (ICEs) from donor cells to recipient cells 2) DNA uptake/release, mediate exchange of DNA with the extracellular milieu and, 3) Effector translocators, deliver DNA and/or protein substrates to eukaryotic cells and are directly involved in virulence (See (1, 16, 30, 36, 37)). This figure was modified from Figure 1 in *"The versatile bacterial type IV secretion systems."* *Nature Reviews Microbiology* 1, 137-14; November 2003, (doi:10.1038/nrmicro753).



① Conjugation



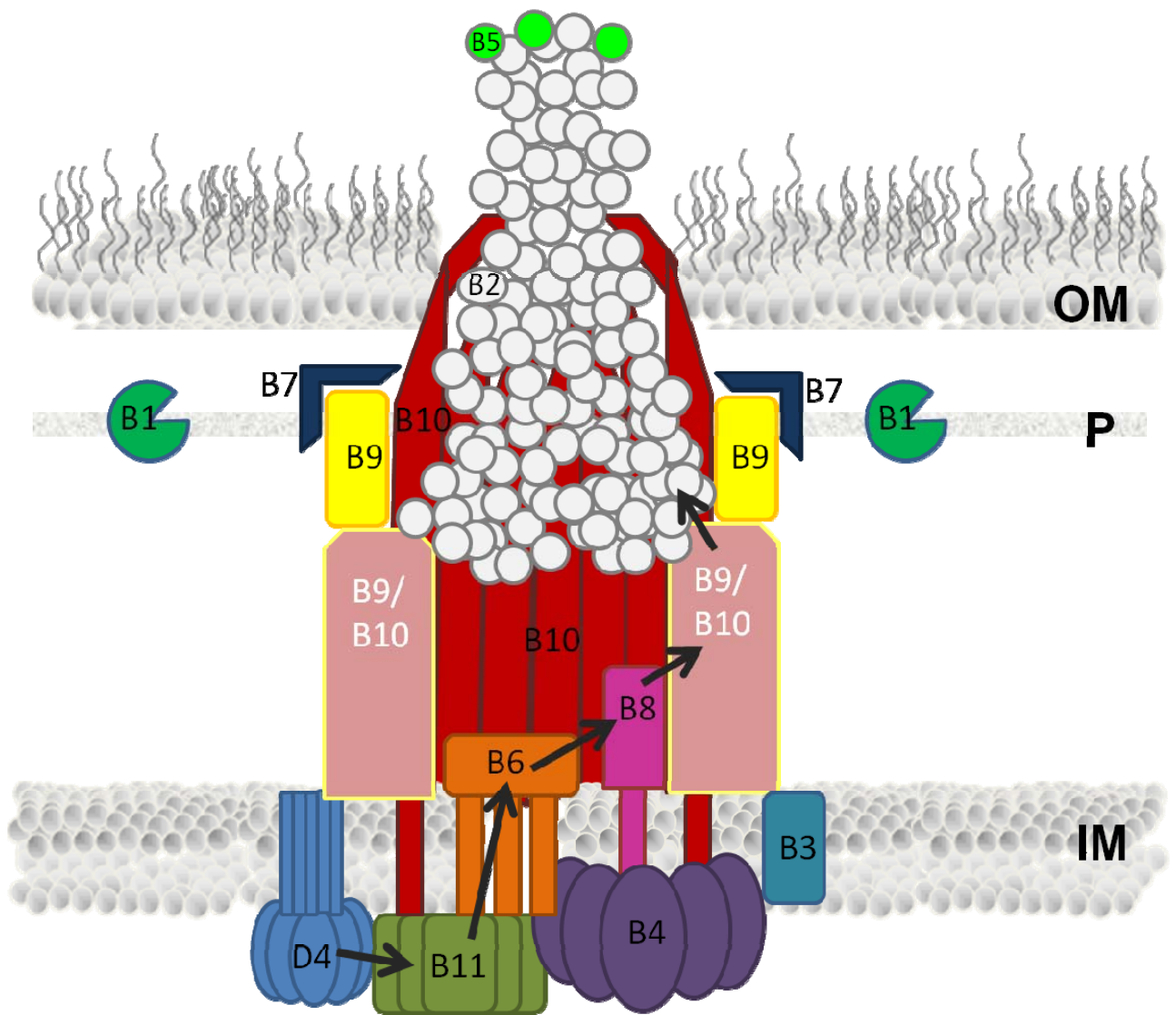
② DNA uptake / DNA release



③ Effector translocators

Figure 1.2 Schematic of the localization of the *Agrobacterium tumefaciens* VirB/D4 type IV secretion components and the T-DNA secretion pathway

The VirB1-VirB11 and VirD4 type IV secretion system (T4SS) components are shown according to their proposed localization and interactions. Black arrows indicate the path of the translocating T-DNA. The T-DNA interacts directly with VirD4, VirB11, VirB6, VirB8, and finally VirB2-VirB9. P: periplasm; IM: inner membrane; OM; outer membrane.



transduction system (38). VirA detects signals released from wounded plant tissues and VirG activates transcription of the *vir* operon. The VirB/D4 system delivers an oncogenic nucleoprotein complex into plant cells, resulting in the formation of tumors called Crown Galls which can devastate agriculturally important crop species (1, 5, 39).

The majority of genes required for tumorigenesis are found within pathogenic *A. tumefaciens* strains on large (~180kb) extrachromosomal elements called Tumor-inducing (Ti) plasmids (40, 41). *A. tumefaciens* can conjugatively transfer the Ti-plasmid to *Agrobacterium* and *Rhizobium* recipients, and upon transfer these strains can now infect plants through T-DNA transmission (14, 41). The Ti plasmid harbors the T-DNA and the virulence (*vir*) genes involved in T-DNA transfer to susceptible plant cells. The T-DNA carried on a separate region of the Ti-plasmid, is typically 10-30 kb in length and delimited by the left and right border repeat sequences. None of the T-DNA genes are required for its secretion, and therefore, all DNA between the border repeats can be excised and substituted with DNA of interest for delivery to plant or other eukaryotic target cells (42-44). The VirB proteins are encoded by the *virB1 through virB11* genes expressed from a single promoter (1, 39). VirB1 - VirB11 are mating pair formation proteins (mpf) that form the translocation channel and the T-pilus (5). The *virD* operon encodes the relaxase VirD2 substrate and ancillary protein VirD1 required for excision of the T-DNA and its export from the bacterium, as well as the coupling protein VirD4 that functions as a receptor for the T-DNA transfer intermediate and several independently translocated proteins (45, 46).

Following signal perception and *vir* gene induction, T-DNA is processed and exported across the *A. tumefaciens* cell envelope via the T4SS encoded by the *virB* operon. It then moves through the plant cell to the nucleus where it integrates into the plant genomic DNA. The *virE* operon encodes the single-stranded DNA-binding protein (SSB) VirE2 that interacts with the T-DNA, forming the T-complex. VirE2 protects the T-DNA from cytoplasmic nucleases in the plant cell and mediates delivery of the T-DNA to the plant nuclear pore with the help of VirE3 (47-52). VirF, another translocated effector protein, appears to be involved in targeted proteolysis of VirE2 after its arrival in the host nucleus (53). Once integrated in the plant genome, the T-DNA genes are expressed and the protein products catalyze synthesis of novel amino acids, called opines. Opines are released from the plant cell and can be taken up and catabolized for use as carbon and energy sources by the infecting bacteria. The T-DNA genes also code for proteins that disrupt biosynthetic pathways of the plant hormones auxin and cytokinin. The resulting hormonal imbalance

leads to uncontrolled cell proliferation and formation of the unorganized tumors, termed 'Crown Galls' (40).

IV) Substrates Transferred by the Secretion Channel

A. tumefaciens uses the VirB/VirD4 T4SS to translocate the T-DNA as a single-stranded DNA particle bound covalently at its 5' end to the VirD2 relaxase. *A. tumefaciens* also uses this T4SS to translocate protein substrates only. These include the VirE2 SSB, VirE3, and VirF (54). The first evidence for protein translocation independently of T-DNA transfer derives from mixed infection experiments in which it was shown that the co-infection of plants with two avirulent *A. tumefaciens* strains, one deleted of T-DNA but with an intact *vir* region, and a second mutated for *virE2* or *virF*, resulted in tumorigenesis (55, 56). More recent studies showed that protein substrates fused to reporter proteins such as the Cre recombinase (57) can mobilize the transfer of the reporter protein to target cells. Most T4SSs recognize substrates by detecting a signal sequence located within the protein components, e.g. relaxase or effector proteins. These 'secretion' signals are located close to the C termini and mainly consist of hydrophobic or positively-charged clusters of amino acids (15).

The T-DNA substrate was shown to form close sequential contacts with channel subunits along the secretion pathway (Fig. 1.2) (58). VirD4, termed a coupling protein or substrate receptor, initiates the transfer process by recruiting the T-DNA substrate to the T4SS. Additional studies have also shown that VirD4 recruits protein substrates such as VirE2 to the secretion channel (45, 59). The DNA substrate next makes contacts with ATPase VirB11 (45), and VirB11 in turn transfers the substrate to the inner membrane-associated subunits VirB6 and VirB8. Finally, the T-DNA forms close contacts with the outer-membrane-associated VirB9 and the VirB2 pilin. On the basis of these demonstrated T-DNA – T4SS subunit close contacts, it was proposed that the VirB/VirD4 secretion channel that spans the cell envelope is composed minimally of VirD4, VirB11, VirB6, VirB8, VirB2, and VirB9. Other subunits are required for substrate transfer, and it is thought that some of these might form a scaffold for the assembly of the transenvelope channel. One of these proposed scaffold proteins is VirB10, and recent findings suggest that VirB10 spans the entire *Agrobacterium* cell envelope and participates in energizing substrate transfer through the distal portion of the transfer channel (58).

The VirB/D4 translocation system also mediates the conjugal transfer of RSF1010, a non-self-transmissible IncQ plasmid, into plant cells as well as between *Agrobacterial*

cells (60, 61). This transfer requires the plasmid's origin of transfer (*oriT*) and the RSF1010-encoded MobA nicking enzyme, suggesting that the VirB complex recognizes the IncQ transfer intermediate, capped at its 5' end with MobA. The RSF1010 transfer intermediate was shown to follow the same substrate transfer pathway as the T-DNA, and it also was shown to competitively interfere with T-DNA and VirE2 substrate binding to the VirD4 receptor (62). Taken together, these observations support the idea that the VirB/D4 T4SS is a multifunctional translocation apparatus that exports diverse substrates through recognition of amino acid sequence or structural motifs. The VirD4 substrate receptor and all VirB proteins except for the VirB1 transglycosylase are required for transfer of the VirD2-T-strand and MobA-RSF1010 transfer intermediates, VirE2, and VirF (61, 63, 64).

V) **General Architectural Features of VirB/D4 T4SS**

The T4SSs of Gram-negative bacteria span the entire cell envelope and present substrates with a conduit to transit through the periplasm and bacterial membranes (2, 3, 15, 30). Based on recent structural, functional, and biochemical studies, these proteins can be grouped by function/location (Fig. 1.2, see below for more detailed introduction). There are three cytoplasmic-associated ATPases, VirB4, VirB11, and VirD4, which provide energy for substrate transfer and machine assembly (30, 45). VirB6 through VirB10 and possibly VirB3 form the bulk of the channel scaffold that spans from the inner membrane to the outer membrane (2, 58, 65-67). VirB3, VirB6, and VirB8 all reside at the inner membrane and form portions of the base of the channel (58, 65, 66). VirB7, VirB9, and VirB10 interact to form a multi-subunit 'core' complex that spans the entire cell envelope (67, 68). VirB2 and VirB5 form part of the secretion channel but also polymerize to form the extracellular T-pilus (25, 69).

VI) **Structure-Function Analysis of Type IV Secretion System Core Components**

VirB7, VirB8, VirB9, and VirB10 are conserved among most T4SS of Gram bacteria (39, 70) and are postulated to comprise the T4SS 'core' subunits (67, 68, 71-73). VirB7 is a small lipoprotein that stabilizes VirB9, partly through a disulfide crosslink (74, 75). VirB9 subunits are hydrophilic but associated with the outer membrane. VirB8 and VirB10 are bitopic membrane proteins that both possess a globular periplasmic domain. The periplasmic domains of the *A. tumefaciens* and *Brucella suis* VirB8 subunits were solved by X-ray crystallography (76). VirB8 has been shown to be important for spatial positioning of the VirB proteins and may, therefore, function as a nucleation center for the T4SS (29, 77).

VirB10 subunits have a short N-terminal domain, a transmembrane region, a proline-rich region, and a C-terminal β -barrel domain (73, 78, 79). VirB10 is an energy sensor/transducer that undergoes a conformational change in response to ATP hydrolysis from VirB11 and VirD4 to activate substrate transfer through the distal portion of the secretion channel (58).

Recent studies have shown for the related pKM101 T4SS that VirB7-like TraN, VirB9-like TraO, and VirB10-like TraF assemble as a stable 'core' complex (67, 68). This core complex was visualized as a large (185 Å wide and long) ring-shaped channel by cryoelectron microscopy (CryoEM) and X-ray crystallography. The complex, composed of 14 copies of each subunit, consists of two stacked layers (I- and O-layers) linked by a thin density stretch. The I- and O-layers are double-walled, ring structures that create a hollow chamber that is thought to span the cell envelope. The I-layer is anchored at the inner membrane while the O-layer is stacked on top and inserted into the outer membrane. The I-layer is composed of the N-terminal domains of TraO and TraF; the O-layer is formed by TraN and C-terminal domains of TraO and TraF.

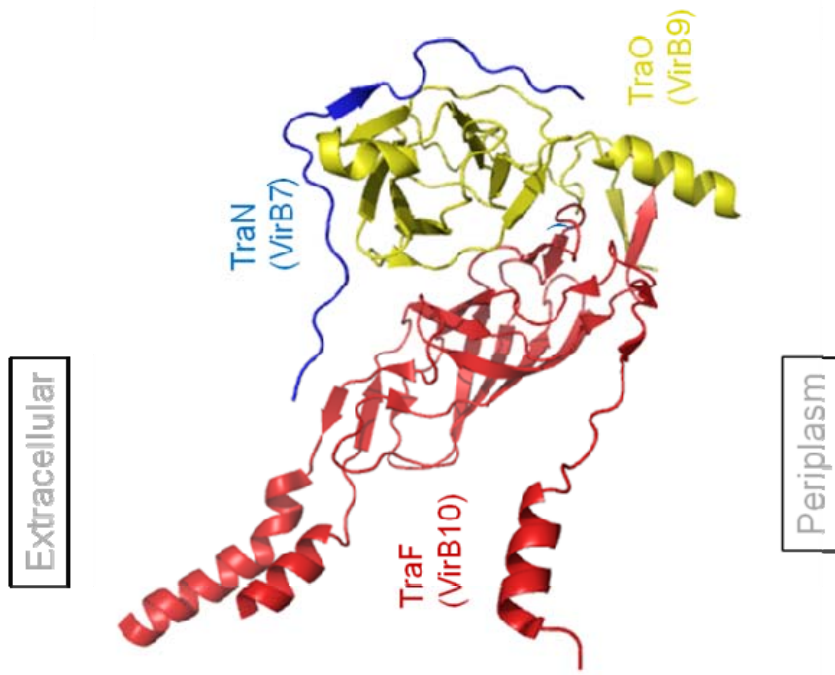
Outer Membrane Core Complex Structure

The structure of the distal portion of the core complex, presumptively located near the outer membrane, was resolved by X-ray crystallography (68). This complex corresponds to the O-layer visualized by CryoEM and contains 14 copies of the C-terminal domains of TraO and TraF and the full-length TraN (Fig. 1.3A and B). Alpha helical projections extending from the top the TraF β -barrel create a halo which forms the outer membrane 'pore'. The remainder of the C-terminal domain of TraF shapes the inner chamber of the O-layer surrounded by the TraN-TraO complex (Fig. 1.3 A and B). The C-terminal domains of TraO and TraF interact directly, while full-length TraN interacts with the C-terminal domain of TraO but not with TraF [Fig. 1.3A and refer to (68)]. Given the sequence conservation between these pKM101 Tra proteins and the VirB as well as other T4SS core subunits, the Tra core structure is postulated to represent a structural paradigm for core complexes of all Gram-negative bacterial T4SSs. Notably, no other proteins were found associated with this outer membrane core complex (67, 68) and the T-DNA substrate was never shown to form a close contact with VirB10 (58). VirB2, which is required for substrate transfer and T-pilus formation, forms the distal portion of the secretion channel and may, therefore, form a secretion conduit inside the VirB10 pore. The core complex may in addition serve as a base for assembly of the extracellular T-pilus; however,

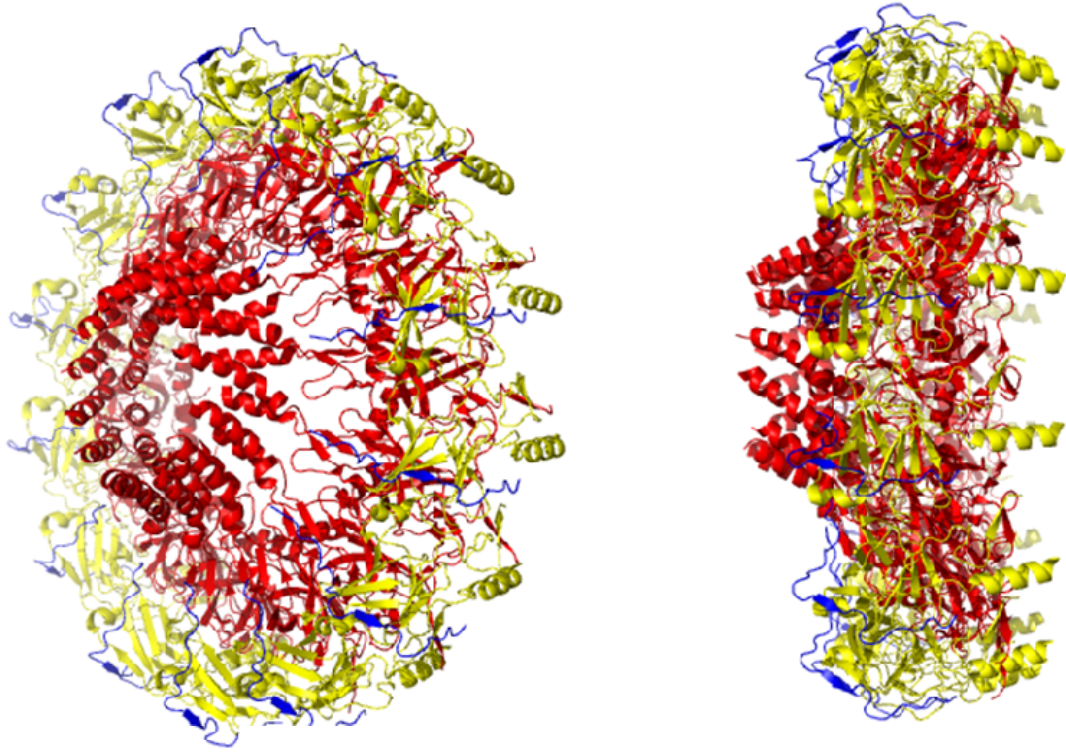
Figure 1.3 Structure of the 'core' type IV secretion system

A) Crystal structure of the outer membrane complex, comprising the O-layer. TraN, TraO, TraF are colored blue, yellow, and red respectively. VirB7, VirB9, VirB10 homologues encoded by pKM101. VirB7, VirB9CTD, VirB10CTD heterotrimer, side view with periplasmic side facing downwards B) Crystal structure of complete pKM101 outer membrane core complex Top: Tilt-view from outer-membrane Bottom: Side view with periplasmic side facing downwards. Modeled with coordinates from pKM101 core outer membrane complex X-ray structure (DOI:10.2210/pdb3jqo/pdb) (68) using the PyMOL (<http://pymol.org/>) to construct the figure.

A



B



at this point, no studies have outlined the functional relationship between the VirB2 pilin and core component VirB10.

Structure of the Inner Membrane Complex

The I-layer was resolved at ~15 Å by cryoelectron microscopy (67). The I-layer is composed of the N-terminal domains of TraO and TraF. TraF inserts into the inner membrane forming a portion of the base of the core structure (67, 68). In the *A. tumefaciens* system, we propose that the VirB7/VirB9/VirB10 complex represents a scaffold for the T4SS, and that the other channel subunits assemble within the core chamber to form the translocation channel. Correspondingly, the ring formed by 14 copies of the VirB10 transmembrane (TM) sequence would encircle the translocase, comprised of polytopic VirB6, bitopic protein VirB8 and, possibly, other subunits (3, 80, 81). VirB6 and VirB8 form close contacts with the T-DNA (58) (3, 80, 81). VirB6 has 5 transmembrane domains and a large periplasmic region that has been shown to be important for making T4SS interactions (65, 82). VirB8, as mentioned above, may play a key role in localization of the T4SSs (29, 77). VirB9 likely forms portion of the translocation channel extending through the periplasm to the outer membrane. Finally, VirB2 would assemble within the core chamber to comprise the distal-most portion of the transfer channel (Fig. 1.2) (58).

Inner Membrane-Associated ATPases

Most T4SS have two to three dedicated ATPases that supply energy needed for assembly or function of the translocation channel and T-pilus (15). In *A. tumefaciens*, all three ATPases (VirB4, VirB11, and VirD4) are required for substrate transfer, whereas VirB4 and VirB11 but not VirD4 are required for T-pilus biogenesis. These ATPases interact with each other, likely forming an ATPase complex at the cytoplasmic entrance to the T4SS channel (45). This ATPase complex probably interacts with VirB6, VirB8 and/or VirB10 at the inner membrane in order to energize the T4SS (83). Yet, the exact architecture of this complex and the specific role each ATPase plays during transfer and machine assembly of the secretion channel and the T-pilus remains unknown.

VirB11 and its homologs are widely distributed among Gram-negative and Gram-positive bacteria and several species of Archaea (15). These ATPase are tightly-associated with the inner membrane but do not possess any known transmembrane regions. VirB11 self-associates (84), and structural studies of VirB homologues e.g. TrbB_{RP4}, TrwC_{R388}, HP0525_{Cag}, and *Brucella suis* VirB11 have supplied evidence that this family of ATPases

assemble as double-stacked, homo-hexameric rings (84, 85, 86). The crystal structure of ADP-bound HP0525 from *H. pylori* showed that the N termini and the C termini form two globular domains that are separated by the NTP-binding domain (85). VirB11-like subunits are expected to share structural features, although a comparison of *H. pylori* HP0525 and *B. suis* VirB11 identified structural differences between inter-domain contacts within the respective homo-hexamers (86). VirB11 and homologs contain Walker nucleoside triphosphate (NTP) binding regions; where examined, mutation of the Walker A motif (GxxGxGKT/S) abolishes both channel activity and pilus biogenesis (87-92). Studies from our lab also identified mutations that selectively abolish T-pilus production without affecting substrate transfer (87); how VirB11 regulates biogenesis of either terminal organelle has not been established.

VirD4 is a member of the family of ATPases termed coupling proteins or substrate receptors. Coupling proteins are present in all characterized conjugation systems to date (15). These subunits recruit substrates by serving as substrate receptors at the base of the T4SSs, thus linking the substrate processing and translocation reactions. The VirD4 coupling protein and its homologs TraD_F, TrwB_{R388}, and TraG_{RP4} have been extensively characterized through biochemical and structural studies (93-96). They contain three domains: an NTP-binding region, an N-terminal transmembrane region, and an all- α -domain. A crystal structure was obtained for the coupling protein TrwB_{R388} deleted of its transmembrane region (97). This structure presents as a homo-hexameric ring, and modeling of the N-terminal transmembrane stem yielded an overall F₁F₀ ATPase-like ball-stem structure (97, 98). Mutagenesis of the conserved Walker NTP-binding motifs in VirD4 and homologs abolishes protein function (99-101). Several coupling proteins have been shown to bind single and double stranded DNA (93, 94, 102). Biochemical studies have also supplied evidence that coupling proteins self-associate and also interact with other T4SS components, e.g. VirD2, VirB4, VirB10, and VirB11 (45, 83, 103, 104).

VirB4-like ATPases are ubiquitous across all T4SSs described (15). Studies from our laboratory have demonstrated that the VirB4 protein is a membrane-associated ATPase containing two periplasmically exposed domains (105), however, soluble versions of VirB4 homologs have also been identified in other systems. VirB4 self associates, and also interacts with VirD4, VirB11, VirB8, VirB10, and VirB11 (45, 83, 106, 107). Homology between the C terminus and the coupling proteins TrwB_{R388} suggests that C-terminal domain of VirB4 would form a homo-hexamer (108). Yet, studies have identified both dimeric and hexameric forms of VirB4 homologs (78, 106, 108-110). Phenotypic studies

established the importance of the Walker NTP-binding motif and, by extension, VirB4 NTP-binding and/or hydrolysis activities, for substrate translocation and pilus biogenesis (87, 104, 105, 111, 112). In addition, alleles encoding a VirB4 NTP-binding mutant exhibit transdominant effects over the wild-type *virB4* gene, suggesting that VirB4 functions as a homo- or heteromultimer (105). Biochemical studies showed that a purified VirB4 homolog binds and hydrolyses ATP (113). Although the specific function of these activities is not known, the transmembrane topology of VirB4 and its likely interactions with components localized at the inner membrane, suggest that VirB4 can energize ATP-induced conformational changes necessary for biogenesis of the T4SS.

VII) VirB2 Pilin and the T-Pilus Biogenesis Pathway

The VirB proteins direct assembly of the extracellular T-pilus (25). The T-pilus is composed of VirB2 pilin and the VirB5 minor subunit (25, 31, 114). VirB2 homologs or orthologs, with low levels of similarity yet retaining key residues, are present in several other T4SSs (78). The VirB2-like proteins are typically small and hydrophobic, and they also contain a cleavable signal sequence (Fig. 1.4) (115, 116). Several novel processing reactions are known to be associated with pilin maturation (115). The VirB2 pro-pilin is 121 amino acids, the first 47 comprising an unusually long signal sequence. After cleavage, the 74-residue peptide is further processed by joining of the N- and C-termini, forming a cyclic peptide. The mature pilin is composed of two hydrophobic domains and two short hydrophilic domains (104, 117). When synthesized in *E. coli*, the signal sequence of VirB2 is cleaved but the mature protein is not cyclized (118). In *A. tumefaciens*, the cyclized mature pilin is presumably shunted through the core channel complex and serves as the building block for assembly of a functional secretion channel and the extracellular T-pilus (58) (Fig. 1.5).

The T-pilus has been shown to localize at the *A. tumefaciens* cell poles (104, 119). Little is known about the function of the T-pilus. There is some evidence, using VirB2 in yeast two hybrid screening methods aimed at identifying plant host receptors, that T-pili are involved with sensing of the host cell surface (120). No structural information is available for VirB2 or the T-pilus; however, a structure was solved for a VirB5 homolog, TraC_{pKM101}.

Figure 1.4 Sequence alignment of VirB2 pro-pilin homologues

The homologs of *A. tumefaciens* VirB2 pro-pilins (At VirB2) were aligned using CLUSTAL W program and edited manually. The homologous proteins shown here are LvhB2 in *Legionella pneumophila* (Lp LvhB2), VirB2 in *Brucella suis* (Bs VirB2), PtlA in *Bordetella pertussis* (Bp PtlA), VirB2 in *Bartonella henselae* (Bh VirB2), TraM of IncN plasmid pKM101, TrwM of IncW plasmid R388, TrbC of IncP plasmid RP4, and TraA of IncF plasmid F. The conserved domains and amino acid residues are highlighted in color. The signal peptidase I cleavage site is indicated; it was predicted by the conserved sequences of the cleavage sequences in all homologues and based on the known processed sites of F TraA, RP4 TrbC and At VirB2. The putative hydrophobic transmembrane (TM) helices and the core regions of all processed VirB2 homologues are indicated as single solid lines and double dashed lines, respectively. This figure was modified from from Figure3 in “*The T-pilus of Agrobacterium tumefaciens.*” *Trends Microbiol.* 8, 361-69. (doi:10.1016/S0966-842X(00)01802-3).

Signal peptidase I



Lp LvhB2	MSKLRWSQSLGN.LY.LIAVCTLL...TLSHAQSIES...IINRTINYLQGGIART.
Bs VirB2	MKTASPKKSLRILPH.L...LL..ALIVSIAAIEENLAHAN..GCLD.KVNTSMQKVLDLLSG..
Bp Pt1A	MNPLKDLASLPRLAFMAACTLLSATL...DLAQA...GGGLQRVNHFMASIVVLRGAS
Bh VirB2	MTDTISN.IIFI...IIMLLL.TALVSDPSYAAA..ATGSASGLGN.VDNVLQSIIVT.M
At VirB2	MRCFEYRLHLNRLSLSNAMM.VISSCAPSLCGAIAWSISSSG...AAQSAAGCTDPA.TMVNNICTFI....
pKM101 TraM	MTTLFKK...YGPVAVMGVLSIAL...FOIALA...ACTDTGESTAT.SIQTWLSIW.
R388 TrwM	MATSILTRKTNMKNLNYLRACANGK.L..AALIFGATAAMLTA.QE...AAAO...CLE.KA...RSVLETLQOE.
RP4 TrbC	MTTAVPFRLLTMNGI...LFYLAVFFVLALALSA.HF...AMASEGTGG.SLPYE..SMLTN.LRNS.
F TraA	MNAVLSVQGASAPVKKKSFSLNMLRLARAVTPAAVLMIM...FFEQ.LAMAAGSSQQD.....LWASGNT.T

TM

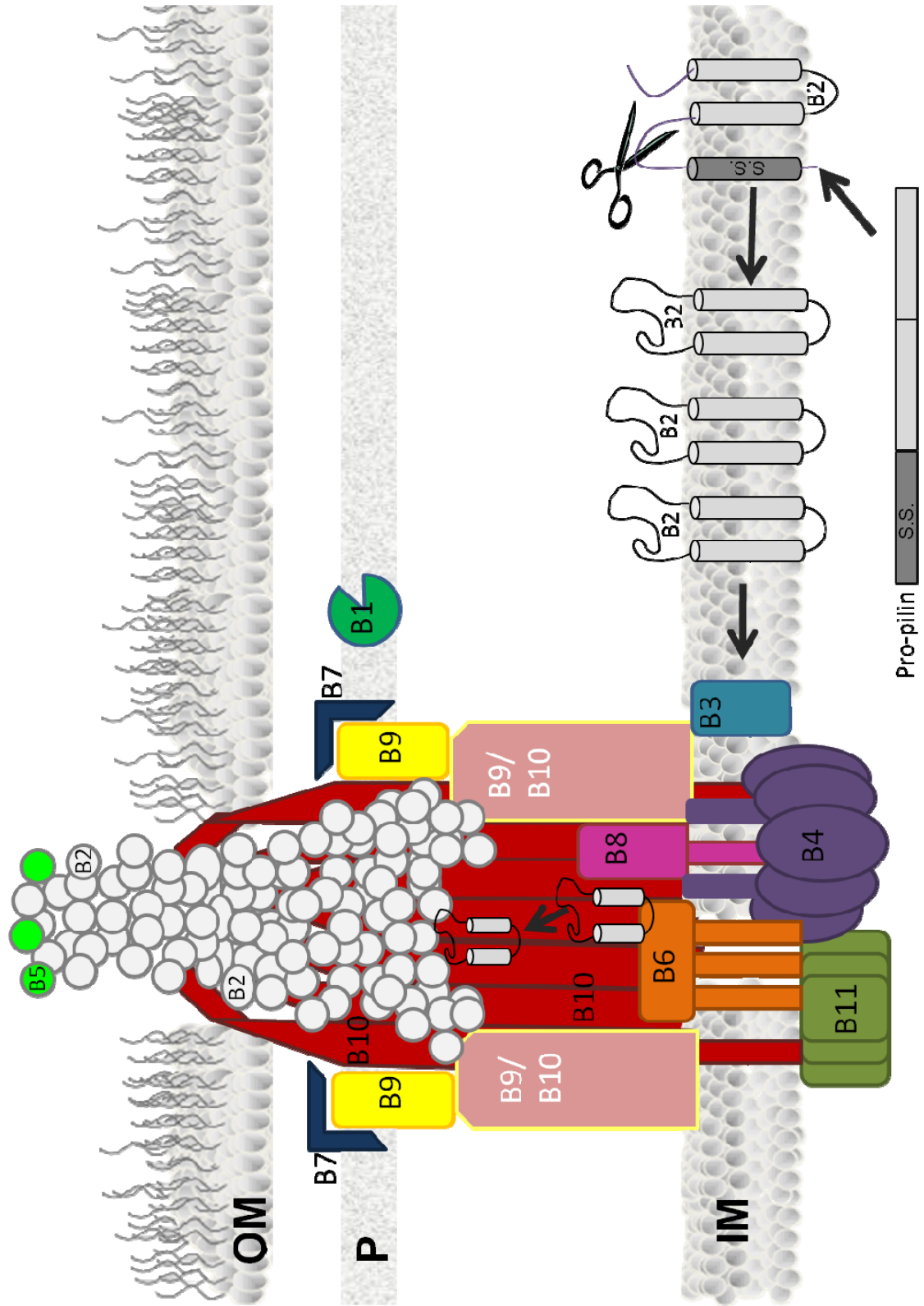
TM

Lp LvhB2	V.....G.VFCIIIAAGY.LCL..A....RQKFPMEYF...VMILVGMGIIFGGSSLYS.TLIG
Bs VirB2	V.....SITIVT.I..A...ITWSGYKMA....FHARFMDVWPVLGGALVWGAAAEIASYLLR
Bp Pt1A	V.....AVT.I..A...ITWAGYKLL....FHADVLDVVRVVLAGLLIGASAEIARYLLT
Bh VirB2	MTGTTAKLIATTC.VA.AVG.IGWMYGFIDL...RVAAY..CLI.GI..GIV..FGASALVSKLTSAS
At VirB2	LGPFGQ.SLAVLG.IV.AIG.ISNMFC.....ASL..GLVAGVGGIVIMFGASFLGQTLTGGG
pKM101 TraM	IPIGCA..IAIM.V..SC.FM.WMLHVIPASFIP.IVIS..LI.GI.....GSASYLV....SLTGVGS
R388 TrwM	LT.....TIVP.IA.AAVIILCLGIAYAG....FIEKDTFVRSIGVTIAGSAVQITAMFLT
RP4 TrbC	VTGPVAFALSIIGIVV.AGGVLI.FGGELNAF....FTLI...FLVLVMAALVGAQNVMMS...TFFGRGAEIAALNGALHQVQVAAADAVRAVAAGRLA
F TraA	VKATFGKDSVVKWVWLAEVLVGAVMVMMT.....VNVK...FLAGFAII....SVFIAVGMVVGL

Core Region

Figure 1.5 Schematic of the pilin processing and proposed T-pilus biogenesis pathway of the *Agrobacterium tumefaciens* VirB/D4 secretion system

The VirB1-VirB11 and VirD4 type IV secretion system (T4SS) components are shown according to their proposed localization and interactions. VirB2 is produced as a 121 amino acid pro-pilin that is inserted into the inner membrane. The 47 residue signal sequence is cleaved by a signal peptidase, resulting in a 74 amino acid product. The N- and C-termini are joined in a head-to-tail peptide bond, forming a cyclic peptide. The mature pilin is composed of two hydrophobic domains and two short hydrophilic domains. The cyclized mature pilin is then predicted to be shunted up the core complex where it can serve as the building block for assembly of a functional secretion channel and the extracellular T pilus. P: periplasm; IM: inner membrane; OM; outer membrane; S.S: Signal Sequence.



T-pili are long, 10nm wide filaments; when treated with sodium dodecyl-sulfate, a 2 nm channel was detected (104). In such a putative channel, it would be possible for the monomeric cyclic VirB2 peptides to be transported to the growing tip of the T-pili, in an assembly mechanism similar to that of flagella. Alternatively, new monomeric protein may be added at the base of the pilus. Immunogold labeling studies confirmed that VirB2 pilins comprise the entire length of the T pilus, and also supplied evidence that VirB5 is localized to the filament tip (121). A VirB4-VirB8-VirB5 interaction sequence was shown to be required for formation of a VirB2-VirB5 complex; assembly of this complex is thought to be a prerequisite for T-pilus assembly (122). Beyond this interaction network, little is known about the subunits involved or the specific steps necessary for T-pilus assembly.

Uncoupling Mutations

Interestingly, various VirB mutations have been isolated that disengage or separate substrate transfer from T-pilus biogenesis. Mutations have been identified in VirB6, VirB9, and VirB11 that abolish formation of detectable T-pilus without disrupting secretion of substrates through the VirB channel (82, 87, 123). In addition, deletion of the VirB1 transglycosylase was shown to abolish T-pilus production without blocking substrate transfer (124-126), whereas, conversely, deletion of the VirD4 coupling protein does not affect T-pilus biogenesis but blocks substrate transfer. On the basis of these findings, it has been proposed that the VirB proteins can alternatively assemble as the T-pilus or the secretion channel. Signals directing assembly of the VirB proteins as the secretion channel or the T-pilus are not known, but could include events occurring at the inner face of the inner membrane e.g. substrate docking, ATP hydrolysis, or the outer face of the outer membrane, e.g. target cell contact, pilus breakage.

VIII) The Importance of VirB2 and VirB10 Subunit Studies of the VirB/D4 T4SS

Both VirB2 and VirB10 are required for substrate transfer and T-pilus biogenesis (25, 127, 128). The movement of VirB2 from the inner membrane to a predicted periplasmic VirB2 polymer (secretion channel portion) (58, 123) and an elaborate extracellular organelle, suggests that VirB2 undergoes dynamic changes in structure and protein-protein contacts. Energy is predicted to play a key role in T-pilus biogenesis but the specific contributions of the VirB ATPases VirB4 and VirB11 have yet to be defined. Biochemical assays have shown that VirB10 is an energy sensor that undergoes a conformation change in response to ATP hydrolysis by VirB11 and VirD4 at the inner membrane (58). Structural

information on the 'core' channel complex of the T4SS encoded by pKM101 showed that a VirB10 homolog forms the outer membrane pore and spans the entire cell envelope (67, 68). Nevertheless, the structural and functional role of VirB10 domains with respect to T-pilus biogenesis and substrate transfer remain undefined. The location of VirB10 and its energy sensing capability suggest that VirB10 could gate the outer membrane channel and VirB10 domains may play specific roles in both secretion and T-pilus assembly. Thus, studies aimed at characterizing the contributions of the VirB2 pilin and VirB10 energy sensor during formation of the T4SS will help develop a more detailed mechanistic understanding of T4SS biogenesis and function, and will also contribute to a broader comprehension of the energetics and molecular events underlying assembly of complex surface organelles.

IX) Dissertation Focus and Specific Aims

In this thesis, I sought to define key reactions required for the integration of the VirB2 pilin into the secretion channel and T-pilus. My work focused primarily on VirB2, VirB4, and VirB10, and the 4 aims were: i) define the VirB2 inner membrane topology and packing architecture in the T-pilus (Chapter 3), ii) characterize the contributions of the VirB4 and VirB11 ATPases to the structural state of membrane-integrated VirB2 pilin during machine biogenesis (Chapter 4), iii) Characterize how VirB10 domains contribute to T-pilus biogenesis and channel activity (Chapter 5), and iv) explore the mechanism by which a VirB10 gating mutant mediates release of secretion substrate while selectively blocking T-pilus biogenesis (Chapter 6).

Chapter 2: Materials and Methods

Strains, plasmids, and induction conditions

Agrobacterium tumefaciens and *Escherichia coli* strains and plasmids used in this study are listed in Table 2.1 and 2.2. Conditions for growth of *A. tumefaciens* and *E. coli* and for *vir* gene induction with 100 μ M acetosyringone (AS) in induction media (ABIM) have been described previously (128). Plasmids were maintained in *A. tumefaciens* and *E. coli* by addition of gentamycin sulfate (100 & 20 μ g/ml, respectively), carbenicillin (100 μ g/ml), tetracycline (5 μ g/ml), spectinomycin (600 μ g/ml) and kanamycin (100 μ g/ml).

VirE2-FLAG tag construction

Cristina Alvarez-Martinez, a postdoctoral fellow in the Christie laboratory constructed a plasmid expressing *P_{virB}-virE1-FLAG-virE2* by site-directed mutagenesis using two-step PCR (129). Primers used to construct this plasmid are listed in Table 2.3. Primers *virE1_for_Nde* and *virE1_rev_FLAG* were used to amplify the region upstream of the FLAG epitope tag (the FLAG sequence was introduced in the *virE1_rev_FLAG* primer). Primers *virE2_for_FLAG* and *E2Down* were used to amplify the region downstream of the FLAG tag (primer *virE2_for_FLAG* contained the desired tag). The 5' and 3' fragments obtained after PCR amplification were used as templates in another PCR reaction using primers *virE1_for_Nde* and *E2Down*, generating the full-length gene containing the desired FLAG tag in frame with VirE2. The fragment was cloned in the pGEMT-Easy vector (Promega) and sequenced.

VirB2-FIAsh tag construction

Plasmids in pJKFIAshHxx series were constructed by cloning a FIAsh Kan^r cassette into the *SphI* site created by the Cys substitutions in VirB2 (See (130)). FIAsh Kan^r cassette was constructed by PCR amplification of the Kan^r cassette from pXZ151 and flanked by an *SphI* site, half of the FIAsh tag, and a *SmaI* site, resulting in: *SphI* – Cys – Cys – Pro – *SmaI* – Kan^r cassette – *SmaI* – Gly – Cys – Cys – *SphI*. Primers used for amplification are listed in Table 2.3, Following cloning into the *SphI* site created by the Cys substitutions in VirB2 (130), the Kan^r cassette was removed by *SmaI* digestion. Imran Shah, a postdoctoral fellow in the Christie laboratory, constructed plasmids pISFIAshH63 and pISFIAshH114 using oligonucleotide-directed mutagenesis. Plasmid pBB8 served as the template (128) and the FIAsh tag was inserted using the primers listed in Table 2.3. Insertions were confirmed by sequencing.

TABLE 2.1: Bacterial strains used in these studies.

Bacterial Strain	Relevant characteristics	Source
<i>E. coli</i>		
DH5 α	$\lambda\Phi80d/lacZ\Delta M15 \Delta(lacZYA-argF)U169 recA1 endA1 hsdR17(r_K - m_K^+) supE44 thi-1 gyrA relA1$	GIBCO-BRL
S17-1	Tra genes from pRP4 integrated into chromosome	BIO-RAD
<i>A. tumefaciens</i>		
A348	A136 containing pTiA6NC	(131)
A348Spc ^r	A348 with Spc ^r by spontaneous mutagenesis	(87)
PC1000	A348 deleted of entire <i>virB</i> operon from pTiA6NC	(132)
PC1001	A348 deleted of <i>virB1</i> and from pTiA6NC	(128)
PC1002	A348 deleted of <i>virB2</i> from pTiA6NC; polar on <i>virB3</i>	(128)
PC1003	A348 deleted of <i>virB3</i> from pTiA6NC	(128)
PC1004	A348 deleted of <i>virB4</i> from pTiA6NC	(133)
PC1005	A348 deleted of <i>virB5</i> from pTiA6NC	(128)
PC1006	A348 deleted of <i>virB6</i> from pTiA6NC	(128)
PC1007	A348 deleted of <i>virB7</i> from pTiA6NC	(128)
PC1008	A348 deleted of <i>virB8</i> from pTiA6NC	(128)
PC1009	A348 deleted of <i>virB9</i> from pTiA6NC	(128)
PC1010	A348 deleted of <i>virB10</i> from pTiA6NC	(128)
PC1011	A348 deleted of <i>virB11</i> from pTiA6NC	(128)
PC1211	A348 deleted of <i>virB2</i> and <i>virB11</i> from pTiA6NC	(123)
JK1002	A348 deleted of <i>virB2</i> from pTiA6NC	(130)
JK1204	A348 deleted of <i>virB2</i> and <i>virB4</i> from pTiA6NC	(130)
C58- <i>fliR</i>	C58 deleted of <i>fliR</i> - Aflagellate, non-motile	Dr. Clay Fuqua

TABLE 2.2: Plasmids vectors used in these studies

Plasmid or Vector	Relevant characteristics	Source
pGEMT-Easy	Crb ^f ; cloning vector	Promega
pBSIIKS ⁺ <i>NdeI</i>	Crb ^f ; cloning vector containing <i>NdeI</i> restriction	(128)
pXZ151	Kan ^r ; broad-host-range IncP plasmid containing <i>P_{lac}</i> with downstream polylinker sequence	(134)
pSW172	Tet ^r ; broad-host-range IncP plasmid <i>P_{lac}</i> with downstream polylinker sequence	(128)
pBBR1MCS2K ^r	Kan ^r ; broad-host-range cloning vector	(135)
pBBR1MCS2G ^r	Gen ^r ; broad-host-range cloning vector	(106)
pML122ΔK ^r	Gen ^r ; IncQ RSF1010 derivative	(60)
pBB50	Kan ^r ; ~3-kb <i>BamHI</i> fragment containing <i>nptII</i>	(128)
<i>virB</i> expression plasmids		
pJEK01	Crb ^f ; pBIIKS ⁺ <i>NdeI</i> expressing <i>P_{virB}-virB2C64S</i>	(130)
pJEK02	Crb ^f ; pBB8 with a <i>virB2</i> internal deletion	(130)
pJEK03	Crb ^f Kan ^r ; <i>sacB</i> -containing pBB50 (128) with the Δ <i>virB2</i> mutation and flanking sequences from pJEK02	(130)
pPC914	Crb ^f ; pBIIKS ⁺ <i>NdeI</i> expressing <i>P_{virB}-virB1</i>	(128)
pPC927	Crb ^f ; pBIIKS ⁺ expressing <i>P_{virB}-virB1</i> , <i>virB2</i> with <i>NdeI</i> at start site, and <i>virB3</i>	(128)
pKA93	Gen ^r ; pBBR1MCS2G ^r expressing <i>P_{virB}-virB4</i>	(45)
pKA96	Gen ^r ; pBBR1MCS2G ^r expressing <i>P_{virB}-virB4K439Q</i>	(130)
pKA94	Gen ^r ; pBBR1MCS2G ^r expressing <i>P_{virB}-virB4</i> and <i>P_{virB}-virB11</i>	(130)
pJKxx series	pJEK01 with VirB2 Cys substitutions; xx denotes the position of the codon replacement	(130)
pJKBxx series	Crb ^f Kan ^r ; pXZ151 ligated to pJKxx plasmids	(130)
pJKBBxx series	Crb ^f Kan ^r ; pBBR1MCS2K ^r ligated to pJKxx plasmids	(130)
pXZB100	Crb ^f Kan ^r ; pXZ151 with <i>P_{virB}-virB11</i>	(136)

pPCB39	Crb ^f Kan ^f ; pXZ151 with <i>P_{virB}-virB11K175Q</i>	(90)
pXZB102	Crb ^f Kan ^f ; pXZ151 with <i>P_{virB}-virB11I265T</i>	(87)
pKVD10	Crb ^f Tet ^f ; pSW172 with P _{lac} -VirB10	(69)
pKVD116	pKVD10 with residues 2-18 deleted from VirB10	(69)
pKVD136	pKVD10 with residues 2-46 deleted from VirB10	(69)
pKVD117	pKVD10 with residues 70-114 deleted from VirB10	(69)
pKVD145	pKVD10 with residues 72-92 deleted from VirB10	(69)
pKVD146	pKVD10 with residues 92-114 deleted from VirB10	(69)
pKVD126	pKVD10 with residues 268-287 deleted from VirB10	(69)
pKVD129	pKVD10 with residues 308-337 deleted from VirB10	(69)
pIG022	pKVD10 with VirB10 Cys substitution at residue 356 in the RDLDF motif	(69)
pKVD Δ 150	pKVD10 with residues 2-150 deleted from VirB10, fused to the 5' end of VirB5 signal sequence from pZD74	(69)
pZD74	<i>virB5</i> signal sequence	(69)
pIGxx series	pKVD10 with VirB10 Ala-Cys codon insertions or cys codon substitutions; xx denotes the codon immediately preceding the insertion or codon of substitution	(69)
pCM48	P _{virB} VirE1-VirE2 FLAG in pGEM-Easy vector	(Dr. Cristinta Martinez, this study)
pCM50	P _{virB} VirE1-VirE2 FLAG cloned as a <i>NdeI/XhoI</i> fragment from pCM48 into pPC914 Nde/Xho	(Dr. Cristinta Martinez, this study)
pCMB50	Crb ^f Kan ^f ; pBBR1MCS2K ^f ligated to pCM50 P _{virB} VirE1-VirE2 FLAG	(Dr. Cristinta Martinez, this study)
pLB100	VirB10 with substitution G272R	Dr. Lois Banta
pJKFLAG85	pBB8 with VirB2 FLAG insertion following residue 85	This study
pJKFIAsHxx series	pVS10 with VirB2 Cys substitution and FIAsH tag insertion; xx denotes the Cys substitution FIAsH tag inserted at the <i>SphI</i> site	This study
pISFLAG62	pBB8 with VirB2 FLAG insertion following residue 62	(Dr. Imran

		Shaw, this study
pISFLAsH63	pBB8 with VirB2 FIAsH tag insertion following residue 63	(Dr. Imran Shaw, this study)
pISFLAsH114	pBB8 with VirB2 FIAsH tag insertion following residue 114	(Dr. Imran Shaw, this study)

Table 2.3: Oligonucleotide primers used for epitope tag construction and insertion

Name	5'Primer
VirE1_for_Nde	5' – AAT ACA TAT GGC CAT CAT CAA G – 3'
VirE1_rev_FLAG	5' – TTT GTC GTC GTC GTC TTT GTA GTC CAT CGT CTC ACT CCT TCT GAC – 3'
VirE2_for_FLAG	5' – ATG GAC TAC AAA GAC GAC GAC GAC AAA ATG GAT CTT TCT GGC AAT– 3'
E2Down	5' – TTC TCG AGT CAA AAG CTG TTG ACG CTT TGG CTA CG – 3'
FIAsH Kan SphI Smal-AS	5' – AAT GCA TGC ACA ACA CCC GGG GTC GAC CTG CAG – 3'
FIAsH Kan SphI Smal -S	5' – AAT GCA TGC TGC CCC GGG TGA GGT CTG CCT C
B2FIAsH 63/64-S	5' – GCT GCC CAG GAT GCT GCA TAT GCA GCT TTA TCC TTG GTC C – 3'
B2FIAsH 114/115-AS	5' – GCA GCA TCC TGG GCA AGC AGC CGA GGA AGC TCG CCC C – 3'
B2FLAG 59/60-AS	5' – CGT GCA TAT ATT GTT AAC CTT GTC ATC GTC GTC
B2FLAG62/63-S	5'- GAT TAT AAA GCG TTT GAT AAC CTG ATA TGC ACG TTT ATC CTT GGT CC – 3'
B2FLAG 64/65-AS	5' – CGG ACC AAG GAT AAA CGT CTT GTC ATC GTC GTC GTC CTT ATA ATC GCA TAT ATT GTT AAC CAT – 3'
B2FLAG 85/86-AS	5'- CCG CCC GAA CAT CCA GGA CTT GTC ATC GTC GTC CTT ATA ATC GAT CCC GAT AGC GAC AAT – 3'
B2FLAG 118/119-AS	5'- TCA ACT ACC GCC CTT GTC ATC GTC GTC CTT ATA ATC AGT GAG CGT TTG GCC GAG – 3'

VirB2-FLAG tag construction

Plasmid pBB8 served as the template for construction of the FLAG tagged VirB2 insertion mutations using oligonucleotide-directed mutagenesis (128) and the FLAG tag was inserted using the primer listed in Table 2.3. Imran Shah, a postdoctoral fellow in the Christie laboratory constructed plasmid pISFlag62.

Virulence assays

Strains of *A. tumefaciens* were tested for virulence on wounded *Kalanchoe daigremontiana* leaves (128). Controls for the tumorigenesis assays included co-inoculating the same leaf with wild-type A348 and the corresponding *vir* gene deletion. Virulence was scored in terms of and time course of tumor appearance and tumor size. Tumors were scored on a scale of – avirulent to +++ wild-type virulence. Assays were performed in triplicate.

Conjugation assays

Diparental mating with *E. coli* strain S17-1(pML122) was used to introduce the IncQ plasmid pML122 (Gen^r) into various *A. tumefaciens* donor strains (82, 87). Conjugative transfer of the mobilizable IncQ plasmid pML122Gen^r from *A. tumefaciens* donor strains of interest to A348Spc^r recipient cells was carried out as described previously (87). Assays were performed in triplicate and transfer frequencies presented as the number of transconjugants per donor for a representative experiment.

Protein analysis and immunoblotting

Proteins were resolved by sodium dodecyl sulfate polyacrylamide gel electrophoresis (SDS-PAGE) using 12.5% or 10% polyacrylamide gels, or Tricine sodium dodecyl sulfate polyacrylamide gel electrophoresis (Tricine SDS-PAGE) using 16.5% polyacrylamide gels (84). Gels were transferred to nitocellulose membranes, and visualized by immunoblot development with goat anti-rabbit conjugated to alkaline phosphatase (BioRad) or blots were developed with anti-rabbit antibodies conjugated to horseradish peroxidase and were visualized by chemiluminescence (Pierce, Thermo Scientific). Pre-stained SDS-PAGE Broad Range from BioRad served as the molecular size markers.

T-pilus isolation and extracellular blot assay

A. tumefaciens strains were grown to an OD₆₀₀ of 0.5 in MG/L media at 28 °C, and then induced for expression of the *vir* genes with acetosyringone (AS) at 25 °C, as described previously (137). The induced culture (1 mL) was spread on ABIM agar plates and incubated for 4 d at 18 °C. Cells were removed from the plates and placed in 1 ml 50 mM KPO₄ buffer (pH 5.5). The cell suspension was passed through a 25-gauge needle. The sheared material was centrifuged for 30 min at 14,000 *x g* at 4 °C and the supernatant was saved. The fraction was centrifuged for 1 h at 100,000 *x g* at 4 °C to recover T- pili or alternatively prepped for analytical gel filtration or viewing in the electron microscope (refer below). T-pili were suspended in 50 µL of Laemmli's buffer and boiled, or suspended in buffer A [100 mM Hepes (pH 7.5), 250 mM sucrose, 25 mM MgCl₂, 0.1 mM KCl] and further fractionated through a 20-70% sucrose density gradient as described previously (138). Alternatively, resuspended T-pili were used in Cys labeling studies, as described below. Extracellular VirB2 and VirB5 were detected by colony surface immunoblotting as described previously (69).

Analytical gel filtration

Recovered T-pili samples were subjected to analytical gel filtration (AGF) by Dr. Hye-Young Yeo (University of Houston) using a Superdex 75 10/300GL column (Tricorn) (69). The column was equilibrated and run with buffer S [50mM Hepes pH 7.0, 2mM MgCl₂, 5% glycerol, 100mM NaCl, 0.1mM EDTA]. The AGF column was calibrated using molecular weight standard markers RNase A (14kDa), chymotrypsinogen A (25kDa), albumin (67kDa), and lactate dehydrogenase (140kDa) (Amercham Biosciences). Recovered gel filtration fractions were analyzed using tricine SDS-PAGE as mentioned above.

Chemical labeling of cysteine residues

Cysteine labeling experiments were performed as previously described (65) with some modifications. Briefly, *A. tumefaciens* strains producing VirB2 Cys derivatives were induced for *vir* gene expression and grown to an OD₆₀₀ of 0.6. Cells from 30 ml cultures were harvested, resuspended in buffer A and distributed into two oakridge tubes to a final OD₆₀₀ of 12 in 500 µl of buffer A. 4-acetamido-40-maleimidylstilbene-2,20-disulfonic acid (AMS; Molecular Probes) was added (5 mM final) to one cell suspension, and cells were incubated at 25 °C for 30 min. Ten ml of buffer A was added to the cell suspension and

centrifuged to remove the AMS. The resulting cell pellet was resuspended in 500 μ l of buffer A. 3-(N-maleimidylpropionyl) biocytin (MPB; Molecular Probes) was added to the AMS-pretreated cells and the second cell suspension at a final concentration of 100 μ M (20 mM stock in dimethyl sulfoxide). The cells were incubated at 25 °C for 5 min. The final concentration of dimethyl sulfoxide in the reaction did not exceed 0.5% (v/v). The biotinylation reaction was quenched by addition of β -Mercaptoethanol (β -ME; 20 mM final) and cells were washed two times in buffer A with 20 mM β -ME. As controls, sonicated cell extracts were treated with MPB. For labeling of the T-pilus, enriched T-pili were suspended in 500 μ l of buffer A, treated with a final concentration of 100 μ M MPB, and incubated at 25 °C for 5 min. The biotinylation was stopped by addition of β -ME (40 mM final). T-pili were recovered by centrifuging at 100,000 \times g , and MPB labeling of Cys-substituted pilin was assessed as described below.

Detection of labeled cysteine residues

MPB-treated T-pili or whole cells were suspended in 200 μ L TES buffer [10 mM Tris pH 7.5, 5 mM EDTA, 2% (w/v) SDS] and vortexed at 37 °C for 30 min. Samples were incubated on ice for 1 h with 250 μ l of buffer B [150 mM Tris (pH 8.0), 0.5 M sucrose, 10 mM EDTA] plus lysozyme (1mg/ml final). Samples were then vortexed at 37 °C for 15 min. Triton X-100 (20 μ l), 13 μ L of 1 M $MgCl_2$ stock solution, and protease inhibitor cocktail EDTA-free (30 μ l; Pierce Biochemicals) were added and the samples were vortexed at 25 °C for 10 min followed by gentle rocking at 4 °C for 3 h. Samples were diluted with 900 μ l of buffer B and centrifuged at 14,000 \times g for 15 min. The resulting supernatant was incubated with a 30 μ l bed volume of Protein A-Sepharose CL4B (Pharmacia) at 25 °C and for 45 min and centrifuged at 5000 \times g to remove protein A-Sepharose and non-specifically bound proteins. The recovered supernatant was incubated overnight at 4 °C with a 60 μ l bed volume of Protein A-Sepharose coupled to anti-VirB2 antibodies. The beads were recovered by low-speed centrifugation at 400 \times g and washed two times in buffer B plus 1% (w/v) Triton X-100 at 4 °C for 10 min, one time in buffer B plus 0.1% (w/v) Triton X-100 at 4 °C for 10 min, and one time in buffer B at 25 °C for 5 min. Beads were recovered and 15 μ L buffer B plus 15 μ l of 5X Laemmli's buffer was added prior to boiling samples (5min). Boiled samples were centrifuged at 400 \times g for 5 min and proteins were subjected to Tricine-SDS-PAGE and transferred to nitrocellulose as described above. Membranes were blocked with buffer C [1X PBS, 0.1% Tween 20, 5% (w/v) bovine serum albumin (BSA)] overnight and then for 4 h in the presence of avidin-HRP (Pierce; 2:10,000 dilution from 2

mg/ml stock). Blots were washed 3 times in buffer D (1X PBS, 0.1% Tween 20, 0.5% BSA) and incubated for 10 min with buffer C prior to analysis by chemiluminescence according to the manufacturer's instructions (Pierce, Thermo Scientific).

Growth Curves

A. tumefaciens strains were grown to an OD₆₀₀ of 0.5 in MG/L media at 28 °C, and then induced in ABIM at 25 °C for 4 h. Cells were normalized and diluted in ABIM (OD₆₀₀= 0.1). Greiner Bio-One flat-bottom, 24- well PS microplates (Sigma-Aldrich, Prague, Czech Republic) were filled with the cell suspension (1mL in each well). Plates were covered with a sealing membrane (Breathe-Easy; Sigma-Aldrich). Growth over time (18 h) was monitored using a Synergy™ Mx Multi-Mode Microplate Reader (Biotek Instruments). The absorbance in each well was measure at 600 nm at given intervals (30 min) with continuous shaking of the microplate. The absorbance data, with background absorbance subtracted, were exported to MS Excel for further processing. Data are shown for a representative experiment.

FLAG-VirE2 Release Screen

Surface-exposed FLAG-VirE2 was detected by colony immunoblotting as described previously for VirB2 detection (69) with minor modification. Monoclonal FLAG antibody was used as the primary antibody followed by immunoblot development with goat anti-mouse conjugated to alkaline phosphatase (BioRad).

Assays for vancomycin and SDS sensitivity

Growth of each strain in ABIM supplemented with 0.5% SDS or Vancomycin (50 µg/ml and 100 µg/ml) was monitored over 18 h using Synergy™ Mx Multi-Mode Microplate Reader (BioTek Instruments) as described above.

Assays for outer membrane integrity

RNase I release from intact cells was assayed according to Lazzaroni and Portalier (139). Briefly, ABIM induced cells were normalized (OD₆₀₀ = 0.6) and 20 µl was spotted on ABIM RNase agar [standard ABIM agar supplemented with 0.1% yeast extract and 1% RNA type VI from *Torula* yeast (Sigma)]. After overnight growth at 28 °C, RNA was precipitated with cold 10 % trichloroacetic acid (TCA), and RNase I leakage was detected by identification of clear zones surrounding colonies. Alternatively, after overnight incubation, colonies were scraped from the plates, resuspended in 50 µl ABIM, and sonicated. Lysed cells were spotted on fresh ABIM RNase agar for 1h prior to TCA

precipitation and monitored for clearing. ChvE release was monitored by colony immunoblotting with anti-ChvE antibody (69). Alternatively, after incubation, colonies were scrapped from the plates, resuspended in 50 μ l ABIM, and sonicated. Lysed cells were spotted on 0.45 mm nitrocellulose membrane, allowed to sit for 5 min, and developed by immunostaining as mentioned above (69).

Co-immunoprecipitation

Coimmunoprecipitation was performed as described previously (82). Briefly, 500 ml cultures induced by AS were harvested and cells were lysed by the French press. Ultracentrifugation was used to recover total membranes. Membrane were cross-linked with dithiobissuccidimidyl propionate (DSP; 0.5 mg/ml final) and solubilized with RIPA buffer (50 mM Tris pH 7.6, 0.1% SDS, 150 mM NaCl, 0.5% sodium deoxycholate, 1% NP-40). The solubilized membranes were used in immunoprecipitation experiments probing with anti-VirB2, anti-VirB4, or anti-VirB11 antibodies coupled to Protein A-Sepharose CL-4B beads (Amersham Biosciences).

Osmotic shock

Cells were subjected to osmotic shock treatment as previously described (140). Briefly, *A. tumefaciens* strains were induced and grown to an OD₆₀₀ of 0.5. Cells from 65 ml cultures were harvested and normalized to final OD₆₀₀ of 18. Cells were pelleted by centrifugation at 10,000 \times g, resuspended in 8 ml of ice-cold osmotic shock solution [20% (w/v) sucrose, 5 mM CaCl₂, 33 mM Tris-HCl pH 8.0, 0.5 mM Na₂ EDTA] and incubated while shaking at 4 °C for 15 min. Cells were pelleted by centrifugation at 10,000 \times g for 10 min and the supernatant was removed. The pellet was resuspended in 1 ml ice-cold reverse osmosis water and incubated at 4 °C for 10 min while shaking. The cell suspension was centrifuged at 8000 \times g for 10 min, and the osmotic shockate (supernatant) was recovered and the cell pellet was reserved. The shockate was concentrated by precipitation with 5 % trichloroacetic acid or alternatively by ultracentrifugation at 100,000 \times g at 4 °C for 1 h. the resulting pellet was resuspended in 20 μ l of 5X Laemmli's buffer. The remaining cell pellet was resuspended in 400 μ l 5X Laemmli's buffer. Samples were boiled (5 min) and then analyzed using 12.5% SDS-PAGE and Tricine SDS-PAGE as described above.

Electron microscopy

T-pili in the saved supernatant from ABIM plates, mentioned above, were precipitated with 1M MgCl₂ (0.1 M final) by incubation overnight at 4 °C. T-pili were collected by centrifugation at 16,000 x g at 4 °C for 1.5 h. The resulting pellet was resuspended in 100µl of 10 mM Tris-Cl (pH 8.0) and further fractionated through a 20-70% sucrose density gradient at 99,000 x g at 4 °C for 4 h. Fractions (~400 µl) containing T-pili were pooled and centrifuged at 100,000 x g at 4 °C for 1 h. The pellet was resuspended in 100µl 10 mM Tris-Cl (pH 8.0) and fractionated through a 1.1-1.5g/mL CsCl step-gradient for at 120,000 x g at 5 °C 18 h (115). Fractions (~250 µL) harboring T-pili were pooled and centrifuged at 100,000 x g at 4 °C for 1 h. The pellet was resuspended in 10 mM Tris-Cl (pH 8.0) and further diluted to 4 mL to remove excess CsCl prior to centrifuging at 100,000 x g at 4 °C for 1 h. The final pellet was resuspended in 50 µL of 50 mM Hepes, a 5 µl sample was placed on a 300-mesh carbon-Formvar grid (Ted Pella, Inc.). Grids were stained with 1% uranyl acetate (Ted Pella, Inc.) and examined with a JOEL 1400 electron microscope.

Disulfide crosslinking

Isolated T-pili (as described above) were resuspended in non-reducing Laemmli's buffer [125 mM Tris-HCl, pH 6.8, 20% (v/v) glycerol, and 4% (w/v) SDS) containing 50 mM EDTA and no reducing agent] or standard β-ME-containing Laemmli's buffer, boiled, and electrophoresed through a Tricine SDS-PAGE gel, as described above. Alternatively, isolated T-pili were suspended in PBS (pH 7.4), and samples were cross-linked by incubation with 1 mM Cu₂-(phenanthroline)₃ as the oxidant at 37 °C for 5 min. The reactions were stopped by addition 5 mM EDTA followed by addition of non-reducing Laemmli's buffer. Samples were subjected to Tricine-SDS PAGE gels and proteins were detected as described above.

Immunofluorescence microscopy

Cells induced with AS for synthesis of the Vir proteins were washed once in 1 X phosphate buffered saline (PBS; 150 mM NaCl, 15 mM KCl, 0.11% Na₂HPO₄, 0.03% NaH₂PO₄) and a 30 µl suspension (OD₆₀₀=2) was applied onto a 0.1% poly-L-lysine-coated glass cover slip and briefly air dried. Cells were fixed by incubation overnight at 25 °C in fixation solution (37.5% methanol + 12.5% acetic acid), and unbound cells were removed by three 20 min washes in PBS containing 0.05% Tween-20 (PBS-T). Cells were treated

overnight at 4°C with primary antibodies (1:100 dilution in 2% BSA), followed by three PBS-T washes. Cells were then incubated in the dark with Alexa fluor^R 488 goat-anti-rabbit IgG (1:100 dilution in 2% BSA) (Molecular Probes) at 25 °C for 1 h. Cells were washed one time with PBS-T and two times with PBS. Cover slips were treated with anti-fade solution (50% glycerol in PBS), sealed with base coat of nail polish (Revlon) on a microscopic slide, and visualized Nomarski microscopy.

Chapter 3: T-pilus Maturation as Monitored by Cysteine Accessibility

NOTE: *This chapter is derived from work that has been published in 2010: "Evidence for VirB4-Mediated Dislocation of Membrane-Integrated VirB2 Pilins during Biogenesis of the Agrobacterium VirB/VirD4 Type IV Secretion System." Journal of Bacteriology 192(19): 4923-34. PMID: 20656905. I am the primary author on this paper. I performed all experiments described in this chapter. I have been given permission by the publisher of Journal of Bacteriology, the American Society for Microbiology, to reproduce any/all of my manuscript in print or electronically for the purposes of my dissertation (License Number 2510961139325).*

Introduction

A fundamental question of interest for bacterial surface organelles is how the machine subunits are processed and delivered to their sites of assembly. In *A. tumefaciens*, VirB2 is an essential component of the two organelles elaborated by the VirB/VirD4 type IV secretion system (T4SS), the membrane-spanning translocation channel and the extracellular T-pilus (25, 31, 141). The assembly of VirB2 into the channel and T-pilus is poorly understood, although a few early processing reactions have been biochemically defined. Upon synthesis, VirB2 pro-pilin is first integrated into the inner membrane and then cleaved of its 47-residue signal sequence. Next, the N- and C-termini are covalently joined by a novel head-to-tail cyclization reaction (115). The protein catalyzing cyclization has not been identified in *A. tumefaciens*, but in *E. coli* the VirB2 homolog TrbC (24/51 % identity/similarity) of plasmid RP4 (115, 142, 143) is also cyclized and the cyclization reaction is carried out by the TraF protein (115). Cyclization of VirB2 and TrbC is required for functionality of these pilins, whereas another VirB2 homolog, TraA (19/47 % identity/similarity) of *E. coli* plasmid F (113), is not cyclized although its N terminus is N-acetylated (144).

Despite differences in these early processing reactions, a common feature of T4SS-encoded pilus biogenesis pathways is that the pilin subunits integrate into the inner membrane as a pool for subsequent use in building the pilus. Topology models for VirB2, TraA_F, and TrbC_{RP4} were developed from computer-derived hydropathy profiles and limited reporter fusion studies with periplasmically-active alkaline phosphatase (PhoA) (144, 145). These profiles generally predict that two hydrophobic domains of these pilins span the inner membrane, resulting in localization of hydrophilic terminal domains in the periplasm and small central hydrophilic loops in the cytoplasm. However, these hydropathy predictions are often only 60-70% accurate in predicting topology organization (146), and computer algorithms also do not account for interactions between transmembrane (TM) helices, contacts with another subunit(s), and/or specific lipid - protein interaction(s) (146-148). Strategies used to verify membrane protein topologies often rely on general principles including: impermeability of the membrane bilayer to hydrophilic molecules, the difference in properties between the compartments separated by the membrane, or incorporation of reporter groups whose orientation is thought to reflect the topology of the protein (146, 149). While there are other methods available to experimentally determine VirB2's predicted protein topology, cysteine scanning remains one of the least invasive and is less likely than other methods to perturb function and overall structure (149).

If we consider the membrane-integrated pool of VirB2 as a starting-point in a pilin assembly pathway, the secretion channel and T-pilus represent the terminal organelles. VirB2 is required for substrate transfer, even in cells that do not elaborate T-pili (123). Moreover, on the basis of a demonstrated close contact with translocating T-DNA and associated genetic studies (58) we predict that the pilin subunit is delivered to and comprises part of the distal region of the secretion channel near the outer membrane. With regard to the T-pilus, nothing is known about the pilus structure or the packing geometry of pilin. However, studies of the related TraA_F pilin have led to a proposal that the two α -helices comprising the TM domains form anti-parallel helix-helix interactions in the F-pilus resulting in surface-exposed N- and C-termini and a charged central domain lining the pilus lumen (145).

Here, I sought to exploit the power of the substituted cysteine accessibility method (SCAM) to define the inner membrane topology of VirB2, and then to identify differences in the structural states of the pilin when assembled as a component of the secretion channel vs. the T-pilus. This work represents the first detailed *in vivo* structural analysis of the VirB2 pilin.

Results

Phenotypes of VirB2 Cysteine Substitution Mutations

Native VirB2 contains 3 Cys residues, two within the signal sequence and Cys64 in the mature protein. The Christie laboratory reported in an earlier study that a Ser substitution of Cys64 results in an attenuated virulence phenotype (87). In those studies, virulence assays were carried out at room (25 °C) temperature; however, more recent studies have shown that the VirB/D4 T4SS functions optimally at 18 – 20 °C (150). At this lower temperature, I determined that the C64S mutant exhibits near wild-type substrate transfer frequencies, as monitored by two assays, virulence on plants and conjugative transfer of an IncQ plasmid to agrobacterial recipient cells (Fig. 3.1B). T-pili produced by the C64S mutant at the lower temperature also were indistinguishable from pili from the wild type strain, as monitored by sucrose density gradient fractionation and electron microscopy (Fig. 3.1C and D). The wild-type properties of the C64S mutant enabled its use as a platform for construction of single Cys substitution mutations at 5-7 residue intervals along the length of VirB2.

In initial phenotypic studies, I determined that all 16 Cys mutant proteins migrated at the same position and most accumulated at comparable steady-state levels as native VirB2 with minimal to no effect on function, as monitored by pilus production and DNA transfer (Fig. 3.1). However, two mutant proteins (G51C and T54C) accumulated at diminished levels in whole cell extracts, although both proteins were detectable in membrane fractions (Fig. 3.1A). These mutations, as well as T58C, L117C, and G119C which reside near N/C processing and cyclization sites, completely abolish substrate transfer (Fig. 3.1B). Cys substitution of the aromatic residue F71 also abolished substrate transfer. Of these mutations, only G51C, F71C, and L117C also completely abolished T-pilus biogenesis (Fig. 3.1B). Notably, the transfer minus (Tra⁻) strain producing the G119C mutant pilin assembled morphologically wild-type pili as monitored by sucrose fractionation and electron microscopy (Fig. 3.1C and D). This mutant therefore selectively blocks substrate transfer without detectable effects on pilus biogenesis.

Inner Membrane Topology of VirB2

VirB2 contains two hydrophilic regions and two hydrophobic stretches. For the purposes of discussion, I will depict VirB2 as consisting of 4 domains (I-IV). This domain architecture derives from *in silico* hydropathy analyses (Fig. 3.2A), and is consistent with that described for the VirB2 homolog, TraA pilin of the F plasmid T4SS (151, 152).

Figure 3.1 Phenotypes of VirB2 Cys substitution mutations.

(A) Effects of mutations on total cellular and membrane levels of VirB2. Total cellular material and membrane fractions were subjected to SDS-PAGE, and immunoblots were developed with anti-VirB2 antibodies. Protein samples were loaded on a per-cell-equivalent basis. (B) Upper panel, effects of mutations on T-DNA transfer as monitored by virulence on wounded *Kalanchoe* leaves (black bars) (–, avirulent; +++, WT virulence) and transfer of the mobilizable IncQ plasmid pML122 to *A. tumefaciens* recipients (gray bars) (Tc's/Donor, number of transconjugants per donor cell). Lower panel, effects of mutations on T-pilus production, as monitored by VirB2 abundance recovered from the shear fraction by ultracentrifugation (top) and colony immunoblots developed with anti-VirB2 antibodies (bottom). (C and D) Pilin fractionation profiles and pilus morphologies produced by $\Delta virB2$ mutant strains synthesizing native VirB2 (Cys64; WT) or the Cys64Ser (C64S) or Gly119Cys (G119C) mutant protein. (C) Distribution profiles of extracellular pilins in identically prepared 20 to 70% sucrose density gradients, as monitored by immunoblot development with anti-VirB2 antibodies. (D) Morphologies of pili from peak sucrose gradient fractions, as detected by uranyl acetate staining and electron microscopy.

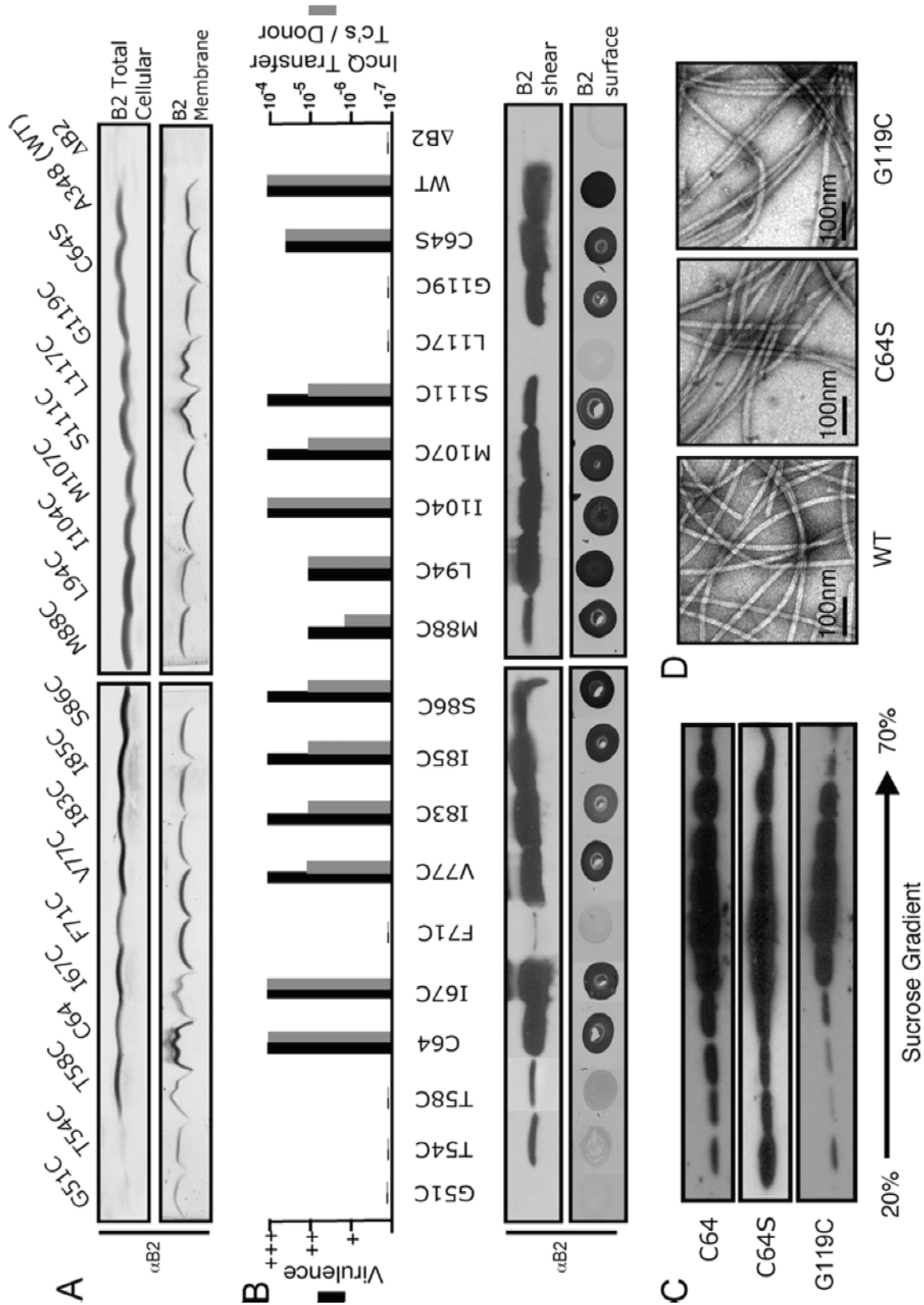
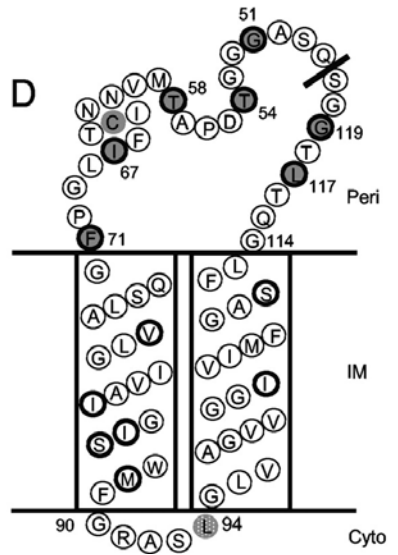
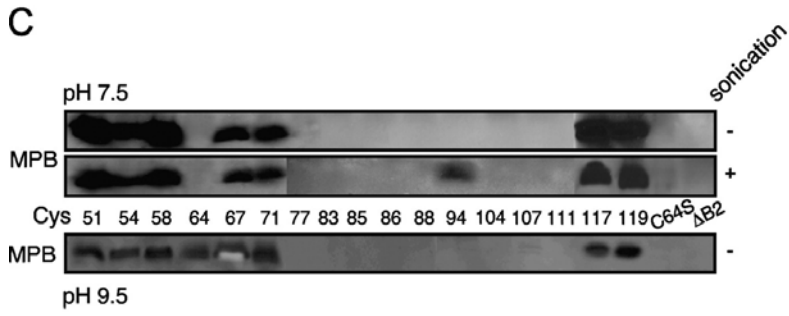
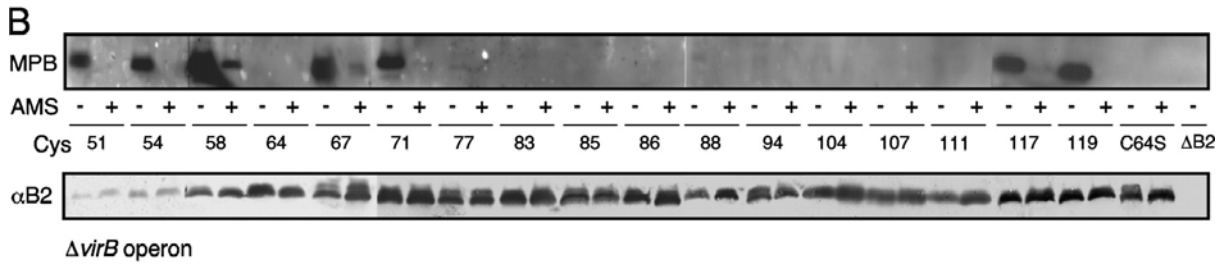


Figure 3.2 MPB accessibility of Cys substitutions.

(A) Predicted domain architecture of VirB2. Numbers correspond to the N and C termini of mature pilin and a compilation of hydrophobic domain (gray cylinders) boundaries as predicted by computer hydropathy programs: TMHMM (boundaries predicted: TM1 66 and 88, TM2 92 and 114), Mobylye (70 and 90, 93 and 113), Phobius (65 and 87, 94 and 113), SOUSI (61 and 83, 91 and 113), and HMMTOP (63 and 85, 92 and 114). Domain numbering (I to IV) follows the nomenclature devised for the VirB2 homolog, TraA, of the F plasmid (117). (B) Δ *virB* operon strains producing pilins with Cys substitutions at the residues indicated were treated with thiol-reactive MPB without and with pretreatment with AMS. Cys-substituted pilins were isolated by immunoprecipitation and analyzed for MPB labeling. Immunoprecipitates also were analyzed for VirB2 protein abundance by blot development with anti-VirB2 antibodies (Δ B2). (C) MPB labeling profiles obtained by treatment of intact and lysed cells (by sonication) at neutral and alkaline pH. (D) A topology model for membrane-integrated VirB2 pilin. Thick black-outlined circles with gray centers, Cys substitution mutations at these positions were labeled by MPB treatment of intact cells; thick black-outlined circles with white centers, substitutions at these positions were not labeled under any condition; gray circles with gray outlines, substitutions labeled upon sonication (Cys94) or MPB treatment at alkaline pH (Cys64). Peri, periplasm; IM, inner membrane; Cyto, cytoplasm. Bar, N-C cyclization junction.



As shown in Fig. 3.2A, it has been proposed that hydrophobic domains II and IV form transmembrane α -helices and hydrophilic domains I and III reside in the periplasm and cytoplasm, respectively. To examine the disposition of the pilin at the inner membrane (IM), I analyzed the accessibility of the substituted Cys residues to the biotinylated sulfhydryl-specific maleimide probe MPB. MPB has a molecular size of 542 daltons and crosses the outer membrane (OM) through porins, but inefficiently traverses the inner membrane (153-155). MPB therefore labels residues located in the periplasm but not residues located in the cytoplasm or those buried in transmembrane regions or structural folds. VirB2 has been shown to undergo processing, cyclization, and membrane insertion independently of other VirB proteins (156). Thus to define the inner membrane topology of the cyclized pilin, I developed an MPB-labeling profile for Cys substitution mutants produced in the $\Delta virB$ operon strain.

As shown in Fig. 3.2B, upon treatment of whole cells, Cys residues throughout Domain I were MPB-labeled. To confirm the periplasmic location of hydrophilic Domain I, I pretreated cells with the highly hydrophilic, non-biotinylated sulfhydryl-specific maleimide probe AMS, which also crosses the OM but not the IM. Labeling of Domain I Cys residues was efficiently blocked by AMS pretreatment. Curiously, MPB did not label Cys64 in Domain I even though neighboring Cys substitutions were labeled (Fig 3.2 B). To examine the possibility that Cys residue may be buried in a structural fold within the periplasmic loop, MPB-labeling was carried out at alkaline pH 9.5. This alkaline reaction condition has been shown to render Cys residues in a structural fold - but not those embedded in the membrane - accessible to MPB labeling (155). As shown in Fig. 3.2 C, Cys64 but not Cys residues in the TM helices were labeled, supporting the proposal that Cys64 is buried in a pH-sensitive structural fold.

Cys substitutions present in the hydrophobic Domains II and IV or in the small hydrophilic loop III (Domain III) were not MPB-labeled in alkaline or neutral conditions (Fig. 3.2C). However, MPB treatment of sonicated cell extracts resulted in the labeling of Cys94 (Fig. 3.2 C), suggesting that Domain III is cytoplasmically localized. Cys residues in Domains II and IV were not detectably labeled in whole cells or sonicated cell extracts, supporting predictions that these correspond to membrane α -helices.

Taken together, these MPB-labeling patterns favor a membrane topology model depicted in Fig. 3.2 D. This model is consistent with the positive-charge-inside rule for membrane proteins (157) since Domain III (GR⁺ASL) has an overall net positive charge. This model is also compatible with earlier predictions that the cleavage and cyclization

reactions (Domain I) for the related pilin TrbC of the RP4 T4SS are carried out in the periplasm (115).

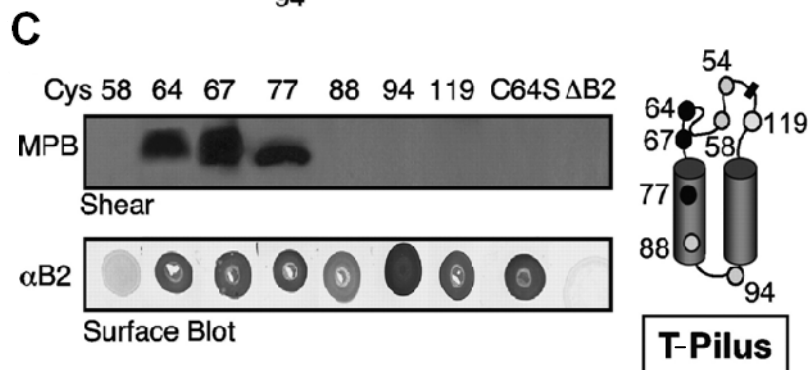
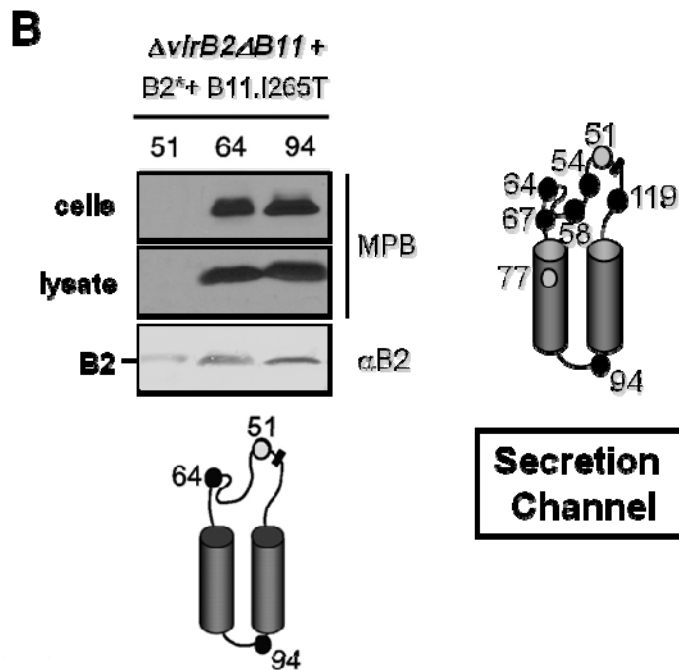
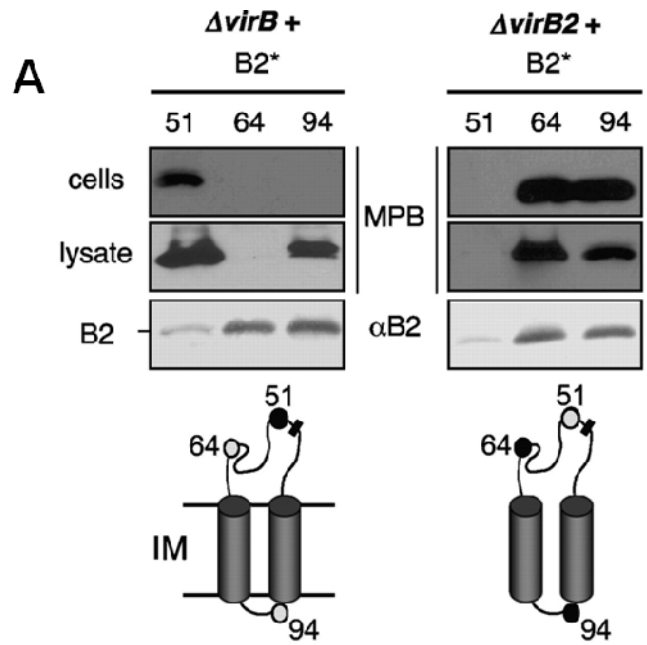
SCAM Reveals VirB2 Topology Changes in the Presence of Other Secretion Subunits

In the above studies, the membrane topology of VirB2 was determined in a strain lacking other VirB proteins. I predict that this topology model is also valid for pilin monomers that accumulate in the membrane as a pool early during T4SS biogenesis in wild-type cells. I next sought to identify differences in the VirB2 structural organization when produced together with the other T4SS subunits; any differences detected with the Cys-labeling profile presented above might reflect the altered structural organization of VirB2 when assembled as a component of the secretion channel. I detected differences in MPB-labeling patterns for 3 of the Cys substituted pilins when produced in $\Delta virB2$ (presence of VirB proteins) vs. $\Delta virB$ operon (absence of VirB proteins) mutant strains (Fig. 3.3 A). Specifically, Cys51 in hydrophilic Domain I was not detectably labeled in the presence of VirB proteins but was strongly labeled in their absence. Conversely, Cys64, also in Domain I, was strongly labeled in the presence of VirB proteins but was unlabeled in their absence. Finally, and most strikingly, Cys94, in the hydrophilic loop Domain III, was labeled in the presence other VirB proteins even when intact cells were MPB-treated, whereas as shown above Cys94 was only labeled upon sonication of cells lacking other VirB proteins. We previously demonstrated, using the same experimental protocol, that Cys substitutions in the cytoplasmic regions of bitopic protein VirB10 (69) and polytopic protein VirB6 (65) were not MPB labeled during treatment of intact cells but were labeled in cell lysates. These data suggest that Cys94 MPB-labeling, observed in a functionally wild-type strain, is unlikely attributable to cell rupture or permeation of MPB across the inner membrane. Remaining Cys mutant proteins exhibited the same labeling patterns in both the $\Delta virB2$ and $\Delta virB$ operon mutant backgrounds (refer to figure 3.2).

Although the differences in MPB-labeling of Cys51, Cys64, and Cys94 observed in strains producing vs lacking VirB proteins could reflect differences in the membrane-integrated vs secretion channel form of VirB2, the former strain also produces T-pili. T-pili are rarely detected on the surfaces of intact cells but are instead readily sloughed into the extracellular milieu. Nevertheless, I sought to characterize the structural organization of pilin in a strain that produces a functional secretion channel but lacks extracellular T-pili. Such strains have been isolated previously in the Christie laboratory as a result of mutations generated in various VirB subunits including VirB6, VirB9, VirB10, and VirB11

Figure 3.3 Disposition of VirB2 in VirB-producing cells and T-pili

(A) Comparison of MPB labeling patterns of Cys-substituted pilins synthesized in the absence ($\Delta virB$) or presence ($\Delta virB2$) of other VirB proteins and Pilins (B2*) carried Cys substitutions at the residues indicated at the tops of the blots. Intact cells and cell lysates were MPB treated and analyzed as described in the text. VirB2 protein abundance in immunoprecipitates was assessed by immunoblot analysis with anti-VirB2 antibodies ($\Delta B2$). Schematic diagrams of MPB labeling patterns are presented below the blots for each strain. Thin lines, hydrophilic loops; gray cylinders, hydrophobic domains; bar, cyclization junction; black-filled circles, MPB labeled upon treatment of intact cells; gray-filled circles, no MPB labeling. IM, inner membrane. Data are presented only for Cys replacements displaying differences in labeling patterns between the two genetic backgrounds. (B) the patterns in an uncoupler mutant (B11-I265T) that does not produce T-pili but is substrate positive. (C) MPB labeling patterns of pilins incorporated into the T-pilus. Corresponding colony immunoblots developed with anti-VirB2 antibodies are shown for each mutant strain. The schematic at the right shows MPB accessibility of Cys residues in the isolated T-pilus. Black and gray circles, accessible and inaccessible residues, respectively.



(69, 82, 87, 123). These Tra^+ , Pil^- mutations are postulated to ‘uncouple’ pathways mediating assembly of the T-pilus and the secretion channel and therefore are termed ‘uncoupling’ mutations. Importantly, mutant strains with the Tra^+ , Pil^- phenotype still require VirB2 for substrate translocation (123), indicating that the pilin is a component of the secretion channel.

I introduced these three Cys-substituted pilin genes into a strain producing a VirB11 mutant (I265T) that confers the Tra^+ , Pil^- “uncoupling” phenotype (87). Upon treatment of these strains, I found that the Cys-substituted pilins exhibited the same MPB-labeling patterns as observed for strains producing native VirB11 together with the other VirB proteins (Fig. 3.3 A and B). The differences in MPB-labeling of Cys51, Cys64, and Cys94 in strains lacking vs. producing other VirB proteins therefore likely reflect differences in structural organization of the pilin when integrated in the membrane vs assembled as a component of the secretion channel.

The T-pilus is the alternative terminal organelle produced during T4SS biogenesis. I sought to examine the pilin structural organization when polymerized as the T-pilus, and to this end I isolated T-pili from the Pil^+ strains producing Cys-substituted pilins. MPB treatment of the isolated T-pili yielded a labeling profile that was in stark contrast to that obtained for the cell-associated pilins. In the T-pilus, Cys residues at positions 64 and 67 in hydrophilic Domain I and position 77 in hydrophobic domain II were labeled (Fig. 3.3 C). Other Cys residues in Domain I (at positions 54, 58, and 119) and Cys94 in Domain III did not MPB label upon treatment of isolated T-pili (Fig. 3.1 B & 3.3 C). These data suggest that hydrophilic and hydrophobic residues 64-77 in Domains I and II, respectively, are surface-displayed in the T-pilus. Other residues in Domain II, and those in Domains III and IV, were MPB-inaccessible and therefore likely buried in packing interfaces or the lumen of the T-pilus.

Discussion

Here, I developed a topology model for the membrane-integrated VirB2 pilin by SCAM. I then used SCAM to identify differences in the structural organization of pilin when it is incorporated as part of the VirB/D4 T4SS machine. My data supplied the first evidence that VirB2 adopts distinct structural states when assembled as a component of the secretion channel vs. the T-pilus. I discuss my findings below in the context of available data on other conjugative pili.

The topology model derived from my MPB labeling studies was for VirB2 pilin produced in the absence of other VirB proteins. The data confirmed and extended previous studies of VirB2 and the related pilins TraA_F and TrbC_{RP4} based on *in silico* secondary structure analyses and PhoA fusion studies (152, 158, 159). Essentially, I found that the two hydrophobic regions (domains II and IV) span the IM, the intervening hydrophilic loop (domain III) is located in the cytoplasm, and a large hydrophilic region comprised of N- and C-terminal hydrophilic residues joined by cyclization (domain I) is located in the periplasm (31, 143, 152). The general model for biogenesis of T4SS pili is that the pro-pilin subunit integrates into the inner membrane and is then processed into the mature pilin. Pilin monomers then accumulate in the membrane until a signal that is currently unknown activates pilin dislocation and subsequent assembly reactions. Although the formation of a pilin pool remains untested for the *A. tumefaciens* VirB/VirD4 T4SS, at this point it is reasonable to assume that the topological profile of pilin synthesized in the absence of other VirB proteins corresponds to that of the pilin pool in wild-type cells. It is important to test the pilin pool model and studies presented in the Future Studies section (see Chapter 7) are designed to evaluate this model.

Contribution of Domains and Residues to VirB2 Function

Mutational studies of VirB2, as well as TraA_F and TrbC_{RP4}, have identified residues generally in the hydrophilic loops that are critical for pilin processing, stability, and function (Fig. 3.4) (160, 161). VirB2 mutations within the signal sequence near the cleavage site disrupt processing of the pro-protein and cyclization (115) and similar results have been seen with TraA_F and TrbC_{RP4} (Fig. 3.4). Here, I found that Cys substitutions near the N-terminus of the mature pilin (Cys51, Cys54) disrupted protein stability (Fig. 3.1) Mutations within both the N- and C-termini of VirB2 that do not appear to affect processing, also resulted in loss of substrate transfer (Cys51, Cys54, Cys58, Cys117, Cys119). Correspondingly, effects on pilin function as monitored by pilus production and transfer

Figure 3.4 Mutations in domains of related pilin subunits have similar effects on function

Comparison of select mutant phenotypes of related pilin subunits: VirB2_{A.t.}, TraA_F, and TrbC_{RP4}. The core pilin sequence for each subunit is shown, including the predicted transmembrane regions (TM). Related pilin subunits show similarities in predicted structure with two hydrophobic regions, a long hydrophilic loop, and a shorter cytoplasmic loop. This summarizes the phenotypes of a subset of point mutations made along the length of VirB2 (Fig.3.1), TraA_F (161), and TrbC_{RP4} (160).

TM
lumen
TM

VirB2: ⁵¹QSAGGG⁵⁴DPATM⁵⁸VNNIC⁶⁴T⁶⁷ILGP⁷¹FGQSLA⁷⁷VLGIVAIGISW⁸¹MF **GRASL** GLVAGVGGIVIMFGASFLGQTL¹¹⁷TGGS¹¹⁹ *

TraA: ⁷AGSSQ¹¹DLMASGNTTV¹⁷KA²³TFGK²⁸SSW³⁴K⁴²WVLA⁴⁶EVLVGAMV⁵²MMT ⁴⁶KNVK⁴⁹ ⁵⁰FLAGFAIISV⁵⁴FLI⁶⁰AVGMAVVGL * * * *

TraB: ³⁷SEGTGGSLP⁴²Y⁴⁷ESWLTNLRNSVT⁵⁹GPVAFALSIIGIVVAGGV⁷⁸IFGGEL NAFFRTL IFLV⁹⁶LMALLVGAQNVMST¹¹⁰FFGRGAEIA¹¹⁹ * * * *

DNA Transfer Defect Italic = lumen * Uncoupler, Pil+ Tra⁻ ↓ Positive-Inside-Rule Residue
Surface Exposed Bold Underline = Hydrophobic Region ● Piliin Stability or Processing

frequencies have been reported for mutations located near the N-termini of mature TraA_F pilin (161) and N- and C-termini of TrbC_{RP4} pilin (160) (Fig. 3.4). Together, these data suggest the hydrophilic domain is important for pilin processing but independently of processing also contributes in unspecified ways to protein function.

My finding that Cys51 and Cys64 residues showed differences in MPB-labeling in the absence and presence of other VirB proteins suggests the periplasmic domain is important for machine assembly, possibly by mediating a critical contact(s) with another VirB subunit(s). In the absence of other VirB proteins, native Cys64 was not labeled in reactions carried out at pH 7.5, but was labeled at pH 9.5 (Fig. 3.2 C). These conditions are expected to favor alkylation of an extramembrane cysteine as well as expose Cys residues buried in secondary structure. At this elevated pH, maleimides can nonspecifically label amine groups(162), but the controls showed that Cys-less VirB2 or derivatives with Cys residues located in the two hydrophobic TM domains did not label. In the absence of other VirB proteins, therefore, Cys64 is probably buried in secondary structure as opposed to associating with or embedding into the membrane. In contrast to Cys64, Cys51 was labeled in a strain lacking other VirB proteins but was not labeled in a strain producing the other VirB proteins. This mutant pilin might adopt a structure rendering Cys51 inaccessible only in the context of the assembled VirB machine. Other T4SS subunits may be shielding MPB-labeling directly or they might indirectly induce a change in the secondary structure of the VirB2 periplasmic loop. However, because the Cys51-substituted pilin is both less stable and also confers a Tra⁻, Pil⁻ phenotype, the observed labeling pattern could reflect an interaction(s) between the mutant pilin and other VirB subunits that perturbs machine assembly or function.

The Cys94 substitution constitutes a topological marker for the cytoplasmic loop, as deduced from its accessibility only in treated cell lysates. Although VirB2 tolerated a L94C substitution in the central hydrophilic loop, other mutations altering positively-charged residues in the central loop of TraA_F disrupted function (160) (Fig. 3.4), consistent with the proposed general importance of a positive charge in this cytoplasmic domain for topological orientation at the IM (163, 164). Interestingly, however, in other studies of VirB2 summarized in Chapter 7, I introduced epitope tags at various sites in the pilin both to identify permissive regions and to facilitate pilin and pilus purification. Although insertions at most sites abolished protein function, a mutant pilin with a FLAG tag (DYKDDDDK) inserted immediately after residue 85 fully supported both pilus biogenesis and substrate transfer. This FLAG-tagged pilin will be the subject of further investigations, but at this

junction it is intriguing to note that this tag is highly negatively-charged and therefore would change the overall net charge of the cytoplasmic domain from positive to negative. The fact that this is a functional protein raises fundamental questions about the requirements for membrane insertion of this pilin and/or the validity of the model that this pilin integrates into the membrane during T4SS biogenesis.

Finally, VirB2 generally tolerated Cys substitutions in both hydrophobic domains, as was also reported for TraA_F (161). However, for both VirB2 and TraA_F, mutations of aromatic (VirB2 F71C; TraA_F F50A, F54V, F60V) or charged (TraA_F E34A) residues in the hydrophobic domains disrupt pilus assembly, DNA transfer, or phage attachment. These mutations could affect membrane insertion of the pilin or packing of hydrophobic helices during assembly of the pilin into the secretion channel or pilus (161) (Fig. 3.4).

Pilus vs. Secretion Channel

The pilin structural organization or the nature of its homo- or heteromeric contacts in the two terminal organelles, the secretion channel and T-pilus, are not defined. At least two lines of evidence suggest that VirB2 pilin assembles not only as the T-pilus but also as a component of the secretion channel. First, VirB2 was shown to form formaldehyde-crosslinkable contacts with translocating T-DNA by use of the transfer DNA immunoprecipitation (TrIP) assay (58). Further TrIP studies with various *virB* mutant strains also suggested that VirB2 is positioned at the distal portion of the secretion channel, probably near the OM (58). Second, several “uncoupling” mutations that selectively block pilus assembly without affecting substrate transfer have been isolated in VirB subunits, e.g., VirB6, VirB9, VirB10, and VirB11 (69, 87, 123). The Tra⁺, Pil⁻ strains harboring these mutations require synthesis of VirB2 for formation of a functional secretion channel, confirming the importance of pilin - not the T-pilus - for substrate transfer. Here, I also isolated the opposite class of “uncoupling” mutation, VirB2 G119C, conferring a Tra⁻, Pil⁺ phenotype (Fig. 3.1). This class of mutations also was isolated in the TrbC_{RP4} (e.g., G114A) (160) and TraA_F (e.g., K49A, F50A, F54A, F60V) (161) pilins (Fig. 3.4). The Tra⁻, Pil⁺ “uncoupling” mutation of VirB2 is located in the C-terminal hydrophilic domain (domain I). In my studies, I determined that Cys94 and Cys119, as well as other Cys substitutions in domain I, are accessible to MPB-labeling, raising the possibility that one or both of these hydrophilic domains are exposed within the lumen of the secretion channel. In addition, I showed that the MPB-labeling patterns of Cys mutants produced in a Tra⁺, Pil⁻ uncoupling mutant strain (VirB11. I265T) (87) matched the isogenic, phenotypically wild-type strain, but

differed appreciably from MPB-labeling patterns of pilins assembled into T-pili (Fig. 3.3). This is further evidence that VirB2 adopts distinct structural states when assembled as a component of the secretion channel vs. the T-pilus. However, deciphering the quaternary structure of VirB2 in the secretion channel is technically challenging and will require further studies of VirB2 binding partner interactions and definition of residues or regions in close contact with translocating substrate.

The T-pilus structure is not yet known, although a structure of the F-pilus has been presented at ~20 Å by cryoelectron microscopy. This structure yielded dimensions for the pilus (8 nm) and interior lumen (30 Å) but was insufficient for definition of the pilin packing geometry (145). The hydrophobic helices of VirB2 and TraA_F likely pack against one another, resulting in exposure of hydrophilic residues on the surface and interior of the respective pili (165). To gain insight into the pilin packing geometry, I analyzed the accessibility of the engineered Cys residues in isolated pili. My accessibility studies identified a surface patch, marked partly by MPB-labeling of Cys64 and Cys67 in hydrophilic domain I (Fig. 3.3 C). Residues 64-69 of VirB2 correspond to residues 17-24 of TraA_F, a region also exposed laterally on the pilus, as shown by bacteriophage binding and antibody labeling of immunodominant epitopes (161, 166) (Fig. 3.4). For both VirB2 and TraA_F, the surface patch extends into hydrophobic domain II, as shown by labeling of Cys77 and phage attachment data for a TraA_F K28 substitution mutant (161). Cys substitutions at residues 51, 71 and 117 blocked pilus assembly, and therefore it is possible that additional residues in domain I of the native protein are also surface-displayed. Cys substitutions of other hydrophobic residues in domains II and IV were inaccessible to MPB and are probably buried in pilin-pilin subunit interfaces.

It is interesting to note that hydrophobic domain IV possesses a GG₄ dimerization motif (167, 168) (Fig. 3.5). This motif has been shown to be important for stabilizing intermolecular helix-helix interactions (169, 170) as well as for stabilizing folding of certain protein monomers (171-173). In addition, I. Garza in the Christie lab identified a glycine zipper motif (G-XXX-G-XXX-G) within domain IV (Fig. 3.5). This motif has also been shown to mediate helix-helix interactions (174). Conceivably, the GxxxG dimerization motif or the glycine zipper mediates formation of domain IV helix – helix interactions among adjacent VirB2 pilins in the assembled T-pilus.

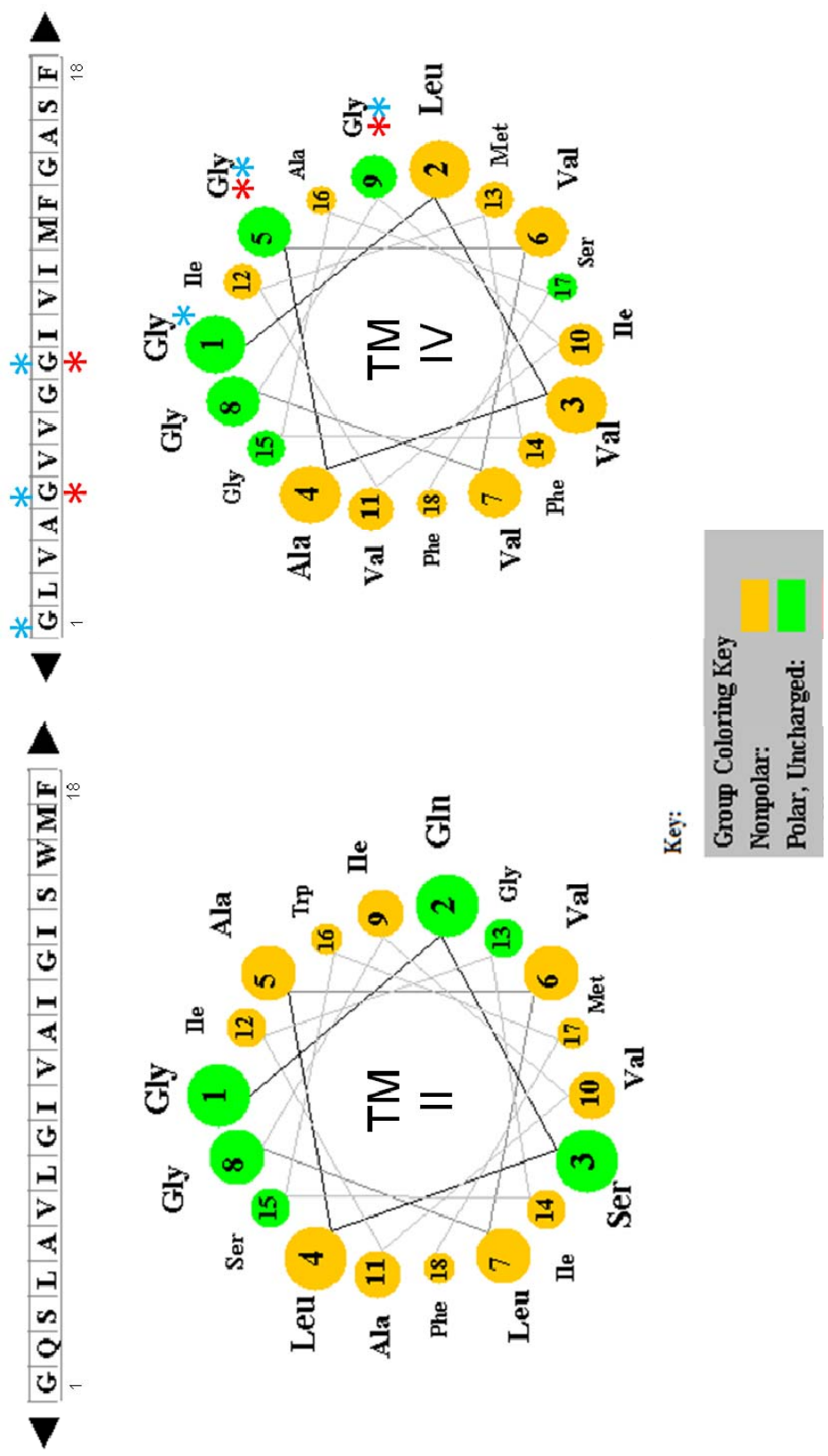
Cys94 in the hydrophilic central loop did not label and might reside in the interior of the T-pilus, as also proposed for TraA_F in the F pilus (165, 175). Interestingly, TraA_F can

Figure 3.5 Helical wheel representations of VirB2 transmembrane helices, regions II and IV

Helical wheel patterns shown for VirB2 regions II and IV defined by MPB-labeling shown in figure 3.1D. Red asterisks denote the predicted GG₄ dimerization motif (Gly-X-X-X-Gly) in VirB2 domain IV. Blue asterisks denote the predicted glycine zipper motif (G-XXX-G-XXX-G) identified by I. Garza. This figure is modified from a screen capture of the Java Applet written by Edward K. O'Neil and Charles M. Grisham (University of Virginia in Charlottesville, Virginia).

The applet is available at:

<http://cti.itc.Virginia.EDU/~cmg/Demo/wheel/wheelApp.html>.



accommodate epitope tags at its C terminus without loss of pilus assembly, and these epitopes are surface displayed (161, 166, 175). By contrast, VirB2 G119C was inaccessible to MPB, suggesting that it is buried in pilus. I have been unable to generate functional forms of VirB2 pilin with epitope tags inserted at the C terminus probably because these tags disrupt one or more of the cyclization, folding, or oligomerization reactions.

The absence of Cys77 labeling upon treatment of intact cells is consistent with previous findings for this T4SS and the RP4 conjugation system that few T-pili remain attached to cells (104, 115). Additionally, at this time there are two general models describing the mechanism of pilus assembly: i) the T-pilus might assemble from an IM VirB-platform such that the pilus extends across the periplasm and OM, or ii) the T-pilus might assemble from a VirB platform at the OM in which case no pilus polymer would project through the periplasm. My inability to detect Cys77 labeling in intact cells, a diagnostic for T-pilus polymerization, is more consistent with the latter scenario. This is of particular interest in view of properties that have been ascribed to T-pili and related conjugative pili. Unlike the F-pilus, which dynamically extends and retracts to mediate mating pair formation in liquid media, T-pili and related pili are sloughed or broken from the cell surface and readily form bundles in solution. The released T-pili are thought to promote nonspecific cell-cell aggregation and formation of mating junctions with target cells(116). I gained evidence that VirB2 assembles in the T-pilus in a way that exposes hydrophobic residues in domain II. This patch of surface hydrophobicity along the length of the T-pilus could account for pilus bundling and pilus-mediated aggregation and mating pair formation.

In conclusion, this work provided the first detailed analysis of the inner membrane topology of VirB2, showed that VirB2 forms distinct structural states as part the secretion channel and T-pilus, and presented new information about the potential packing arrangement of VirB2 in the T-pilus.

Chapter 4: VirB4 and VirB11 ATPases Modulate the Structural State of Membrane-Integrated VirB2 Pilin During Biogenesis of the VirB/D4 Type IV Secretion System

NOTE: This chapter is derived from work that has, for the most part, been published in 2010: "Evidence for VirB4-mediated dislocation of membrane-integrated VirB2 pilins during biogenesis of the Agrobacterium VirB/VirD4 type IV secretion system." Journal of Bacteriology 192(19): 4923-34 PMID: 2065690. I am the primary author on this paper. I performed all experiments described in this chapter. I have been given permission by the publisher of Journal of Bacteriology, the American Society for Microbiology, to reproduce any/all of my manuscript in print or electronically for the purposes of my dissertation (License Number 2501460079655).

Introduction

VirB2 pilin is required for elaboration of the T4SS channel and the extracellular T-pilus (25, 128). The VirB2 propilin is processed in two successive steps involving cleavage of its signal sequence and covalent linkage of the N- and C-terminal residues to form a cyclic polypeptide, and the mature pilin is inserted into the inner membrane by a sec-independent mechanism presumptively as a pool for use in T4SS machine assembly (117). Little is known about the movement of VirB2 from its inner membrane location to its site of assembly in the secretion channel and the extracellular T-pilus. A proposed general feature of T4SS biogenesis is that ATP energy is used to drive pilin extraction and subsequent polymerization reactions. Although three ATPases, VirB4, VirB11, and VirD4, are required for elaboration of a functional T4SS channel, only VirB4 and VirB11 are required for T-pilus assembly (104).

Both VirB4 and VirB11 contain the conserved Walker A nucleoside triphosphate (NTP) binding motif (GxxGxGKT/S) (90, 133). Mutations in the Walker A binding pocket of VirB4 and VirB11 do not produce T-pili (Pil⁻) and are unable to transfer substrate (Tra⁻), establishing the importance of NTP energy use for T4SS assembly (89, 106, 133). All T4SSs described to date contain a VirB4-like ATPase, while VirB11-like ATPases are widespread but not universal (15). Interestingly, conjugative pili, produced by the *Escherichia coli* F-like plasmids, actively extend and retract by a process that requires the VirB4 homolog TraC; yet, these T4SSs lack a VirB11 homolog (15). These observations prompted a hypothesis that VirB4-like subunits drive early steps associated with conjugative pilus biogenesis. However, the specific contributions of each of these ATPases in relation to pilin movement remain to be defined.

The question of how pilin monomers of T4SSs as well as other pilus biogenesis systems are extracted from the inner membrane to build the pilus is not understood. To begin to address this question, we asked whether the VirB ATPases induce structural changes in membrane pilin as monitored with the scanning cysteine accessibility method (SCAM) (146). SCAM has been used not only to verify predicted membrane protein topologies but also to study structure–function relationships and the dynamics of protein function (153, 155, 176-179). In this study, I further defined the requirements for assembly of the mature, membrane-integrated pilin into the VirB/D4 channel and T-pilus. My findings support a model that the VirB4 ATPase functions as a pilin dislocase to extract VirB2 from the inner membrane during machine biogenesis. This function might be a universal feature of the broadly conserved VirB4 ATPase superfamily.

Results

In the preceding chapter, I reported differences in MPB-labeling of Cys51, Cys64, and Cys94 substitution mutations in the presence versus absence of VirB proteins. I proposed that labeling of Cys94 in the presence of VirB proteins was due to a structural change in the pilin that exposed the cytoplasmic domain to the periplasm, a change consistent with membrane extraction. To examine the hypothesis that one or both of the VirB4 and VirB11 ATPases is responsible for Cys94 labeling, I carried out Cys accessibility studies with strains engineered to co-produce Cys-substituted pilins together with i) one or both ATPases or ii) Walker A motif mutants, both in the presence and absence of other VirB proteins.

VirB4 ATPase Influences MPB-labeling Patterns of Membrane Pilin

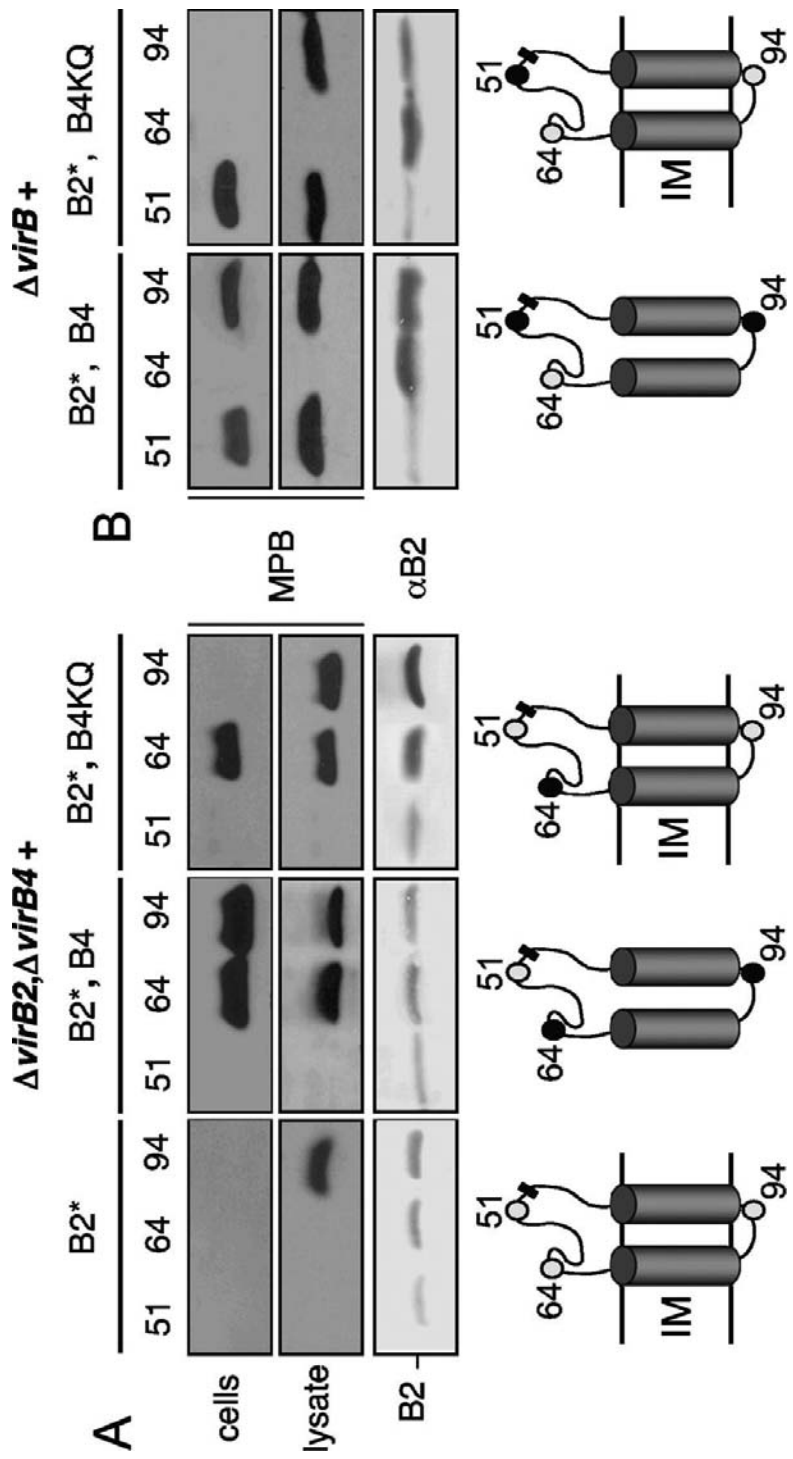
I first assayed for MPB-labeling of Cys-substituted pilins in a $\Delta virB4$ mutant (Fig 4.1A). Interestingly, I found that Cys94 was labeled in a *virB4* null mutant complemented with a plasmid expressing wild-type *virB4*, but was not labeled in the *virB4* null mutant strain or the isogenic strain producing the VirB4 K439Q Walker A mutant. Previous studies have shown that the complemented *virB4* mutant strains produce abundant levels of native VirB4 or the K439Q mutant and exhibit the expected WT (Tra⁺, Pil⁺) and null (Tra⁻, Pil⁻) phenotypes, respectively (133). In addition, the Christie lab has shown that Cys replacements in cytoplasmic domains of VirB6 (65) and VirB10 (69) are not labeled upon MPB treatment of whole cells. Strains producing the Cys-substituted VirB6 and VirB10 proteins synthesized native VirB4, excluding the possibility that this ATPase generally disrupts the inner membrane integrity or otherwise conveys MPB across the cytoplasmic membrane. I conclude that VirB4 with an intact Walker A motif is required for MPB-labeling of Cys94-substituted VirB2.

Cys64 also was labeled in a strain producing native VirB4 but not the isogenic *virB4* null mutant strain (Fig. 4.1A). However, in contrast to Cys94, Cys64 was labeled in a strain producing the VirB4 Walker A mutant, suggesting that accessibility was dependent on VirB4 production but not on ATP hydrolysis. Importantly, steady-state levels of the VirB2 Cys mutants were unaffected by the absence of native or mutant forms of VirB4.

The above findings prompted a test of whether VirB4 similarly would affect MPB-labeling in the absence of other VirB proteins. As shown in Fig. 4.1B, Cys94 was labeled in a $\Delta virB$ operon mutant producing only VirB4, but not in the isogenic strain lacking VirB4 or

Figure 4.1 Effects of VirB4 ATPase on MPB labeling patterns of pilins

(A) Cys-substituted pilins synthesized in strain JK1204 deleted of native *virB2* and *virB4* (nonpolar $\Delta virB2$, $\Delta virB4$). (B) Cys-substituted pilins produced in strain PC1000 ($\Delta virB$ operon mutant). JK1204 and PC1000 were engineered to synthesize mutant pilins (B2*) with Cys substitutions at the residues indicated at the tops of the blots alone or with native VirB4 (B4) or a Walker A mutant (KQ) derivative. Panels showing MPB labeling patterns, VirB2* abundance in the immunoprecipitates. Schematic diagrams of MPB labeling patterns are presented below the blots for each strain. Thin lines, hydrophilic loops; gray cylinders, hydrophobic domains; bar, cyclization junction; black-filled circles, MPB labeled upon treatment of intact cells; gray-filled circles, no MPB labeling. IM, inner membrane. Data are presented only for Cys replacements displaying differences in labeling patterns among the strains analyzed.



producing the K439Q Walker A mutant. By contrast, Cys64 was not labeled in the $\Delta virB$ mutant background regardless of the presence of VirB4, showing that VirB4 promotes MPB-labeling of this periplasmic residue only in the presence of other VirB proteins (Fig. 4.1A). Cys51 was labeled only in the absence of other VirB proteins, and labeling was not altered by the absence or presence of VirB4 alone (Fig. 4.1B).

Together, these findings indicate that VirB4 exerts an ATP-dependent change in the accessibility of the region of VirB2 marked by Cys94, and that VirB4 also exerts an ATP-independent structural change in the region marked by Cys64 but only in the presence of other VirB proteins.

VirB11 ATPase Influences Membrane Pilin Disposition

I next assayed for effects of the VirB11 ATPase on MPB-labeling of Cys-substituted pilins. I observed that Cys94 was MPB-labeled in a $\Delta virB11$ mutant, in agreement with the above proposal that VirB4 alone (among the T4SS ATPases) is responsible for catalyzing the structural change required for labeling of this cytoplasmic residue. I did observe, however, that production of native VirB11 was required for labeling of Cys64. Cys64 was not labeled in a $\Delta virB11$ mutant or an isogenic strain producing a VirB11 Walker A mutant (Fig. 4.2A). These findings suggest that Cys64 accessibility is dependent on VirB11 ATP energy binding or hydrolysis activities.

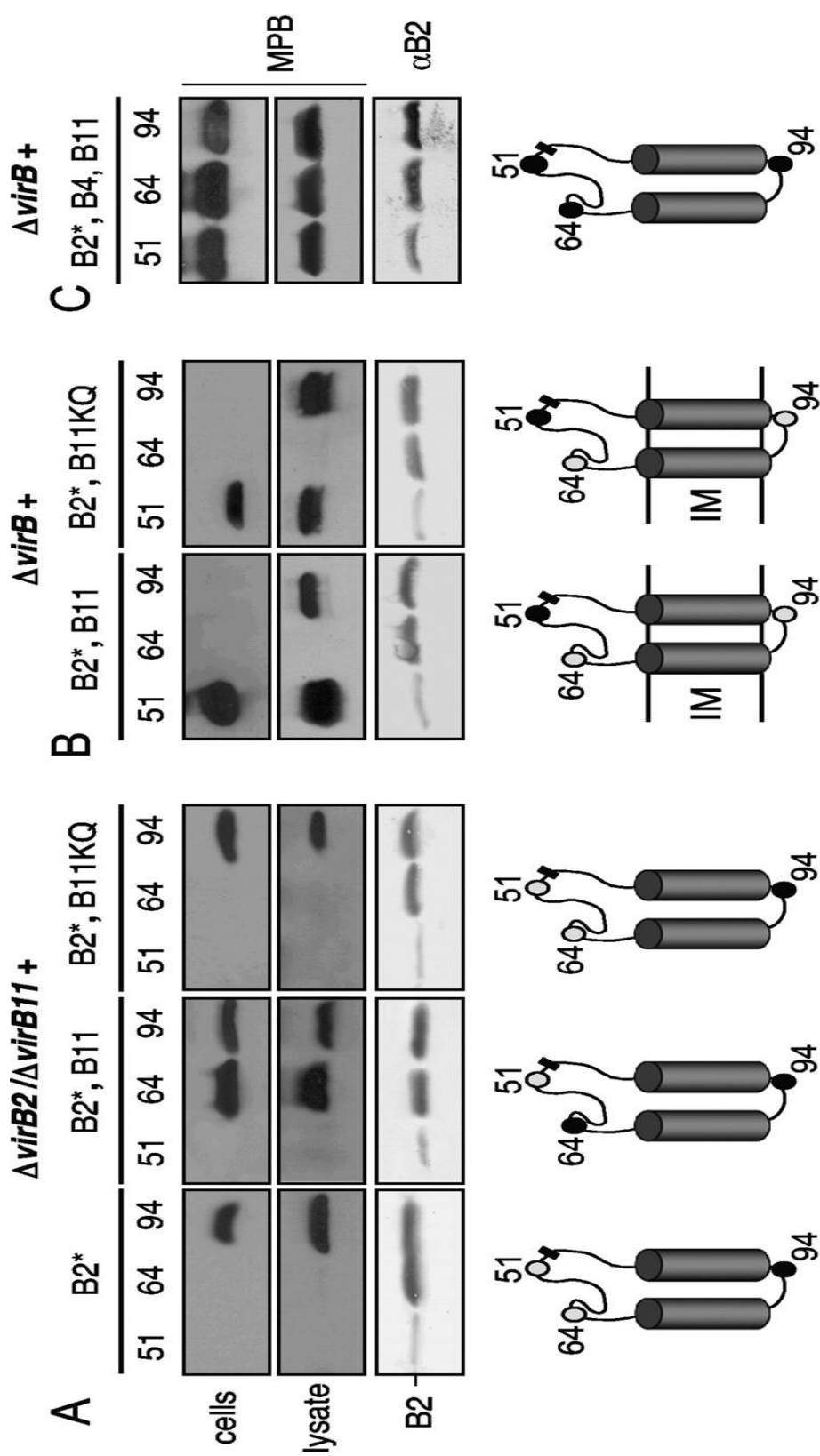
To determine whether the VirB11-dependent effect on MPB-labeling of Cys64 requires the other T4SS proteins, I compared MPB-labeling patterns for VirB2 synthesized in a $\Delta virB$ operon mutant or this strain engineered to co-produce only native VirB11 or the VirB11 K175Q Walker A derivative (Fig. 4.2 B). Cys64 was not labeled in any of these strains, suggesting that VirB11 requires at least one other VirB protein to catalyze a structural change necessary for Cys64 labeling.

VirB4 and VirB11 Act Synergistically to Direct Structural Differences in Membrane-Associated Pilin

In the above studies, I assayed for effects of each ATPase on pilin structure as monitored by SCAM. Next, I sought to determine whether the two ATPases act together to induce structural changes in the cell-associated pilin. To examine this possibility, a $\Delta virB$ operon strain lacking other VirB proteins was engineered to coproduce the VirB2 Cys mutants with VirB4 and VirB11.

Figure 4.2 Effects of VirB11 ATPase on MPB labeling patterns

Effects of VirB11 ATPase synthesis on MPB labeling patterns of pilins. (A) Cys-substituted pilins synthesized in strain PC1211 (nonpolar $\Delta virB2$, $\Delta virB11$). (B and C) Cys-substituted pilins produced in strain PC1000 ($\Delta virB$ operon mutant). PC1211 and PC1000 were engineered to synthesize mutant pilins (B2*) with Cys substitutions at the residues indicated at the tops of the blots alone or together with VirB11 (B11), a VirB11 Walker A mutant (KQ) derivative, or both native VirB11 and VirB4. Panels showing MPB labeling patterns, VirB2* abundance in the immunoprecipitates, and schematic representations of the labeling patterns are as described in the Fig. 4.1 legend. Data are presented only for Cys replacements displaying differences in labeling patterns among the strains analyzed.



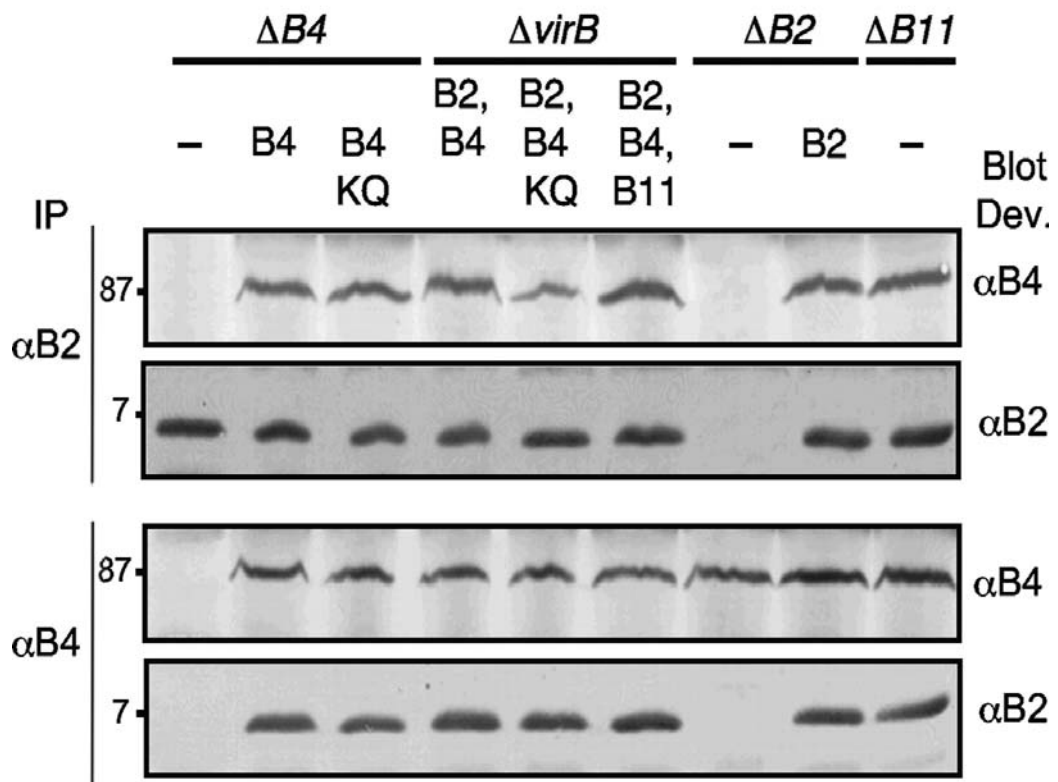
Interestingly, both Cys64 and Cys94 were MPB-labeled when the mutant pilins were co-synthesized with VirB4 and VirB11 but no other VirB proteins (Fig. 4.2C). Labeling profiles of these residues were therefore identical in strains producing just the VirB ATPases or strains producing all of the VirB proteins (see Fig. 4.1A, 4.2A). These findings indicate that VirB4 and VirB11 together coordinate structural changes in pilin necessary for labeling of Cys64 and Cys94, even in the absence of other VirB subunits. However, it is also noteworthy that Cys51 was labeled in the absence of VirB proteins, and synthesis of VirB4 and VirB11 in this background did not alter the labeling pattern (Fig. 4.2C). Synthesis of other VirB proteins thus appears to be necessary for a structural change in the pilin to render Cys51 inaccessible to MPB-labeling.

VirB2 and VirB4 Form a Precipitable Complex

The above findings suggest that VirB2 interacts with one or both of the VirB ATPases at the inner membrane. I assayed for complex formation between VirB2 and both VirB ATPases by immunoprecipitation. To stabilize possible interactions, I treated isolated membranes with the crosslinker dithiobis succidimidyl propionate (DSP) prior to solubilization with RIPA buffer (Containing detergents - 0.1% SDS, 0.5% sodium deoxycholate, 1% NP-40). As shown in Fig. 4.3, anti-VirB2 antibodies coprecipitated VirB2 and VirB4 from membrane extracts of strains producing both proteins both in the presence and absence of other VirB proteins. VirB2 also formed a precipitable complex with the VirB4 Walker A motif mutant, suggesting that ATP binding/hydrolysis is not required for this interaction. In control experiments, anti-VirB2 antibodies did not precipitate VirB4 from extracts of a $\Delta virB2$ mutant, nor was an immunoreactive species the molecular size of VirB4 (87-kDa) precipitated from a $\Delta virB4$ mutant. I attempted but was unable to detect VirB11 in immunoprecipitates recovered with anti-VirB2 antibodies from membrane extracts of VirB11-producing strains. VirB11 thus might exert an effect on VirB2 structure through transient or weak affinity interactions, either directly with the pilin or indirectly through a VirB4 contact. Together, these results suggest that VirB2 does interact in an energy independent fashion with VirB4. Although other VirB proteins are not required for VirB2-VirB4 complex formation, my present findings do not exclude the possibility that another non-VirB protein could mediate this interaction.

Figure 4.3 VirB protein complexes

VirB protein complexes isolated from detergent-solubilized membrane extracts by immunoprecipitation (IP) with anti-VirB2 or anti-VirB4 antiserum. Strains: $\Delta virB4$, PC1004; $\Delta virB2$, JK1002; $\Delta virB$ operon, PC1000; $\Delta virB11$, PC1011 (engineered to synthesize the VirB proteins indicated in addition to those produced from the Ti plasmid). B2, VirB2; B4, VirB4; B4KQ, VirB4K439Q; B11, VirB11. Anti-VirB2 ($\Delta B2$) and anti-VirB4 ($\Delta B4$) antibodies were used for immunoprecipitation (IP) (left) and development of immunoblots (Blot Dev) (right).



VirB4 Domains Exposed in Periplasm

If VirB4 interacts directly with VirB2, it would need to interact with the inner membrane. In early studies, the Christie lab supplied evidence that VirB4 tightly associates with the membrane (180). By PhoA fusion reporter and proteinase K digestion analyses, evidence was also presented for an extracytoplasmic domain(s) of VirB4 (105). Native VirB4 possesses 9 Cys residues, and one of these, Cys57, is predicted to reside in the periplasm on the basis of the earlier reporter fusion studies (105). Interestingly, I found that VirB4 was MPB-labeled both in the presence and absence of other VirB proteins (Fig. 4.4). Moreover, a Walker A motif, mutant form of VirB4 was also MPB-labeled, suggesting that VirB4 spans the inner membrane independently of its catalytic activity. I also detected increased labeling in cells treated with MPB during sonication, consistent with labeling of additional Cys residues located in the cytoplasmic domain. In future studies, it should be feasible to localize the region of VirB4 that interacts with VirB2 through a combination of MPB labeling studies to refine the VirB4 topology model and disulfide crosslinking studies with Cys-substituted binding partners.

VirB4-Mediated Release of Membrane Pilin

To further evaluate a model that VirB4 interacts with VirB2 pilin to catalyze its dislocation from the inner membrane, I assayed for VirB4-dependent release of VirB2 during osmotic shock. I detected appreciably more VirB2 in the shockate of strains producing native VirB4 than strains lacking this ATPase. Additionally, VirB4 alone among the VirB proteins sufficed for release of VirB2 into the shockate fraction (Fig. 4.5A). A VirB4 Walker A mutant did not mediate release of VirB2 into the shockate fraction, consistent with the notion that VirB4 catalyzes VirB2 dislocation by an ATP-dependent mechanism. Furthermore, VirB2 was barely detectable in the shockates of strains producing VirB11 and VirB2 alone, further demonstrating VirB11 does not liberate VirB2 from the membrane.

To confirm that osmotic shock did not result in massive cell lysis or that VirB4 did not somehow disrupt the integrity of the inner membrane, shockates were analyzed for the presence of periplasmic (ChvE) and cytoplasmic (VirE2) markers (Fig. 4.5A), outer membrane markers (VirB7) and inner membrane markers (VirB10, VirB11) (Fig. 4.5B). The VirE2 secretion substrate was present in low amounts in the shockate and levels were independent of the presence of the VirB T4SS as shown previously (47, 181). ChvE was also present at low levels in the shockate fractions of strains producing or lacking VirB4. Inner membrane markers, VirB10 and VirB11 (69, 90), were readily detectable in the cell

Figure 4.4 MPB labeling of VirB4

MPB labeling patterns of native cysteine residues in ATPase VirB4. VirB4 synthesized in strain PC1004 (nonpolar $\Delta virB4$). Wild type VirB2 pilin (B2) and VirB4 or VirB4 Walker A mutant (KQ) derivative produced in strain PC1000 ($\Delta virB$ operon mutant). Panels showing MPB labeling patterns in whole cells and cell lysates following sonication and VirB4 abundance in the immunoprecipitates.

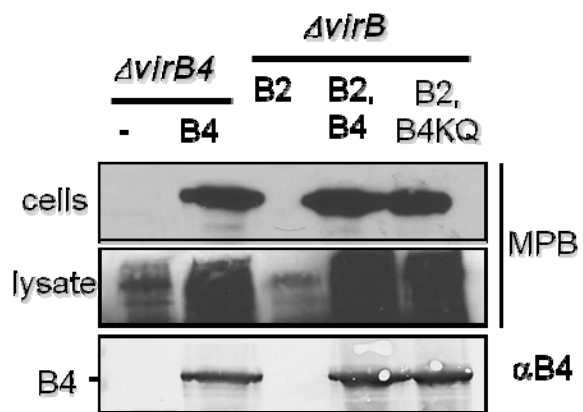
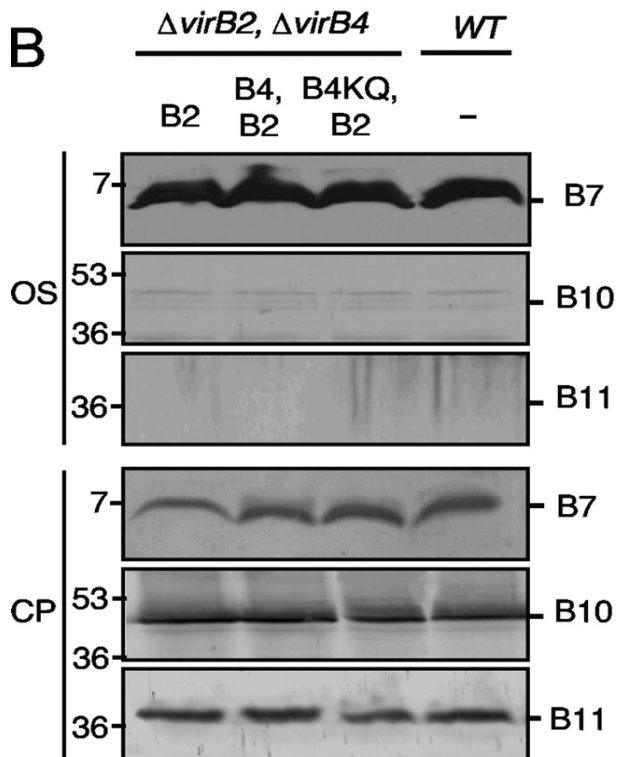
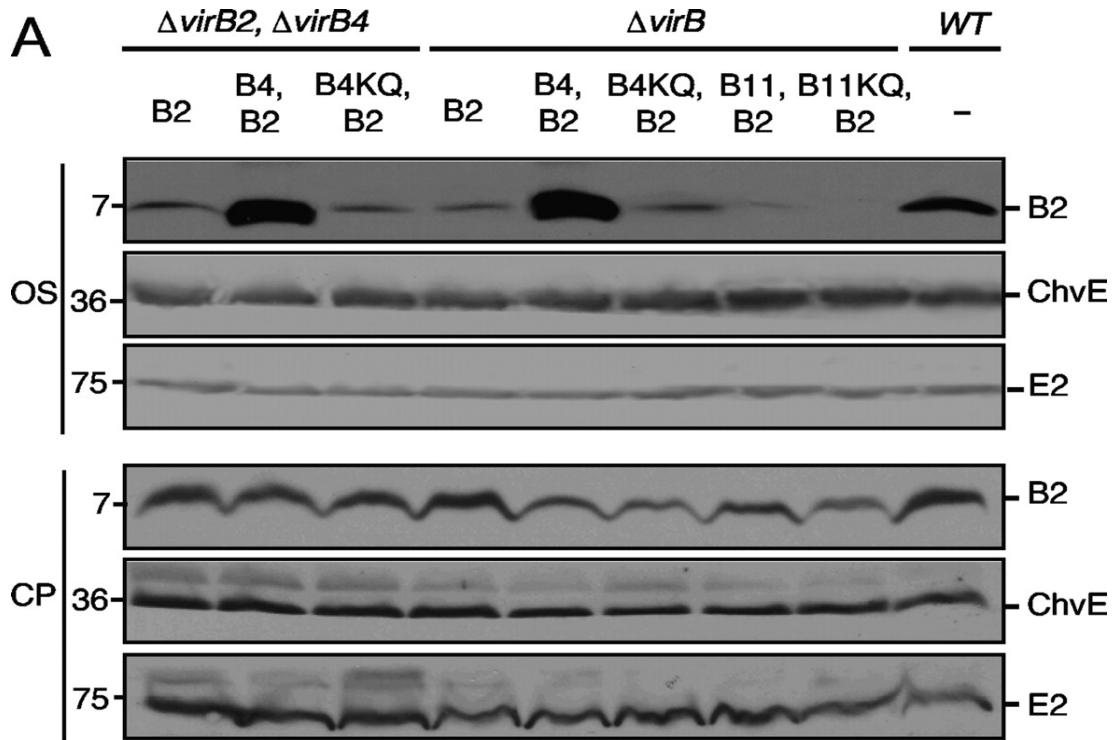


Figure 4.5 VirB4-mediated release of VirB2 upon osmotic shock treatment

Osmotic shock treatment, showing the presence of proteins indicated at the right in material released by osmotic shock (OS) or in the cell pellet (CP) obtained from centrifugation of shocked cells. (A) Detection of VirB2, periplasmic ChvE, and cytoplasmic VirE2. (B) Detection of outer membrane protein VirB7 and inner membrane proteins VirB10 and VirB11. Strains: $\Delta virB2 \Delta virB4$, JK1204; $\Delta virB$, PC1000; WT, A348 (engineered to synthesize the VirB proteins listed in addition to those produced from the Ti plasmid). B2, VirB2; B4, VirB4; B4KQ, VirB4K439Q; B11, VirB11; B11KQ, VirB11K175



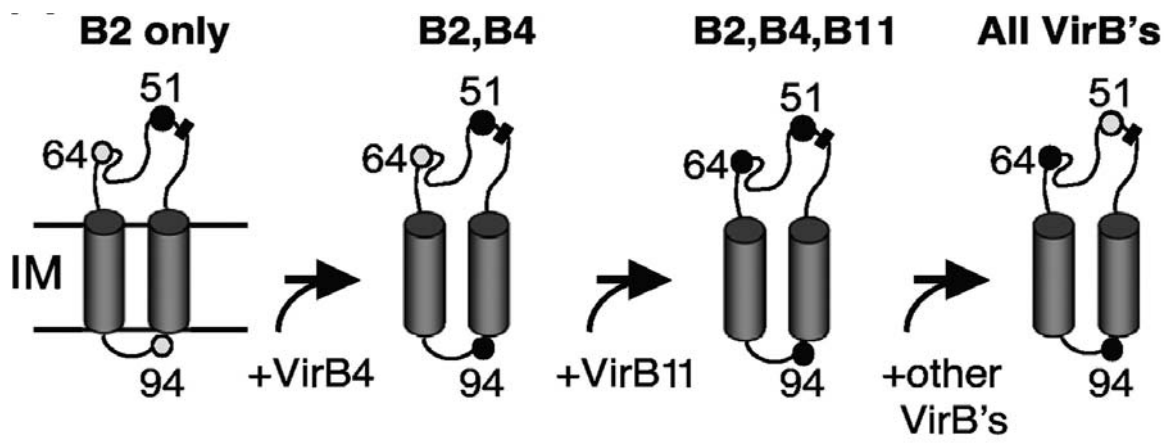
pellets, but not in the shockate fractions. Finally, VirB7 levels were comparable in shockates from all strains. The shockate fractions thus are comprised predominantly of periplasmic material and OM fragments. These findings further support the proposal that VirB4 catalyzes release of VirB2 pilin from the inner membrane.

VirB/D4 Type IV Secretion System Assembly Pathway

Together, results of my studies indicate that VirB4 catalyzes dislocation of the VirB2 pilin early during biogenesis of this T4SS. VirB11 also coordinates with VirB4 to coordinate a structural change(s) in the pilin (Fig. 4.6). Summarizing the proposed steps of pilin maturation: i) VirB11 functions in concert with VirB4 to induce a structural change in membrane-integrated pilin (as shown by labeling of Cys64), ii) VirB4 then liberates VirB2 from the membrane (as shown by Cys94 labeling), and iii) the pilin makes further contacts with remaining VirB proteins to form the secretion channel or T-pilus (resulting in blocking of Cys51 labeling).

Fig 4.6 Schematic summarizing effects of VirB4, VirB11, and other VirB subunits on MPB labeling patterns

MPB labeling patterns are presented. Thin lines, hydrophilic loops; gray cylinders, hydrophobic domains; bar, cyclization junction; black-filled circles, MPB labeled upon treatment of intact cells; gray-filled circles, no MPB labeling. IM, inner membrane.



Discussion

Biogenesis of the VirB/D4 T4SS requires maturation of VirB2 pilin in several steps. The early reactions (signal recognition and cleavage, head-to-tail cyclization, membrane insertion) occur independently of other VirB subunits, whereas subsequent reactions (membrane extraction, incorporation into a functional secretion channel, T-pilus polymerization) require the remaining 10 VirB subunits. To begin defining the mechanistic details underlying these latter *virB*-dependent reactions, I used SCAM to monitor changes in VirB2 pilin. Here, SCAM studies identified effects of the VirB4 and VirB11 ATPases on the pilin structural state. Complementary coimmunoprecipitation and osmotic shock data further supported a model that VirB4 catalyzes dislocation of mature pilin from the IM through direct protein-protein contact and by a mechanism requiring an intact Walker A motif. VirB11 ATPase also contributes to the pilin structural organization, although probably indirectly through a functional interaction with VirB4.

Early studies established the importance of the VirB4 and VirB11 ATPases for assembly of both the secretion channel and T pilus (87, 89, 112, 133, 180), but how these subunits convert chemical energy derived from ATP hydrolysis into mechanical energy for machine biogenesis has remained poorly understood. Here, I showed that VirB4 induces a structural change in VirB2 resulting in MPB accessibility of a Cys substitution located in a cytoplasmic loop (fig 4.1). Importantly, Cys residues located in other cytoplasmic protein domains did not label in any VirB4 producing strains, implying that MPB inner membrane permeability was unaffected by the presence of this ATPase. Thus, I suggest that exposure of Cys94 is the result of VirB4 catalyzing extraction of pilin subunits from the inner membrane into the periplasm. VirB4-mediated Cys94 accessibility and VirB2 release into the shockate fraction required an intact Walker A motif and occurred independently of other VirB proteins, indicating that VirB4 alone catalyzes the observed structural changes by a reaction dependent on ATP binding or hydrolysis. In this study, I examined the Walker A box mutation at K439Q, which has previously been shown to be defective for pilus biogenesis and substrate transfer (106, 133), with similar mutations in VirB4 homologs (*TrbE_{RP4}* and *TrwK_{R388}*) blocking protein function. Interestingly, however, a previous study reported that a different Walker A variant of VirB4_{At} (K439R) from that used here blocked substrate transfer but still elaborated T-pili albeit at low levels (122). The K439R Walker A mutation, which has not been biochemically characterized, is less disruptive structurally than the K439Q mutation and maintains the charge of the binding pocket. Thus, the mutant protein might hydrolyze ATP at levels sufficient for some pilus production. Coupled with

evidence that VirB4 forms a precipitable complex with VirB2 (Fig 4.3) presumably through contacts with VirB4 in the transmembrane region and/or periplasm (Fig 4.4 and (105)), our findings support a working model that VirB4 functions as a dislocation motor to catalyze extraction of pilin subunits from the IM during T4SS biogenesis.

As noted earlier, VirB4-like subunits are signatures for all bacterial and archaeal T4SS (15), and for the F-like T4SS's VirB4-like subunits are the only ATPases required for extracellular elaboration of pilin (182-185). Earlier studies have shown that there are ATPases capable of membrane protein extraction/dislocation (186, 187). The VirB4 ATPases possess physical properties consistent with another well-characterized dislocase, *E. coli* FtsH (186). *A. tumefaciens* VirB4 associates integrally with the IM via one or two membrane-spanning domains (Fig 4.4 and (105)). Other VirB4-like ATPases such as TraC_F, TraB_{pKM101} and TrwK_{R388} also associate with the membrane, although soluble forms of native or mutant forms of these proteins also exist (110, 182, 188). A C-terminal domain of VirB4 also was shown to possess limited sequence homology with the TrwB_{R388} substrate receptor (108), and on this basis the VirB4 C-terminal domain was predicted to assemble as homohexameric rings. In agreement, VirB4 was found to form oligomers under native conditions consistent with the size of a hexamer (122). Moreover, hexameric forms of both TraB_{pKM101} and TrwK_{R388} were detected upon size fractionation of purified forms of these proteins (109, 110). Hexameric but not other oligomeric forms of these ATPases, e.g., dimers, were shown to hydrolyze ATP (110). Lastly, VirB4-like subunits have been found to play a critical role in key protein interactions of the T4SSs (110, 122, 189). Specifically, VirB4_{At} has been shown to interact with ATPases VirB11 and VirD4 (45), bitopic proteins VirB8 (122, 190) and VirB10 (190), and the inner membrane protein VirB3 (66, 189). Taken together, these attributes are consistent with known protein dislocase/protease FtsH and the GspE ATPases predicted to function as pilin dislocases in type IV pilus systems (186, 187, 191, 192). GspE ATPases undergo dynamic changes in structure following ATP hydrolysis (191). While VirB11 is related in sequence to the GspE ATPases, I supplied evidence that VirB4 functions as a VirB2 dislocase. Yet, I also showed that VirB11 coordinates with VirB4 to effect a change in pilin structural organization, as monitored by labeling of Cys64 (Fig. 4.2). Previous work has shown that these two ATPases interact (45) and therefore it is possible that VirB11 acts through VirB4 to induce a structural modification in the pilin periplasmic domain required for subsequent contacts with other assembly factors in the periplasm or at the outer membrane (see below).

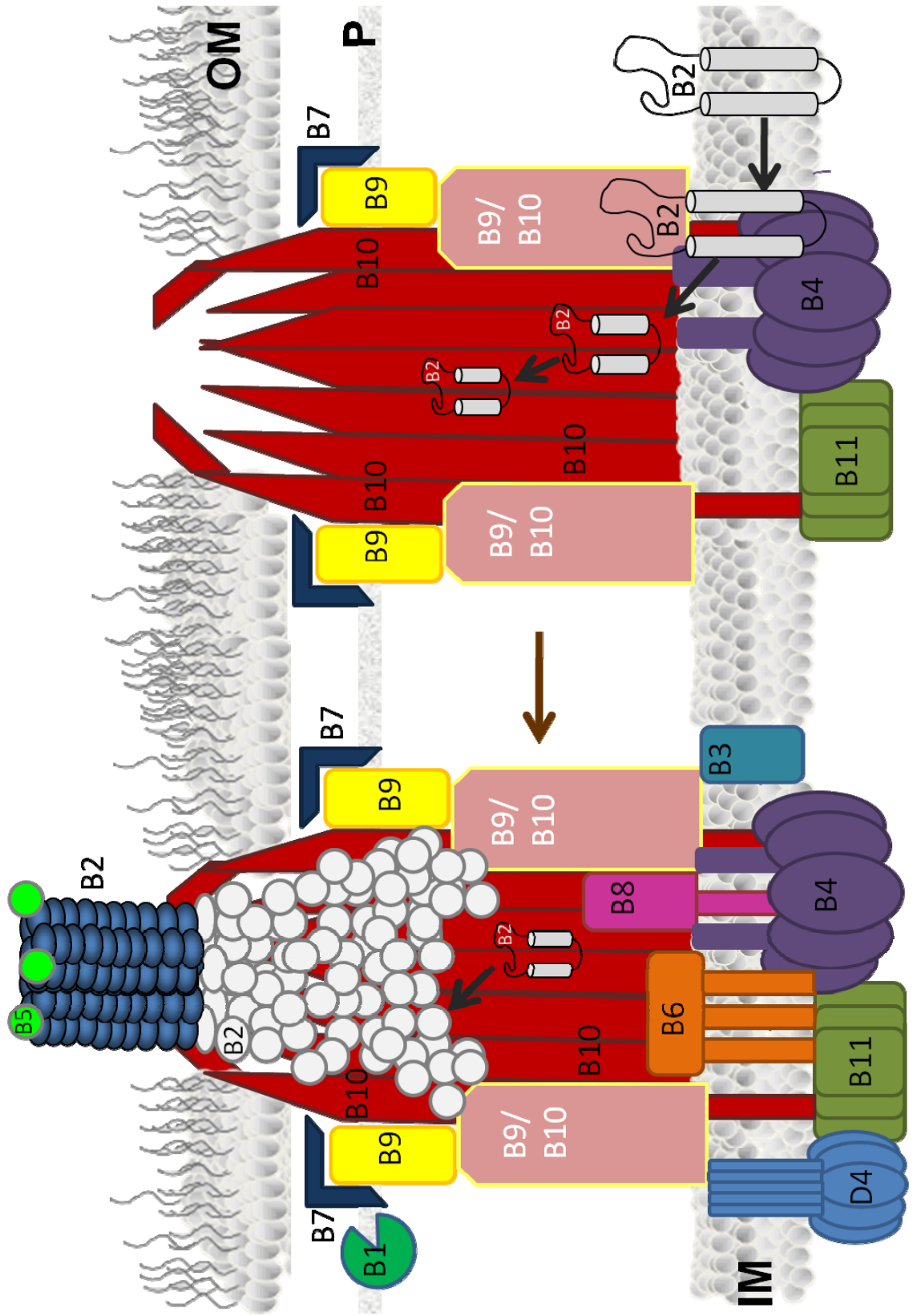
Interactions between the VirB2 pilin and the VirB ATPases have not been previously reported. Here, I supplied evidence for complex formation between VirB2 and VirB4 by coimmunoprecipitation (Fig. 4.3). Furthermore, I showed that VirB4 is MPB-labeled upon treatment of whole cells (Fig 4.4) indicating that at least a portion of the protein is exposed to the periplasm, in agreement with previous studies (105). Presumably, the membrane-spanning or periplasmic domains of VirB4 interact with the membrane-integrated pilin, and further studies in the Christie lab are evaluating this possibility. Small integral membrane proteins, often homologs/orthologs of VirB2_{At} pilin, are commonly found upstream of *virB4* loci (15). Thus, complex formation and/or interaction between VirB4-like ATPases and associated pilin-like subunits may represent a general characteristic of T4SSs.

I propose that a VirB4 dislocase directs an early step in T4SS machine biogenesis. VirB4 forms stabilizing interactions with other inner membrane subunits including VirB3 and VirB8 (66, 122, 189, 190). Furthermore, in agreement with our findings, VirB4 was shown to be required for assembly of a cell-associated complex of VirB2 and the pilus-associated protein VirB5 (122). Although no other VirB2 binding partners have been identified besides VirB4 (this study, Fig. 4.4) and VirB5 (122), a VirB5 interaction with the periplasmic domain of VirB8 was identified (122). In view of this emerging protein-protein interaction network, a model can be proposed wherein VirB11 modulates VirB4 which then functions in the context of a VirB3/VirB4/VirB8 ternary complex to dislocate VirB2. The membrane-extracted VirB2 then interacts with VirB5 to mediate binding with VirB8 (77), which has been postulated to function as an assembly center for building of the VirB/D4 T4SS at specific sites on the cell envelope. Presumably this network of interactions involving VirB2, VirB3, VirB4, VirB5, and VirB8 occurs within the VirB7/VirB9/VirB10 core complex allowing for further protein interactions necessary for pilin subunits to form the distal portion of the secretion channel (58, 87) and polymerize into the T-pilus (Fig 4.7).

My findings add new mechanistic detail to the VirB/VirD4 T4SS biogenesis pathway, and raise the possibility that VirB4 family members function generally as T4SS-specific membrane protein dislocases. Overall, a mechanistic understanding of the T-pilus assembly pathway will provide targets for development of inhibitory compounds that specifically block individual steps of pilus biogenesis. Information about this system also may guide studies exploring the assembly pathways of phylogenetically distinct pilus systems.

Fig 4.7 Model of T-pilus biogenesis pathway

The VirB1-VirB11 and VirD4 type IV secretion system (T4SS) components are shown according to their proposed localization and interactions. Black arrows indicate the path of the pilin. Biogenesis pathway: i) VirB2 inserts into the inner membrane where it is cleaved and cyclized, ii) it then interacts directly with VirB4, iii) VirB11 interacts with VirB4 leading to a change in pilin structure, iv) VirB4 extracts VirB2 from the inner membrane, and, finally, v) pilin subunits are shunted through the T4SS core complex and incorporated in the secretion channel and T-pilus. P: periplasm; IM: inner membrane; OM: outer membrane.



Chapter 5: The Role of VirB10 Domains in T-pilus Biogenesis and Type IV Substrate Secretion

NOTE: *This chapter is derived from work that has been published in 2009: “Agrobacterium VirB10 domain requirements for type IV secretion and T pilus biogenesis.” Molecular Microbiology 71(3): 779-794 (doi: 0.1111/j.1365-2958.2008.06565.x). I am one of the co-primary authors on this paper. Experiments performed by the other authors, Dr. Simon Jakubowski, Vidhya Krishnamoorthy, or Isaac Garza, are indicated in the figure legend or text. I have been given permission by the publisher of Molecular Microbiology, John Wiley and Sons, to reproduce any/all of my manuscript in print or electronically for the purposes of my dissertation (License Number 2501460079655). Crystal structure images were modeled in PyMOL. An educational-use program copy of PyMOL was obtained from <http://pymol.org/ep>, which states that images may be used for thesis/dissertation projects. All structural coordinates were obtained from the RCSB protein data base <http://www.rcsb.org/pdb> and individual identification numbers and specific references are included in the figure legends.*

Introduction

Homologs of the *Agrobacterium tumefaciens* VirB7, VirB8, VirB9, and VirB10 subunits are present in nearly all Type IV secretion systems (T4SSs) of Gram-negative bacteria (39, 70). A number of biochemical and ultrastructural lines of evidence indicate that these subunits assemble as 'core' subcomplexes required for building functional translocation systems (67, 68, 71-73). These 'core' subunits are required for both substrate transfer and T-pilus biogenesis in *A. tumefaciens* (104, 128). Studies of the VirB10_{At} subunit have shown that it forms stabilizing interactions with the VirB7 lipoprotein and the outer-membrane-associated VirB9 (71, 72, 193). Additionally, VirB10 was shown to undergo a structural transition in response to ATP utilization by the VirD4 and VirB11 ATP-binding subunits, as monitored by protease susceptibility (83). This structural change is important for productive complex formation with VirB7 and VirB9, and it allows for transfer of DNA substrates through the distal portion of the secretion channel (58, 123).

A core channel complex composed of homologs of VirB7, VirB9 and VirB10 from the pKM101 T4SS was recently solved by cryo-EM and X-ray crystal structure analysis (67, 68). This 1.05 MDa hollow complex spans both the inner and outer membranes, forming a cylindrical structure composed of 14 copies of each subunit. A striking feature of the structure is that the VirB10-like TraF subunit appears to span the entire cell envelope. An N-terminal transmembrane (TM) domain anchors the protein to the inner membrane. The protein then extends across the periplasm, in part via a Pro-rich domain termed the PRR (69). Part of VirB10-like TraF then extends across the outer membrane pore and may be able to function as a gate or regulator of secretion and/or T-pilus elaboration. This proposed transenvelope topology is unique among bacterial proteins and warrants experimental confirmation as well as further characterization of functional significance. That VirB10-like subunits function as transenvelope bridging proteins is supported by evidence for interactions between VirB10-like proteins from *A. tumefaciens* and plasmids R27 and R388 with at least one ATPase subunit at the inner membrane (45, 107, 194, 195). *A. tumefaciens* VirB10 was shown to form complexes with the three ATPases -VirB4, VirB11, and VirD4 of the VirB/VirD4 system (45, 83, 107, 196). As noted above, at or near the outer membrane, VirB10 also interacts with lipoprotein VirB7 and VirB9 (45, 71, 72, 74, 137, 193, 197, 198).

In light of these findings, VirB10 is thought to function as both a 'structural scaffold' for the core channel, as well as an energy sensor/transducer, possibly gating the outer membrane channel complex during substrate translocation and T-pilus assembly. Similar

to VirB10, TonB from *Escherichia coli* senses energy via the proton motive force through complex formation with the inner membrane proteins ExbB and ExbD (199-202). VirB10 and TonB share similar structural features containing a short N-terminal cytoplasmic domain, a transmembrane region (69), a proline rich region, and a C-terminal periplasmic domain. In one model, TonB was proposed to facilitate active transport by 'shuttling' from the inner membrane to the outer membrane in response to energy (203). More recent findings suggest that TonB is stably anchored to the inner membrane (200), as we have shown is the case for VirB10 (69). How the VirB10 and TonB energy sensors transduce inner membrane energy to mediate outer membrane translocation remains to be determined.

The C-terminal domains of two VirB10 homologs, *Helicobacter pylori* ComB10 and pKM101 TraF, have been solved by X-ray crystallography (68, 73). These structures both present as modified β -barrels with inherent flexible regions. One main feature is the antennae projection (AP), composed of alpha helical regions designated α_2, α_3 , which extends out from the top of the β -barrel. In the TraF structure, solved as a large complex of 14 copies of VirB10-like TraF, VirB7-like TraN and VirB9-like TraO, the AP domains form a pore that was postulated to span the outer membrane (68). A second region that I have named the 'bridging' domain (BD) connects the AP via a flexible section to the core barrel structure. A third region, designated α_1 for ComB10 (73) and α_n1 for TraF (68), extends out to the side of the β -barrel region. In the TraN/O/F structure, the α_n1 helix of one TraF monomer forms contacts with β -barrel domains of neighboring TraF monomers to stabilize the core complex (68). The β -barrel contains a large grooved 'pocket' along its side together with a flexible flap domain and a conserved XDLDF motif at its base (73). The ComB and TraF structures likely represent structural paradigms for VirB10-like proteins, as deduced from the overall extensive primary and secondary structural conservation of the family members (30).

In the previous chapters of this thesis, I presented results of my studies defining early steps in the assembly of the VirB2 pilin into the T4SS channel and T-pilus. Following integration and processing of the pro-pilin, VirB4 and VirB11 work together to mediate pilin structural changes resulting in membrane dislocation and formation of subsequent interactions in the assembly pathway. In view of my model that upon dislocation from the membrane the pilin enters the VirB7/VirB9/VirB10 core chamber, and the current structural information indicating that VirB10 might span both cell membranes (67), I hypothesized that VirB10 contributes to the movement of pilin monomers to their final destinations in the

terminal organelles. The polymerization of pilin monomers into T-pili is easily monitored by assaying for surface-exposed VirB2 and assembly of high-molecular-weight VirB2 complexes. By contrast, at this time little is known about the disposition of VirB2 in the secretion channel and no specific assays are available to monitor pilin incorporation into the channel. Consequently, here I focused my mutational studies on defining the contributions of VirB10 motifs or domains to T-pilus assembly.

I characterized a number of VirB10 mutations generated by V. Krishnamoorthy and I. Garza with the goal of defining the importance of conserved motifs and domains to T-pilus assembly. I collaborated with these lab members and S. Jakubowski, who together analyzed effects of the mutations on protein stability and substrate transfer. A principal finding of interest reported in the publication of this collaborative effort was the discovery of mutations that permit substrate transfer while blocking assembly of T-pili. These so-called 'uncoupling' mutations were isolated in the two regions of VirB10 implicated in spanning the membranes – the N-terminal TM domain and the AP. Our findings support a model in which VirB10 can selectively regulate formation of the extracellular T-pilus or the secretion channel. In the next section, I highlight my contributions to this larger study.

Results

The mutations (see Fig. 5,1) I. Garza and V. Krishnamoorthy created along the length of VirB10 included: i) two residue (Ala-Cys) insertions at 5-residue intervals along the N-terminal region, ii) Cys substitutions within the proline-rich region (PRR), α 1 lever arm, and β -barrel, and iii) deletion of the N-terminus, TM, and/or PRR regions. V. Krishnamoorthy also constructed several deletion mutations within the conserved C-terminal domain based on structural information for the VirB10 homologs crystallography (68, 73). Two regions predicted to be important for function were the antennae projection (AP) which extends from the top of the β -barrel and the 'bridging domain' that connects the AP to the barrel structure (based on the TraF structure) (68). I characterized these mutations, looking for defects in T-pilus production, whereas other lab members assayed for effects on protein stability and substrate transfer.

Mutations Within the N-Terminus of VirB10 Selectively Disrupt T-pilus Biogenesis

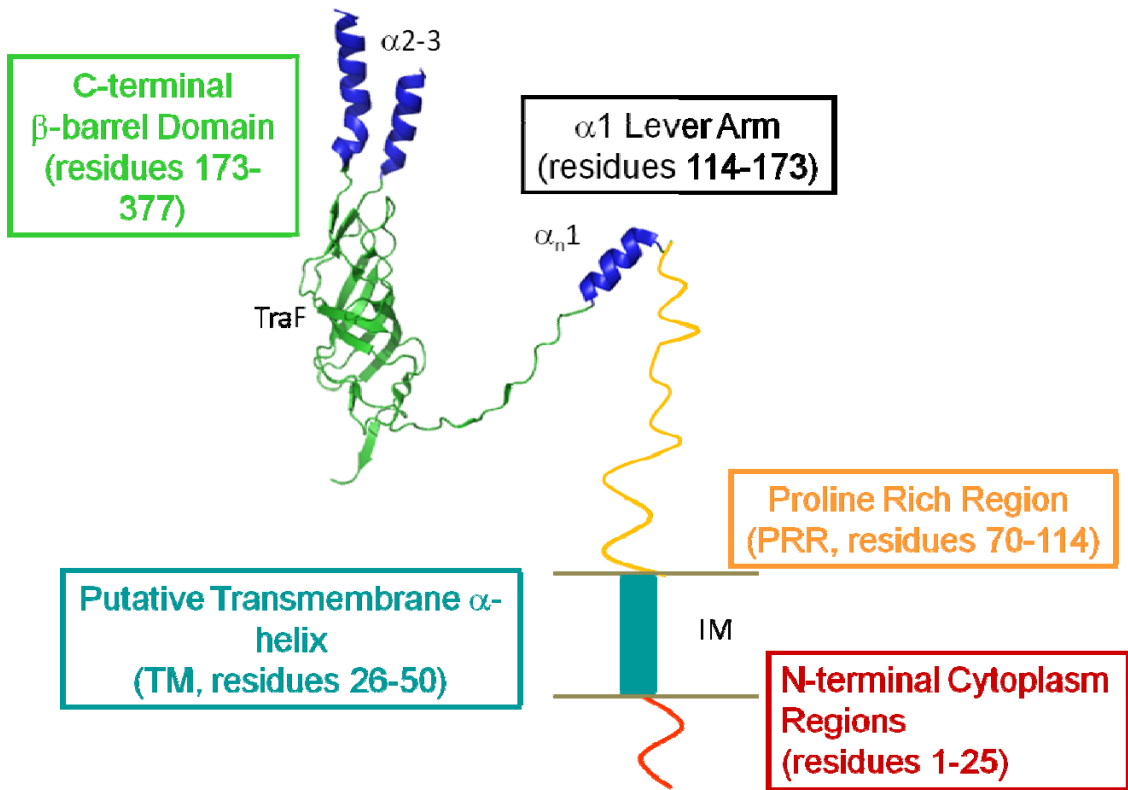
VirB10 has been shown to directly or indirectly interact with all of the ATPases in the VirB/VirD4 T4SS (45, 83, 107, 196). These ATPases are primarily located at the cytoplasmic face of the inner membrane (90, 105, 159). Both the N-terminal cytoplasmic and TM region of VirB10 are predicted to play a critical role in mediating those interactions. The Christie lab predicted that the insertion mutations in these regions should impact substrate transfer as a result of disrupted contacts with one or more of the ATPases. In order to test this hypothesis, I assayed strains producing the N-terminal deletion and 2-residue insertion (i2) mutant proteins for effects on T-DNA transfer and T-pilus production.

The i2 mutations along the cytoplasmic domain did not affect protein function, as monitored by substrate transfer and T-pilus biogenesis (Fig. 5.2) (69). However, a partial deletion (Δ 2-18) completely blocked pilus production but still allowed for a low level of T-DNA transfer, showing the importance of the extreme N terminus of VirB10 particularly for pilus production (Fig. 5.2). A longer deletion of the cytoplasmic and TM domains (Δ 2-46) was nonfunctional (Fig. 5.2) (69). This mutant protein was delivered to the periplasm by fusion to the VirB5 signal sequence and although it accumulated at abundant levels, it was nonfunctional possibly because it failed to form a complex with the VirD4 ATPase [experiment performed by Vidyha Krishnamoorthy, (69)]. Besides the importance of the extreme N terminus for pilus production, I determined that i2 mutations at positions 35, 40, and 45 in the TM domain significantly reduced or abolished pilus production without

Figure 5.1 Schematic of VirB10 domains and mutations

A) Cartoon of VirB10 domains with C-terminal β -barrel domain depicted by crystal structure from VirB10 homologue TraF_{pKM101} (68) and associated structural features (67, 204). B) Top: The various domains of VirB10 and their locations with residue numbers above are depicted. Domain abbreviations: Cyto, cytoplasmic domain; TM, transmembrane helix, PRR, proline-rich region. Ala, Cys (i2, AC; black dots) insertion mutations were engineered at five-residue intervals in the N-terminal 50 residues. Cys substitution mutations in the remainder of the protein are listed at top; Ser substitutions for the two endogenous Cys residues, Cys190 and Cys206 (underlined), also were characterized. Bottom: Deletion mutations of various domains with deleted residues indicated; alternative designations used in the text for some deletion mutations are listed above the corresponding line. The Δ N46 and Δ N150 fragments were exported to the periplasm by fusion to the signal sequence of VirB5 (B5ss). Δ AP, deletion of the antennae projection (see (67, 68, 73)). Deletion mutations were constructed by V. Krishnamoorthy. Cysteine substitutions and two residue insertions were constructed by I. Garza. Shown is the TraF β -barrel modeled with coordinates from pKM101 core outer membrane complex X-ray structure (DOI:10.2210/pdb3jqo/pdb) (67, 68) using PyMOL (<http://pymol.org/>) to construct the figure.

A



B

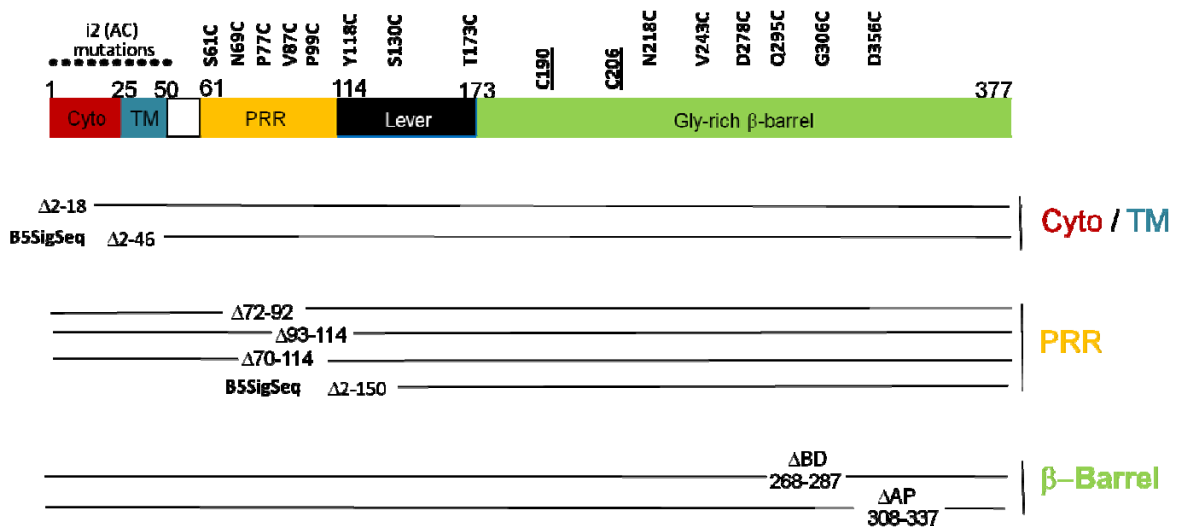
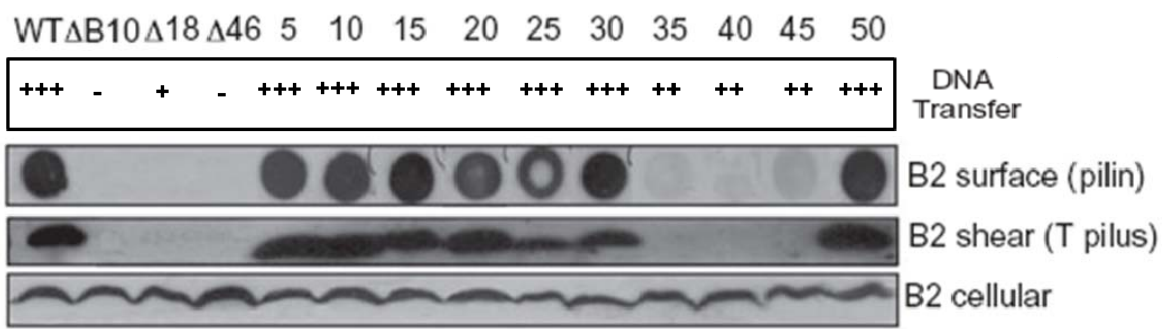


Figure 5.2 Phenotypes of N-terminal insertion and deletion mutations

Effects of mutations on T-DNA transfer as monitored by virulence on wounded *Kalanchoe* leaves (- avirulent, +++ WT virulence) and effects of mutations on T-pilus production. Top-to-bottom: colony immunoblots developed with anti-VirB2 antibodies showing presence of surface-exposed pilin protein (B2 surface); extracellular shear fraction subjected to ultracentrifugation, gel electrophoresis and immunoblot development with anti-VirB2 antibodies revealing presence of high-molecular-weight T-pilus (B2 shear); total cellular material subjected to gel electrophoresis and blot development with anti-VirB2 antibodies revealing total cellular levels of the protein. Strains: WT, wild-type A348; Δ B10, non-polar *virB10* strain PC1010; Δ 18, PC1010 producing VirB10 Δ 1–18; Δ 46, PC1010 producing VirB10 Δ 1–46 fused to the VirB5 signal sequence for export of the C-terminal fragment to the periplasm; 5–50, PC1010 producing i2 (Ala–Cys) insertion mutations at the residue indicated. DNA transfer experiments were performed by I. Garza for i2 insertions and Cys substitution mutations and V. Krishnamoorthy for deletion mutations.



influencing DNA substrate transfer (Fig. 5.2). None of the deletions or insertions impacted the stability of cell-associated VirB2.

Contributions of the Proline Rich Region and β -barrel domain to VirB10 Function

Deletion and Cys-substitution mutations were introduced along the PRR and β -barrel domains of VirB10. These were extensively characterized and the results published (69). Here, I will summarize my contributions to this larger study focusing on testing the effects of the various mutations on pilus biogenesis.

First, with respect to mutations in the VirB10 PRR domain, the most informative mutations were partial or full deletions of this domain. These abolished all protein function, including pilus biogenesis (Fig. 5-3), and they also abolished the capacity of VirB10 to form a precipitable complex with the outer membrane-associated VirB7 and VirB9 proteins (experiments performed by S. Jakubowski, (69)). In earlier studies, it was shown that Proline-rich regions (PRRs) of proteins adopt extended structures and also mediate protein-protein interactions (205). The VirB10 PRR might, therefore, adopt an extended structure necessary for a productive and stable interaction with the outer membrane core subunits (67, 68). In support of this idea, an N-terminal fragment of VirB10 composed of the cytoplasmic domain, TM domain and PRR (Δ 150-377) also was nonfunctional with respect to transfer substrate and T-pilus production (Fig. 5.3). This mutant protein failed to interact with VirB7 or VirB9 (S. Jakubowski, (69)). Conversely, a C-terminal β -barrel fragment (Δ 1-150) delivered to the periplasm by fusion to the VirB5 signal sequence was defective for both substrate transfer and T-pilus production (Fig. 5.3); however, it did show complex formation with VirB7 and VirB9 [S. Jakubowski; (69)]. Together, these results establish the importance of the PRR most likely for enabling VirB10 to extend across the periplasm.

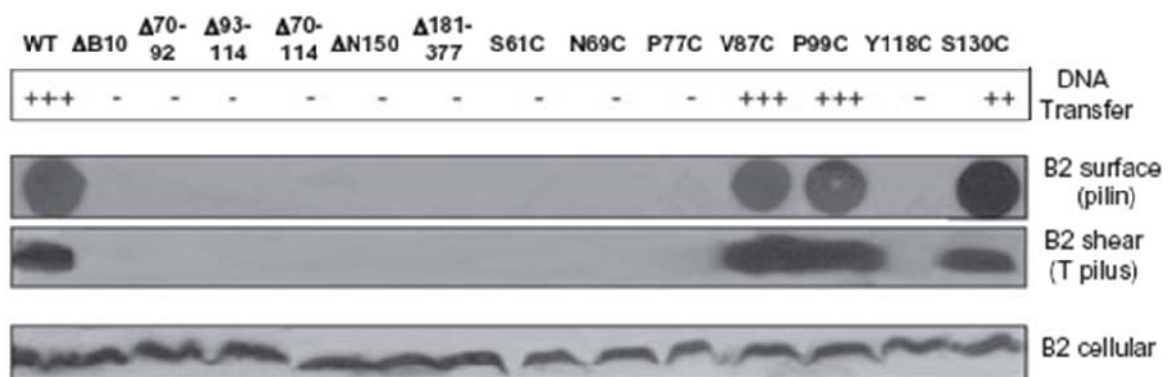
With respect to the β -barrel domain, mutations that abolished substrate transfer also abolished pilus biogenesis (Fig. 5.4). In general, these were Cys substitutions of residues that are conserved among VirB10 homologs. These mutations might affect contacts between adjacent β -barrel domains, or β -barrel domain contacts with other VirB channel subunits, but further studies are needed to examine these possibilities.

The Antennae Projection Selectively Contributes to T-pilus Assembly

The TraF β -barrel domain possesses two extensions, the α 1 lever arm and the antennae projection (AP). The AP is a helix-loop-helix that potentially spans the outer membrane (68) (Fig. 1.3B). In VirB10, the corresponding AP is predicted to span residues

Figure 5.3 Phenotypes of PRR deletions and substitution mutations.

Effects of mutations on T-DNA transfer as monitored by virulence on wounded *Kalanchoe* leaves (- avirulent, +++ WT virulence) and effects of mutations on T-pilus production. Extracellular pilin and T pilus, and total cellular pilin and VirB10 derivatives were detected as described in Fig. 5.1 legend. Strains: WT, wild-type A348; Δ B10, non-polar *virB10* strain PC1010; isogenic PC1010 producing the following PRR mutants $-\Delta$ 70-92, Δ 93-114, Δ 70-114, PRR internal deletion mutants; Δ N150, residues 150-377 containing the β -barrel domain exported to the periplasm by fusion to the VirB5 signal sequence; Δ 181-377, residues 1-180 containing the cytoplasmic, TM, PRR and linker domains; Cys substitution mutants as listed. DNA transfer level experiments were performed by I. Garza, V. Krishnamoorthy and S. Jakubowski.



282-335. Strikingly, partial deletions of the AP (here Δ AP denotes deletion of TraF based alpha 3 and linker region; Δ 308-320, Δ 323-337, Δ 303-337) and a couple of Cys-substitutions in the AP did not affect DNA transfer (Fig. 5.5A and see (69)), suggesting that the AP region is dispensable for DNA transfer. Additionally, TraF also has a predicted flexible section I have denoted as the 'bridging' domain (BD). The BD connects the AP to the β -barrel. Interestingly, a BD deletion mutation (Δ 268-287) diminished but did not abolish substrate transfer (Fig. 5.4A), suggesting that the BD contributes to but is not essential for substrate transfer.

Although the mutational analyses established that both the AP and BD were found to be dispensable for substrate transfer, my further studies showed that both regions are vital for T-pilus biogenesis (Fig. 5.4). Strains synthesizing the Δ AP and Δ BD mutant proteins possessed low levels of extracellular VirB2, as monitored by the colony blot and T-pilus shear assays (Fig. 5.4A). I also analyzed the extracellular fractions by sucrose density gradient centrifugation. Interestingly, whereas pili isolated from the wild-type strain distribute across the gradient as a broad peak, VirB2 from the Δ AP and Δ BD mutant strains distributed predominantly in the low and high density sucrose fractions (Fig. 5.5A). These findings suggest that the mutant strains released VirB2 to the cell surface, but as monomers or short polymers or aggregates as opposed to intact pilus fibers.

To determine if this observed phenotype is restricted to the AP and BD deletion mutations, I subjected extracellular fractions from other mutant strains (e.g., i2.35, i2.45, N218C) whose phenotypes resembled those of the Δ AP and Δ BD mutants, namely, reduced accumulation of extracellular VirB2 but Tra⁺ (see Figs. 5.2 and 5.4) to sucrose density fractionation. All three mutants demonstrated a disperse profile of VirB2 consistent with wild-type pilus assembly; representative data are shown for pili obtained from the N218C mutant strain (Fig. 5.5A).

I further analyzed the extracellular material from AP deletion using an analytical gel filtration (AGF) column. Due to the low production of VirB2 in the AP deletion mutant, ten times the amount of extracellular material relative to wild type was subjected to AGF. VirB2 from wild-type cells partitioned in a size range consistent with high molecular weight T-pili (>100kDa) (fig. 5.5B). By contrast, the majority of extracellular VirB2 from the Δ AP mutant was present in the lower molecular weight species (<10kDa) (Fig. 5.5B). Taken together, these results indicate that the AP and the BD are critical for T-pilus polymerization.

Figure 5.4 Phenotypes of β -barrel deletions and substitution mutations.

A) Effects of mutations on T-DNA transfer as monitored by virulence on wounded *Kalanchoe* leaves (- avirulent, +++ WT virulence). Effects of mutations on T pilus production. Extracellular pilin and T pilus, and total cellular pilin were detected as described in Fig. 5.2 legend. Strains: WT, wild-type A348; Δ B10, non-polar *virB10* strain PC1010; isogenic PC1010 producing Cys substitution mutants as listed. Here, Δ AP denotes deletion of TraF based alpha 3 and linker region (see (69)). B) β -barrel ribbon structure modeled with coordinates from pKM101 core outer membrane complex X-ray structure (DOI:10.2210/pdb3jqo/pdb) (67, 68) using the PyMOL (<http://pymol.org/>) to construct the figure. This C-terminal domain (residues 173–377) presents as a non-canonical β -barrel with a groove marked by the V243C substitution mutation, a flexible base marked by the S173C and N218C mutations and a conserved RDLDF motif, the α 2, α 3 antennae projection (AP) marked by Q295C and G306C and the flexible bridging domain marked by D278C. Cys substitution mutations are in blue. Residue numbers labeled in red indicate pilus defect. Red boxes indicate deletion of region results in pilus defect. Deletion mutations were constructed by V. Krishnamoorthy. Cysteine substitutions were constructed by I. Garza. DNA transfer experiments were performed by V. Krishnamoorthy and S. Jakubowski.

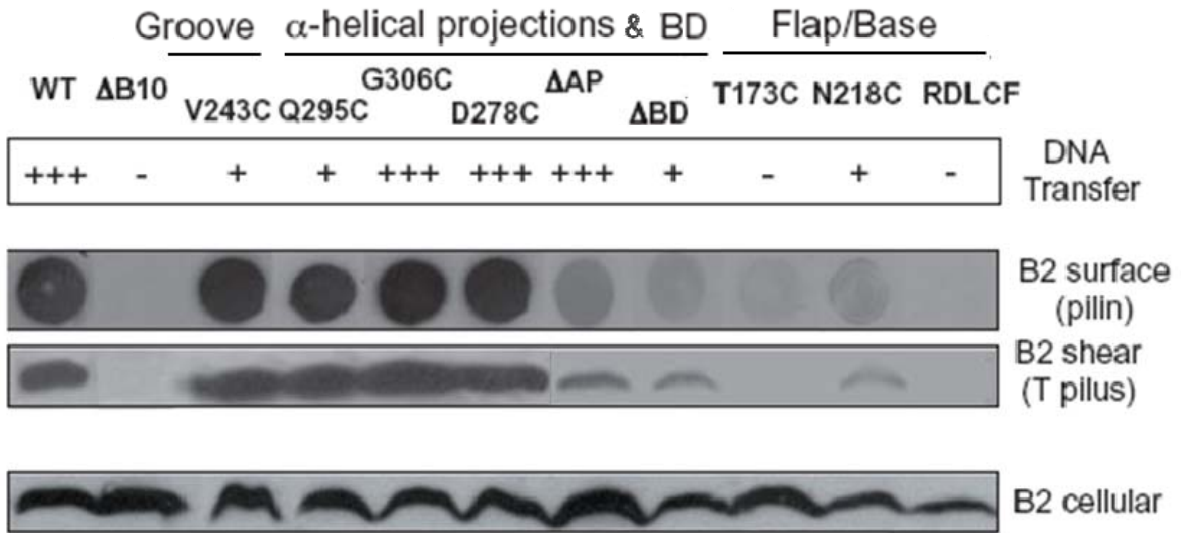
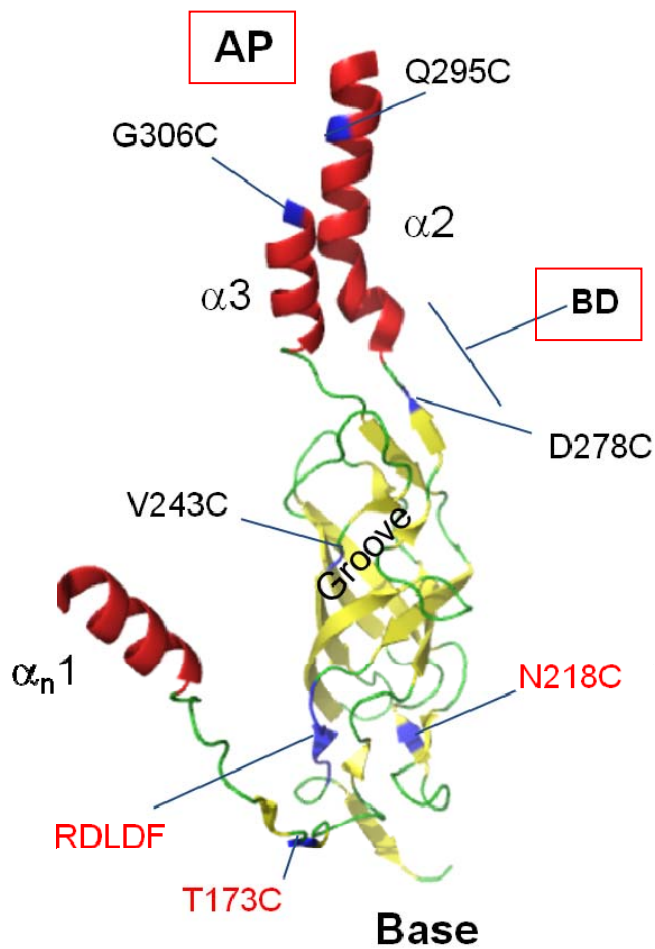
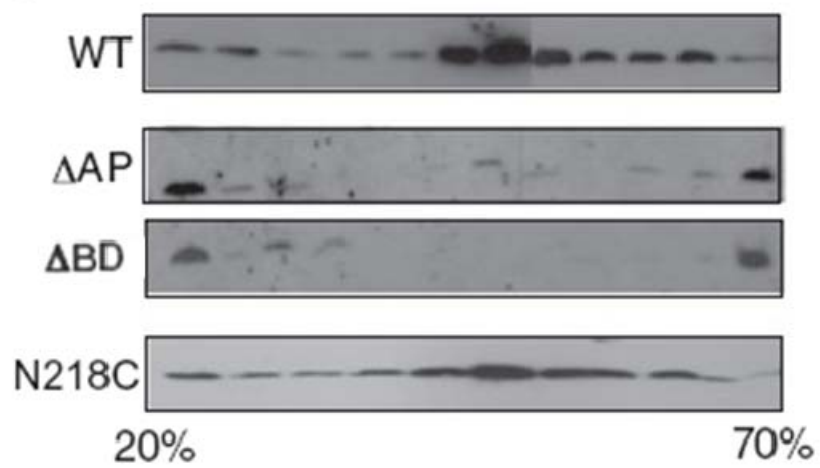
A**B**

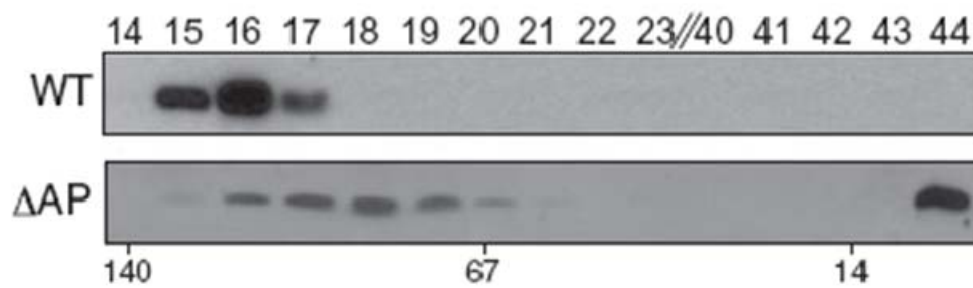
Figure 5.5 Effects of VirB10 helix projection mutations on T-pilus assembly

Effects of VirB10 helix projection mutations on T pilus assembly. A. Sucrose density gradient distribution profiles of extracellular VirB2 pilin/T pili produced by WT cells and the Δ AP and Δ BD helix mutants. Here, Δ AP denotes deletion of TraF based alpha 3 and linker region (see (69)). For comparison, extracellular material from the N218C mutant strain, which also produces low amounts of surface pilin (Fig. 5.4), was similarly analyzed. Immunoblots developed with anti-VirB2 antibodies show the distribution profiles of extracellular pilin in identically prepared 20–70% sucrose density gradients. B. Extracellular material from WT cells and the Δ AP mutant was fractionated through a Superdex 75 10/300 GL gel filtration column and fractions (listed at top) were analysed for the presence of VirB2 pilin by immunostaining. Molecular masses of reference proteins are shown below (in kDa).

A



B



Discussion

VirB10 is predicted to assemble as a structural scaffold as well as a 'communication' bridge between the inner and outer membranes. In this study, I collaborated with other members of the Christie laboratory to characterize the contributions of specific VirB10 domains to DNA transfer and/or T-pilus biogenesis. The most interesting outcome from this work was the demonstration that two transmembrane domains, one spanning the inner membrane and the second spanning the outer membrane, contribute selectively to the biogenesis of T-pili.

VirB10: a 'Communication' Bridge for IM and OM Machine Subassemblies

VirB10 forms close contacts with inner membrane associated T4SS ATPases (45, 107). VirB10 senses ATP binding or hydrolysis activities by the VirB11 and VirD4 ATPases and, in turn, undergoes a conformational change that is necessary for T-DNA transfer through the translocation pathway (58, 123). VirD4 spans the inner membrane (159), while VirB11 associates peripherally at the cytoplasmic face of the membrane (90). Therefore, the short N-terminal cytoplasmic domain and/or TM domain are predicted to interact with one or both of these ATPases. Additionally, VirB10 might interact directly with the VirB4 ATPase, which stimulates dislocation of membrane-integrated VirB2 (see Chapter 4 and (130)). Interestingly, i2 insertions throughout the N-terminal domain and a deletion ($\Delta 2-18$) mutation did not abolish substrate transfer, but did disrupt pilus biogenesis. A longer deletion ($\Delta 2-46$) of both the cytoplasmic N-terminus and the TM domain abolished both activities confirming the importance of both domains for VirB10 function. I suggest that the N-terminal region of VirB10, including the cytoplasmic and TM domains, could mediate productive interactions with the VirB or VirD4 ATPases that are required for protein function. In view of the selective disruption of TM domain mutations on pilus biogenesis and my finding that VirB4 mediates dislocation of the membrane-integrated VirB2 pilin, I favor the hypothesis that a VirB10 TM domain interaction with the VirB4 ATPase serves to coordinate delivery of the pilin into the core chamber. Experimental tests of this hypothesis are proposed in Chapter 7.

VirB10: A Regulator of T-pilus Biogenesis

The isolation of 'uncoupling' mutations that selectively disrupt T-pilus production or substrate transfer suggests that VirB10 might differentially regulate assembly or function of the secretion channel or polymerization of the T-pilus. In collaboration with other laboratory

members, I identified three subclasses of ‘uncoupling’ mutations in VirB10: Class I mutations attenuate substrate transfer levels, but do not disrupt T-pilus production, Class II mutations abolish T-pilus production, but do not affect substrate transfer, and Class III mutations selectively disrupt T-pilus polymerization, allowing for release of VirB2 monomers into the extracellular milieu but without affecting substrate transfer to target cells. The latter two classes were of primary interest as they arose, respectively, through mutation of the N-terminal region at or near the inner membrane and the AP presumptively spanning the outer membrane.

The Class II mutations included N-terminal deletion ($\Delta 2-18$) and i2 insertions with the transmembrane region (i2.35, i2.40, i2.45). As discovered and further characterized by I. Garza, the i2 mutations are located within a sequence (33-LIV*GGVVL*ALSLS*L-46) that resembles a leucine zipper motif (206). The model I. Garza developed from his studies is that this Leu zipper motif participates in homo- or heteromeric interactions that are selectively important for pilus biogenesis. Again, in view of my studies defining a VirB4 dislocase activity, the most reasonable model is that the VirB10 N-terminal region forms a productive interaction with the VirB4 ATPase.

The Class III mutations included the ΔAP and ΔBD mutations (fig. 5.4 and 5.5). On the basis of sequence conservation within this region, most or all VirB10 family members likely contain an α -helical AP. In view of the Class III phenotype, it is enticing to think that the AP may play a direct role in facilitating sequential addition of VirB2 subunits during polymerization. In such a model, the AP might coordinate the packing of pilin monomers to build the pilus polymer. According to this model, the AP functions directly in the morphogenesis of the pilus and might serve as a platform upon which the pili are assembled. However, an alternative possibility is that the AP functions as a gate that opens to allow T-pilus extrusion across the outer membrane. According to this model, the AP functions more passively in the polymerization process, but is still required for extrusion.

The bridging domain is composed of a short β -sheet and flexible sections (Fig. 5.4 B). While the ΔBD mutation did phenocopy the AP deletion, it also showed a significant reduction in substrate transfer. As discussed in more detail in the next chapter, the bridging domain contains a number of conserved glycine residues that might regulate translocation of substrates and extrusion of the T-pilus through the AP pore.

The structures of the pKM101 outer membrane core complex (67, 68) have provided us with a picture of a T4SS subassembly. It is still unclear if T4SSs use this subcomplex to build the secretion channel, T-pilus, both structures, or neither structure. The isolation of

'uncoupling' mutations, however, minimally establishes that biogenesis of the secretion channel and pilus can be genetically separated. Uncoupling mutations have been isolated in a number of T4SS subunits, including polytopic VirB6 (65), outer membrane core subunit VirB9 (123), ATPase VirB11(87, 136), ATPase VirD4 (104), VirB2 and the VirB2-like TrbC pilin of the RP4 plasmid transfer system (130, 160). Future studies aimed at isolating and characterizing T4SS subassemblies in association with substrates or T-pili should help to define the requirements for assembly of these two terminal organelles.

Taken together, results of my studies establish that both the TM and AP regions of VirB10 are critical for T-pilus assembly. Here, I present two models that could account for the mutant phenotypes (Fig, 5.6).

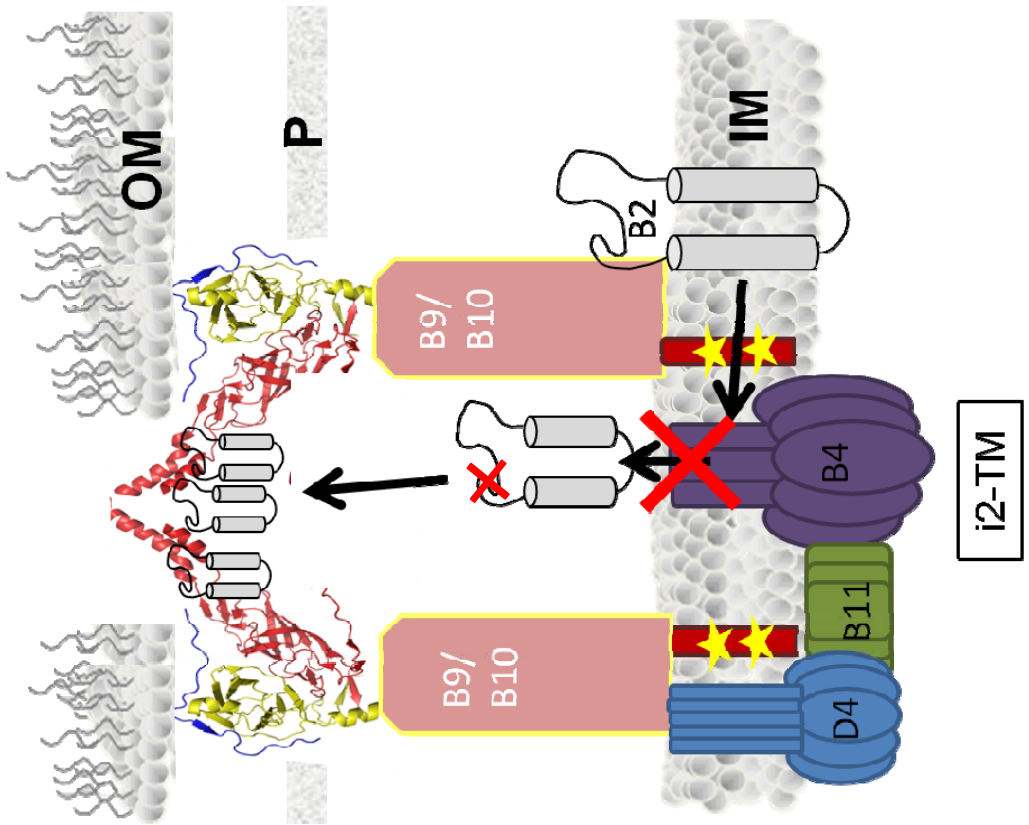
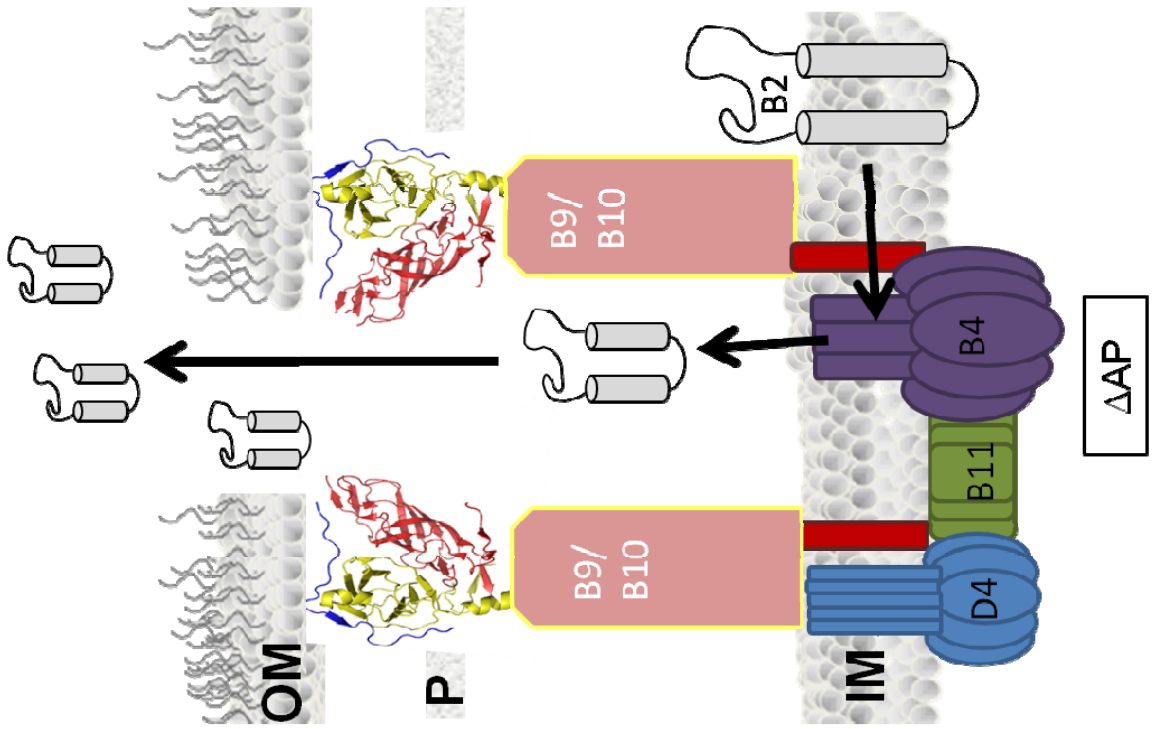
Model I: The VirB10 TM domain interacts with the pilus assembly factor VirB4 to enable pilin dislocation directly into the core complex. According to this model, the i2 mutations disrupt the VirB10-VirB4 interaction and this in turn blocks entrance of the pilin monomers into the core chamber or alternatively may prevent a necessary structural transition for incorporation into the T-pilus versus the channel. In earlier studies, the Christie lab identified VirB subunits that form close contacts with the translocating T-DNA (58). While VirB4 was required for substrate translocation (45), it did not form close contacts with the T-DNA substrate. Therefore, VirB4 appears to selectively regulate delivery of the pilin monomer into the channel without directly regulating passage of secretion substrates. A disruption in the VirB10-VirB4 interaction mediated by the i2 mutations could thus account for the $\text{Tra}^+, \text{Pil}^-$ 'uncoupling' phenotype. This model is also compatible with unpublished data by S. Jakubowski in our lab that VirB10 interacts with VirB4.

Model II: The AP region serves as a gating domain or polymerization chaperone. In wild-type cells, the AP regulates passage of the pilus polymer across the outer membrane, whereas in the ΔAP mutant pilin monomers or short oligomers are extruded. This deletion may induce a leakiness to the secretion channel that allows for nonspecific release of both substrate and pilin monomers. As noted above, an alternative possibility is that the AP is directly involved in T-pilus polymerization, perhaps similar to the mechanism used by the chaperone-usher pathway of pilus biogenesis, via donor-strand exchange (207).

In conclusion, our findings support the notion that VirB10 functions as a 'communication' bridge between the inner and outer membranes and possibly also serves as an outer membrane gated pore. Moreover, on the basis of the "uncoupling" phenotypes identified in the TM and AP regions, I propose that VirB10 differentially regulates assembly of the T-pilus or the secretion channel.

Figure 5.6 Models of VirB10 TM and AP domain involvement during T4SS T-pilus assembly

Left figure depicts the proposed function of the VirB10 TM domains in establishing productive contacts with VirB4. Two residue transmembrane insertions (i2-TM; depicted by yellow stars) were shown to specifically block T-pilus biogenesis without affecting substrate transfer. VirB2 may be blocked (red 'X') from entering the core channel complex or fail to make a structural transition (small red 'x') necessary for incorporation into the T-pilus due to loss of specific contacts between VirB10 and VirB4. Right figure highlights a model in which the VirB10 AP serves as an outer membrane gate and/or polymerization chaperone for VirB2. Removal of the AP (Δ AP) allows both substrate and VirB2 monomers to be released into the extracellular milieu. In the absence of the AP, VirB10 cannot mediate polymerization through an indirect (e.g. channel gating, promoting contact with another VirB subunit) or possibly direct mechanism (e.g. donor-strand exchange to promote pilus assembly, see (207)). Outer membrane complex was modeled with co-ordinates from pKM101 core outer membrane complex X-ray structure (DOI:10.2210/pdb3jqo/pdb) (67, 68) using the PyMOL (<http://pymol.org/>) and modified to construct this figure. OM: outer membrane; P: periplasm; IM: inner membrane.



Chapter 6: Characterization of a *virB10* Mutant Conferring Release of VirE2 to the Extracellular Milieu While Selectively Blocking T-Pilus Biogenesis

NOTE: This work was performed as part of a collaboration between the laboratories of Dr. Peter Christie and Dr. Lois Banta (Williams College - Biology Department - Williamstown, Massachusetts). This work describes a mutation that was first isolated in an experimental screen designed and performed by Dr. Lois Banta. Further characterization of this mutation was performed by Dr. Eric Cascales and Jennifer E. Kerr under the supervision of Dr. Peter Christie. Each person contributed to the development and design of the experiments. Members of the collaboration responsible for data discussed are indicated.

Introduction

Type IV secretion systems (T4SS) mediate the movement of DNA and/or protein substrates into a variety of recipient cells or into the milieu (2, 3, 15, 30). The *Agrobacterium* VirB/VirD4 T4SS is dedicated to the movement of both T-DNA and protein substrates into plant and other cell types based on a cell-contact dependent mechanism (33, 34, 60, 64, 208). These T4SSs span the entire bacterial cell envelope and comprise a conduit for substrates to pass *en route* to target cells (2, 3, 15, 30). Three VirB/VirD4 T4SS components, the cell-envelope-spanning subunit VirB10 together with the outer-membrane-associated subunits VirB7 lipoprotein and VirB9, form a stable T4SS subassembly that is known as a 'core' complex (2, 30). These 'core' subunits are phylogenetically conserved among T4SSs of Gram-negative bacteria (15), and therefore structure-function studies of paradigmatic 'core' complexes likely will identify mechanistic features of broad biological importance.

Recently, structural information was obtained for a 'core' complex of the *Escherichia coli* pKM101 conjugation system by cryoelectron microscopy (cryoEM) and X-ray crystallography (67, 68). In this 'core' complex, homologs of VirB7, VirB9 and VirB10 assemble together as a 185 Å ring composed of 14 copies of each subunit. On the basis of the cryoEM images, VirB10-like TraF was postulated to span the inner membrane and project through the periplasm to the outer membrane. In view of the more recent X-ray structure, it was further suggested that an α -helical domain of TraF termed the antennae projection (AP), spans the outer membrane, such that the 14 AP's in the core complex form an α -helical outer membrane pore with an opening of ~20 Å in diameter. At the inner membrane, an N-terminal transmembrane (TM) domain anchors TraF in the membrane, and the 14 copies of TM domains in the core complex form a ring of a 55 Å in diameter.

As suggested for the pKM101 core structure, a presumptive VirB7/VirB9/VirB10 core complex likely functions as a structural scaffold during machine biogenesis. In support of such a function, the three VirB proteins mutually stabilize each other as well as other VirB subunits. Moreover, S. Jakubowski in our laboratory recently succeeded in enriching a ring-shaped complex resembling that of the pKM101 core and composed minimally of these 3 subunits (unpublished data). Another interesting feature identified for the VirB10 subunit is that it senses ATP binding or hydrolysis activities of the VirD4 and VirB11 ATPases. In response, VirB10 undergoes a structural transition, identified as a change in susceptibility to an endoprotease. This structural change is important for stable complex formation between VirB10 and the VirB7/VirB9 complex (83).

E. Cascales, a postdoctoral fellow in the Christie laboratory, developed a substrate trapping assay based on the chromatin immunoprecipitation assay (ChIP). In this assay, cells are treated with formaldehyde to crosslink the translocating T-DNA to subunits of the T4SS channel. Following solubilization, subunits are immunoprecipitated with the anti-VirB antibodies, and co-precipitated crosslinked T-DNA is assessed by PCR amplification. With this assay, E. Cascales supplied evidence that the energy-activated form of VirB10 regulates substrate transfer through the distal portion of the channel composed of the VirB2 pilin and VirB9 subunits (58, 83). Accordingly, VirB10 is postulated to function as a 'gate-keeper' that regulates substrate translocation across the outer membrane by a mechanism dependent on sensing of inner membrane ATPase activities. One potential protein that undergoes gated release is VirE2, a single-stranded DNA-binding protein that interacts with the T-DNA, forming the T-complex. VirE2 protects the T-DNA from cytoplasmic nucleases in the plant cell and mediates delivery of the T-DNA to the plant nuclear pore with the help of VirE3 (47-52).

The proposed role of VirB10 as an energy-activated regulator of substrate transfer across the outer membrane remains to be experimentally tested. In this investigation, I participated in a study with our collaborator Dr. Lois Banta (Department of Biology, Williams College, Williamstown, MA, USA) aimed at testing the model that VirB10 regulates substrate translocation across the outer membrane. In a genetic screen, Dr. Banta's lab isolated a substitution mutation in VirB10 that confers leakage of a secretion substrate across the outer membrane. Here, I present results of my studies confirming both the 'substrate leaky' phenotype and an observed disruption of T-pilus biogenesis. I also report results of experiments indicating that the mutation, which is located near the AP region, does not confer nonspecific disruption of outer membrane integrity. Our collective findings add to a body of evidence that VirB10 functions as an energy-activated, outer membrane 'gate-keeper',

Results

The VirB/D4 T4SS translocates substrates across the entire cell envelope by a mechanism requiring direct contact with target cells (33, 34, 209). The Lois Banta lab designed and performed a screen to identify 'leaky' T4SS channels. Her lab screened ~12,000 strains expressing *virB10* mutant alleles for the release of functional, FLAG-tagged VirE2 (FLAG-VirE2) derivative to the cell surface. One mutant strain was isolated that showed a significant increase in release of FLAG-VirE2 in comparison with a wild type T4SS. The *virB10* allele was sequenced and found to harbor a single mutation that resulted in a substitution of an arginine for glycine at residue 272. Here, I present additional characterization data for this VirB10 G272R mutant. Modeling of the G272R mutation within the pKM101 core complex was performed by Dr. Gabriel Waksman.

***virB10* Mutant Confers Release of VirE2 to the Extracellular Milieu**

In agreement with the Banta lab finding, I found that the G272R mutation confers increased levels of surface exposed FLAG-VirE2 substrate in comparison to both the isogenic $\Delta virB10$ mutant or the $\Delta virB10$ mutant producing native VirB10 (Fig. 6.1A). FLAG-VirE2 accumulated at comparable total cellular levels in each strain background. The G272R mutation also did not affect cell viability in *virB* induction medium (ABIM) (Fig. 6.1B).

The G272R mutation may directly affect secretion channel gating or it could non-specifically disrupt outer membrane integrity. In order to test this, I measured growth of a $\Delta virB$ mutant producing native VirB10 or the G272R mutant in the presence of the large antibiotic vancomycin or anionic detergent SDS. I also assayed for the release of periplasmic-localized proteins RNase and ChvE. The outer membrane of Gram-negative bacteria normally provides a barrier to potentially harmful molecules. Porins at the outer membrane allow only the transit of small molecules (<600 Da) (210-212). Vancomycin is a large antibiotic (~1,500 Da) that targets the N-acetylmuramic acid and N-acetylglucosamine peptide subunits from incorporating into the peptidoglycan matrix and therefore predominantly affects Gram-positive bacteria cell wall synthesis (213, 214); however, an ungated channel or pore at the outer membrane could allow for transit of the drug into the periplasm of Gram-negative bacteria (215). Likewise, the outer membrane also protects from the effects of anionic detergents (216).

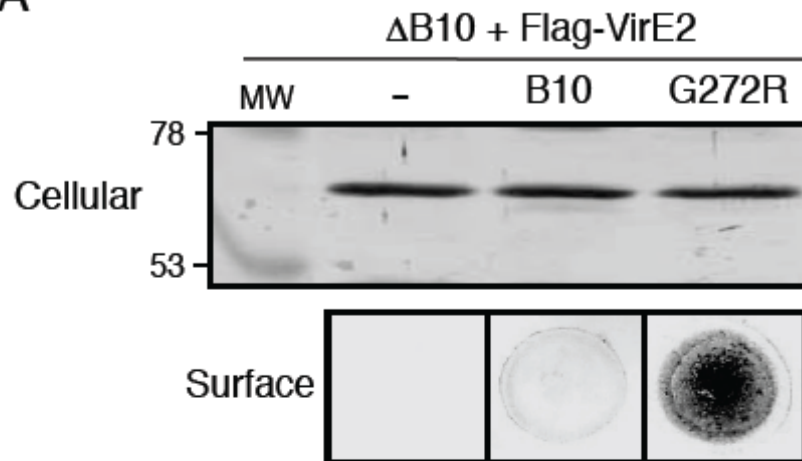
The G272R mutant showed increased sensitivity to both vancomycin and sodium dodecyl sulfate (SDS) (Fig. 6.2A and B). The G272R mutant strain grew slower in the

Figure 6.1 Effects of the G272R mutation on VirE2 release and growth

A) N-terminally FLAG-tagged VirE2 (Flag-VirE2) was produced in a nonpolar $\Delta virB10$ mutant strain (PC1010) and the $\Delta virB10$ mutant synthesizing native VirB10 or the G272R mutant protein. Upper, total cellular levels of FLAG-VirE2 assessed by immunostaining with anti-Flag antibodies. MW, molecular weight markers with sizes in kilodaltons (kDa) listed at left. Lower, FLAG-VirE2 surface display on the corresponding *vir*-induced strains as monitored by colony immunoblotting with anti-FLAG antibodies. B) Growth curves of PC1010 producing native VirB10 or the G272R mutant upon resuspension of cells in *vir*-induction media, as described in Materials and Methods.

Note: FLAG release phenotype first observed in the Lois Banta lab. Shown here is a repeat of that assay in A lower panel.

A



B

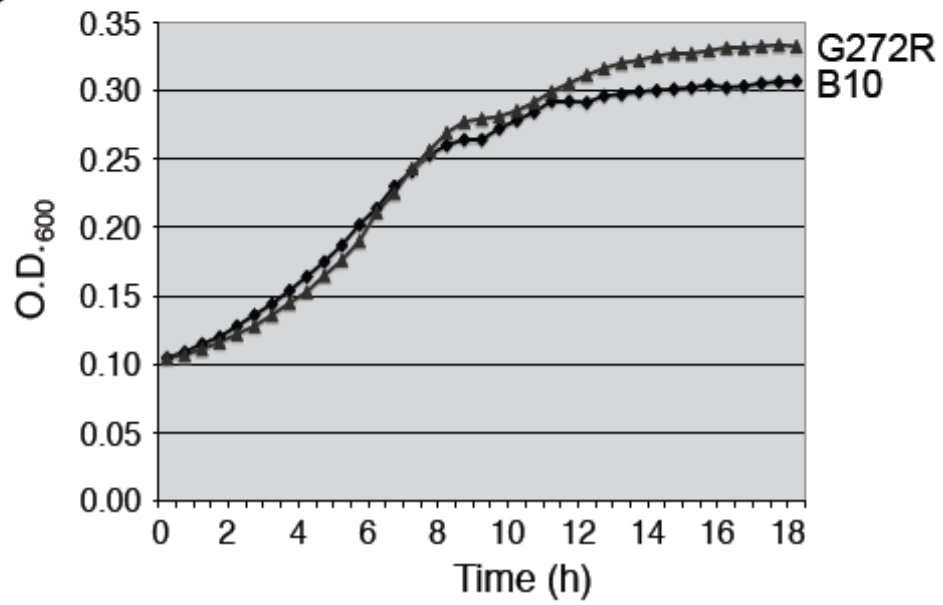
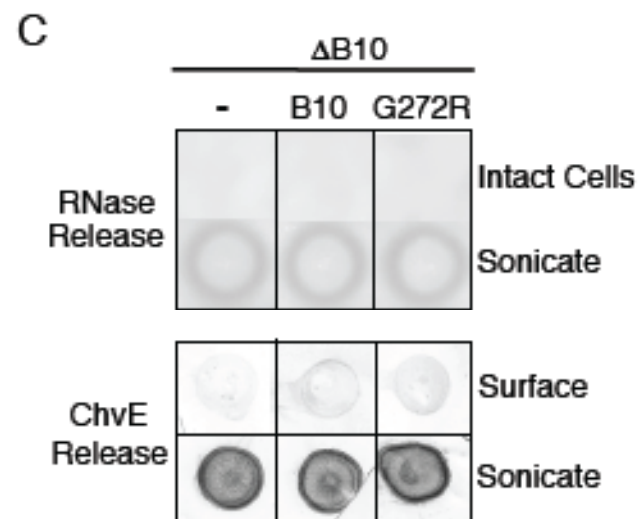
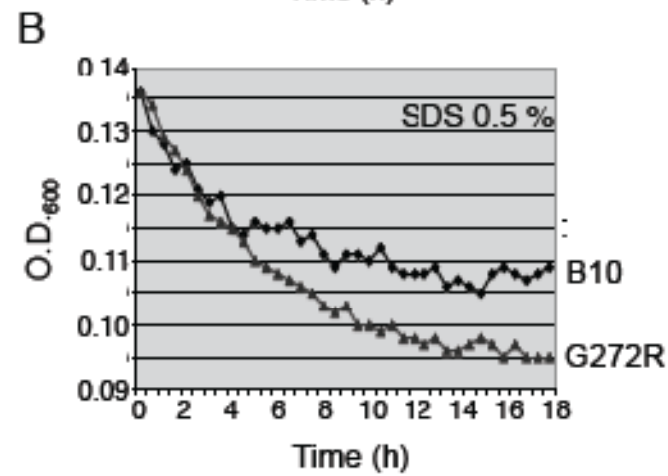
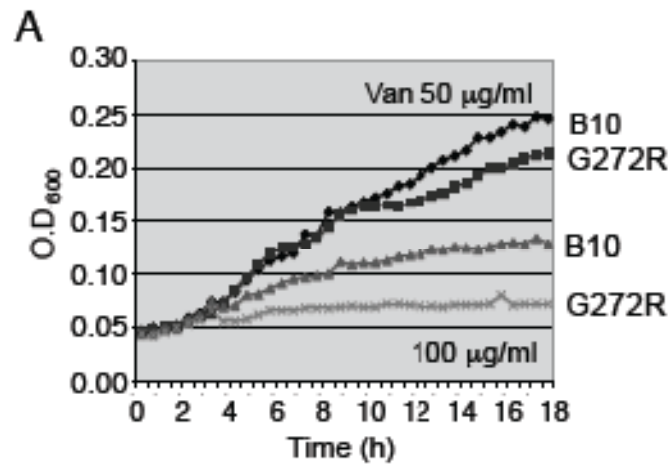


Figure 6.2 Effects of G272R on membrane integrity, as monitored by vancomycin and SDS sensitivity and release of preiplasmic proteins

A & B) PC1010 (Δ B10) producing native VirB10 or the G272R mutant were suspended in *vir*-induction media containing vancomycin (50 or 100 μ g/ml) or SDS (0.5 %) and growth/lysis was monitored for 18 h. C) PC1010 (Δ B10) cells lacking or producing native VirB10 (B10) or G272R were assayed for RNase release from intact cells on RNA-containing plates as described in Materials and Methods. Presence of cellular RNase was confirmed by addition of sonicated cell extracts to RNA-containing plates. Strains were assayed similarly for release of periplasmic ChvE as monitored by development of colony blots with anti-ChvE antibodies. Production of cellular ChvE was assessed by spotted in sonicating cell extracts on nitrocellulose and development with anti-ChvE antibodies.



presence of 50 $\mu\text{g/ml}$ vancomycin compared to an isogenic strain producing native VirB10 and the difference was more evident with the addition of 100 $\mu\text{g/ml}$ vancomycin (Fig. 6.2A). Growth was prevented and cells were presumably lysed in both the G272R mutant and the functionally wild-type strain by addition of 0.5% SDS; however, the G272R mutant showed a more pronounced sensitivity (Fig. 6.2B). In addition to inhibiting molecules from entering the cell, the outer membrane prevents periplasmic proteins and large molecules from exiting the bacterium. *A. tumefaciens* possesses RNase and the sugar-binding protein ChvE in the periplasm (217). If the G272R mutant disrupted outer membrane integrity, these proteins might be released to the cell surface. However, the G272R mutant did not show increased release of the periplasmic proteins as monitored by surface colony blots for ChvE and an RNA degradation assay for RNase in comparison to a ΔvirB10 mutant or an isogenic strain producing native VirB10 (Fig. 6.2C) (139). Thus, G272R likely disrupts the gating of the secretion channel at the outer membrane pore, allowing for release of FLAG-VirE2 substrate and increased uptake of molecules that are typically unable to cross the outer membrane.

G272R is Locked in an Energy-Activated Conformation

In wild type cells, VirB10 undergoes a conformational change in response to sensing ATP binding or hydrolysis by VirD4 and VirB11. This energy-activated structural transition results in exposure of a protease cleavage site that can be monitored by the presence of a $\sim 40\text{-kDa}$ degradation product following protease treatment of spheroplasts (83). In the absence of ATPases VirD4 and VirB11 or in cells depleted of cellular ATP levels with arsenate treatment, VirB10 maintains a protease-resistant conformation (48 kDa) (83). Interestingly, Dr. E. Cascales showed that the G272R mutant protein is degraded to the $\sim 40\text{kDa}$ species even in the presence of arsenate (E. Cascales, personal communication). The data suggest that the G272R mutant protein might 'lock' VirB10 into the energy-activated conformation.

G272R is Permissive for Intercellular Substrate Transfer, but Blocks T-Pilus Biogenesis

Next, the G272R mutation was tested for its potential impact on substrate transfer to recipient cells or T-pilus biogenesis. Substrate transfer to target cells was monitored by a plant tumor assay and conjugative transfer of a mobilizable IncQ plasmid. Interestingly, despite the apparent 'leaky' phenotype, the G272R mutation did not disrupt substrate

transfer of oncogenic T-DNA and protein substrates to plant cells as shown by appearance of plant tumors, or the conjugative transfer of an IncQ plasmid substrate to bacterial recipient cells (Fig. 6.3A). In contrast, neither the VirB2 pilin nor the pilus-associated protein VirB5 were detectable on the cell surfaces or in the high-molecular-weight shear fraction of the G272R mutant strain (Fig. 6.3B). These findings indicate that the G272R mutation completely blocked extracellular T-pilus production. Cellular levels of VirB2 and VirB5 were unaffected by production of the G272R mutant protein. Therefore, the G272 mutation is another example of an ‘uncoupling’ mutation that renders cells Tra⁺ and Pil⁻.

An AP Deletion Mutation Confers a Partial Gating Defect

VirB10 is postulated to form the outer membrane pore in the pKM101 core complex structure by creating a halo of interlocking alpha-helical projections extending from the top of the β -barrels. In Chapter 5 and our publication reporting the results of the VirB10 mutational analysis (69), I reported that deletion of these antennae projections (AP) and the associated bridging domains also resulted in Tra⁺, Pil⁻ phenotype. Unlike the G272R mutation that completely abolished release of extracellular VirB2, these deletion mutants mediated the release of pilin monomers into the milieu. I hypothesized that since these deletion mutants release nonpolymerized VirB2, they may also release VirE2 to the surface, even in the absence of a target cell. Interestingly, strains producing the Δ AP or Δ BD mutant proteins did not release FLAG-VirE2 to the milieu (representative data are shown for the Δ AP mutant strain in Fig. 6.4A). Both deletion mutants were also evaluated for nonspecific effects on the outer membrane. As shown for the Δ AP mutant (Fig 6.4), the mutant strains did not show enhanced vancomycin sensitivity or release of periplasmic proteins RNase or ChvE. The strains showed only a mild defect in the presence of 0.5% SDS relative to the isogenic strain complemented with native *virB10* (Fig. 6.4D-E). These results suggest that deletion of this region does not phenocopy the putative ‘open’ channel defect associated with the G272R mutation. Deletions in or around the AP region of VirB10 appear to selectively release VirB2 monomers without influencing secretion channel substrate gating or outer membrane integrity.

Figure 6.3 Effects of G272R mutation on DNA transfer, surface display of VirB2 pilin and the pi

lus-associated protein virB5

A) Levels of substrate transfer to plants, as monitored by virulence assays, and IncQ plasmid transfer to agrobacterial recipients. B) PC1010 ($\Delta virB10$) lacking or producing native VirB10 or the G272R mutant were assayed for surface-accessible VirB2 and VirB5 by colony immunoblotting, and for the presence of both proteins in material recovered in the shear fraction. Corresponding analyses with PC1002 (nonpolar $\Delta virB2$ mutant) shows specificity of the anti-VirB2 antibodies, and also the G272R mutation also blocked delivery of VirB5 to the cell surface independently of VirB2 production. Bottom panels show steady-state cellular levels of VirB2 and VirB5 in the various strains.

A

	$\Delta B10$		
	-	B10	G272R
Virulence	-	+++	++
Conjugation	$<10^{-8}$	2.3×10^{-5}	2.2×10^{-5}

B

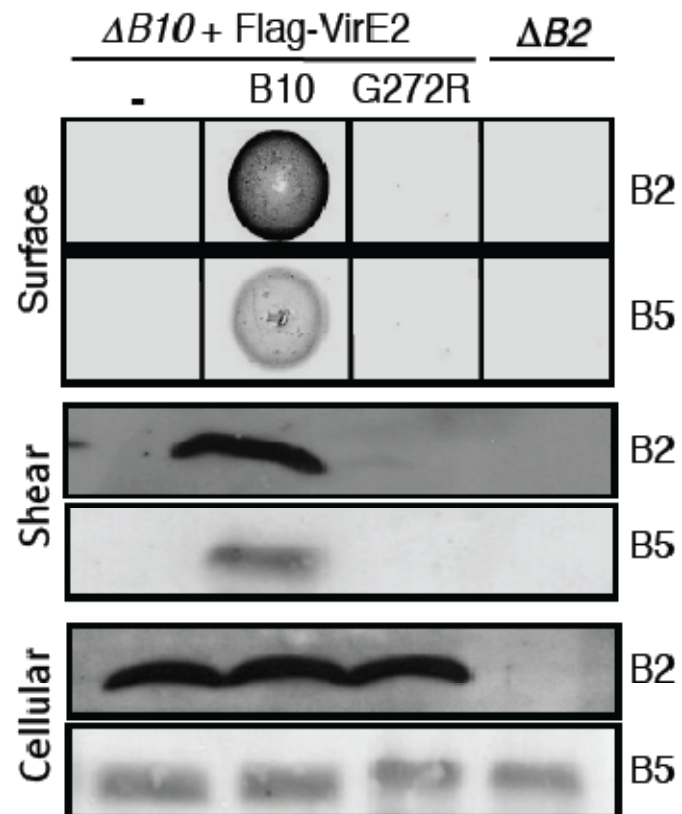
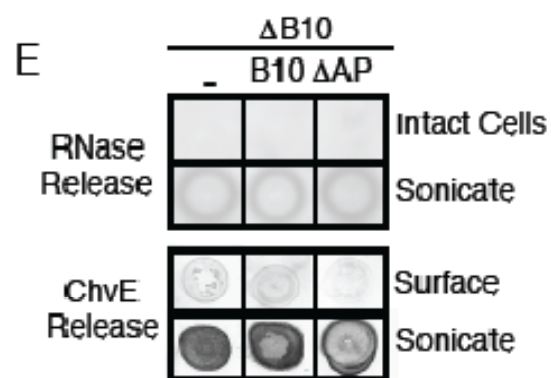
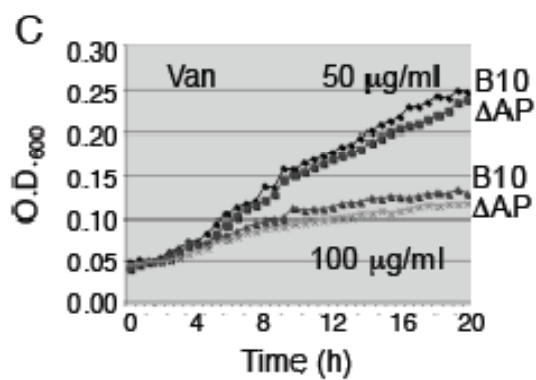
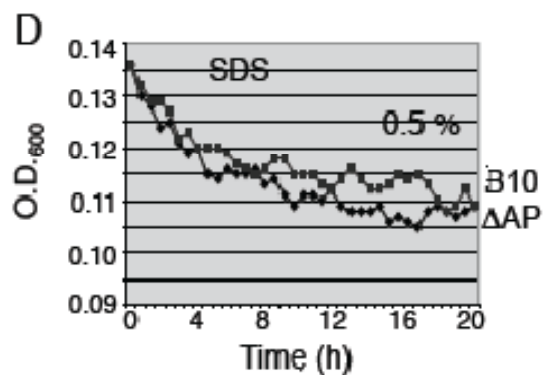
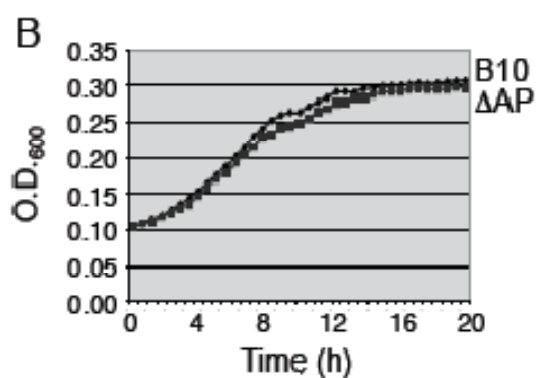
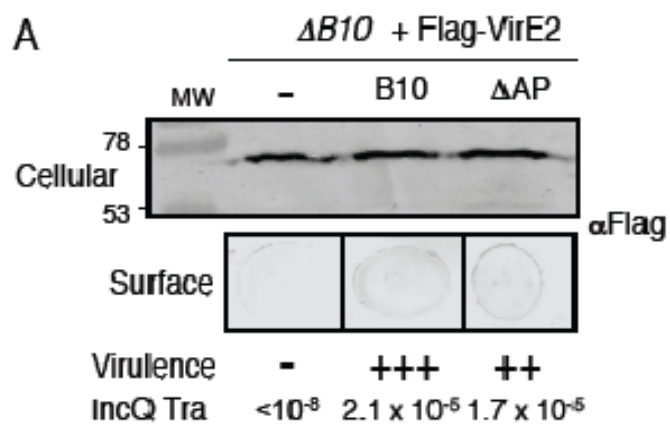


Figure 6.4 Effects of the Δ AP (Δ 302-337) mutation on VirE2 release, DNA transfer, cell growth, and outer membrane integrity

A) Effect of the Δ AP mutation on release of FLAG-VirE2. Samples were prepared and analyzed as described in Fig. 6.1A. The Δ AP mutant strain displayed only slightly reduced levels of substrate transfer to plants, as monitored by virulence assays, and IncQ plasmid transfer to agrobacterial recipients. B – E) as described in Fig. 6.2 legend, showing that the Δ AP mutation did not result in diminished cell growth, enhanced sensitivity to vancomycin or SDS, or release of periplasmic RNase or ChvE. My earlier studies showed that the Δ AP mutation disrupts polymerization of VirB2 into the T-pilus (See Chapter 5).



Discussion

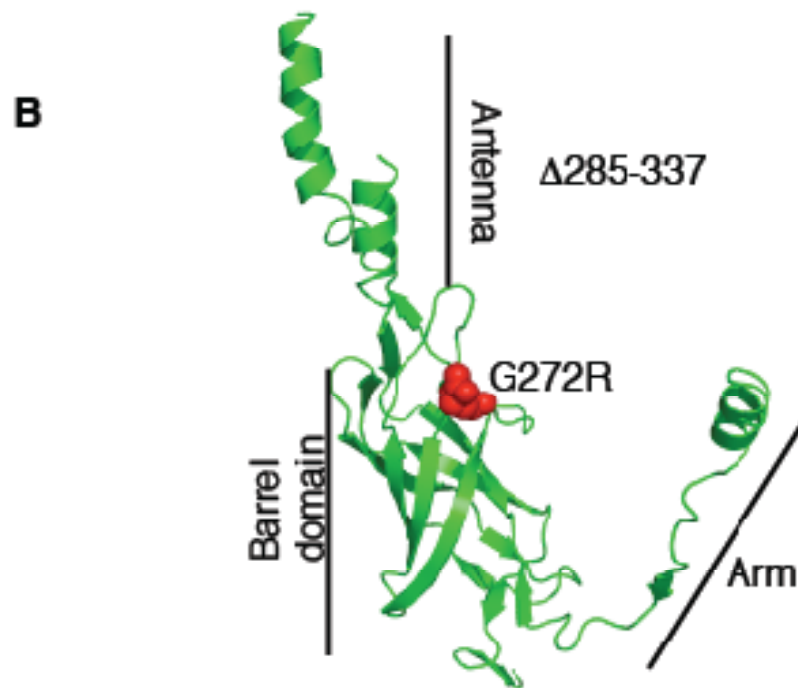
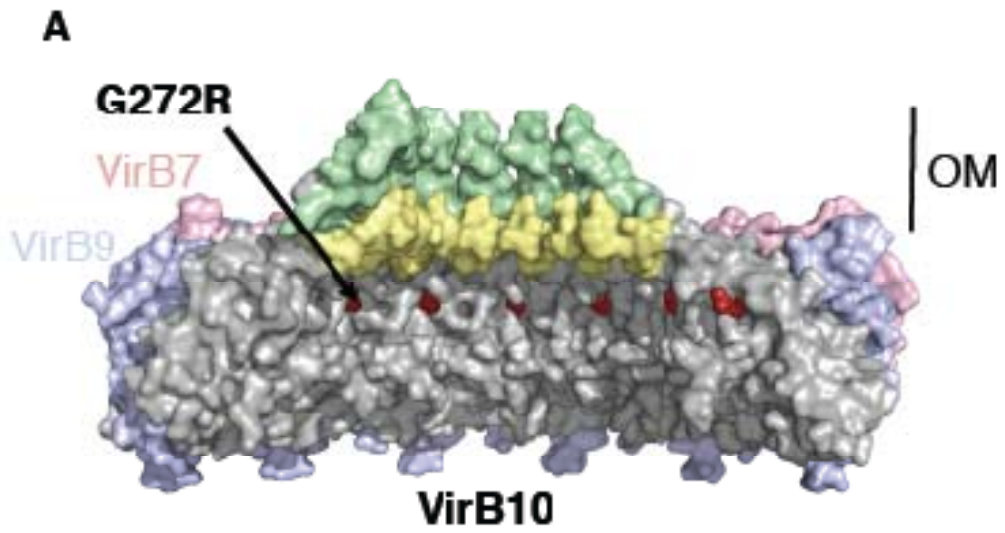
Export of virulence factors is typically tightly regulated in response to environmental as well as host-derived signals, and in many cases requires physical contact with a recipient cell (33, 34, 60, 64, 208, 218). The outer membrane location of a portion of VirB10 in the pKM101 core channel complex led to a hypothesis that VirB10 may directly serve as a gate for the T4SS substrate channel. To test this model, VirB10 mutant strains were screened for leakage of protein substrate to the surface in the absence of target cell contact. The VirB10 G272R mutation conferring such a phenotype was mapped to a highly-conserved glycine residue in the bridging domain (BD), which links the antennae projection (AP) to the β -barrel of VirB10 homolog TraF_{pKM101}. Previously, I showed that deletion of this BD resulted in attenuated levels of DNA transfer (see chapter 5). Here, I show that, unlike the G272R substitution mutation, deletion of this region as well as the associated AP that extends from the β -barrel forming the outer membrane cap of the core complex does not result in leakage of protein substrates to the milieu. This work emphasizes not only the importance of the bridging domain but also the general role of VirB10 in mediating translocation of substrates across the outer membrane.

The features of VirB10 as a putative envelope spanning subunit (67, 68) and as a coupler of inner membrane energy to outer membrane translocation (83) suggests VirB10 might regulate channel activity at the outer membrane. Here, I showed that the G272R mutation appears to specifically disrupt the T4SS channel gating versus non-specifically disrupting the outer membrane (Fig. 6.1). The data from E. Cascales that this mutation confers a constitutive 'energy-activated' conformation even in ATP-depleted cells is in line with the idea that the G272R mutation locks the channel into an 'open' configuration.

It is important to note, however, that in wild-type cells the energy-activated form of native VirB10 is also proteolytically degraded. Yet, wild-type cells do not release detectable levels of protein substrates (Fig. 6.1 A and data not shown). G. Waksman located the G272R mutation in the VirB7/VirB9/VirB10 core complex modeled from the pKM101 X-ray structure, showing its exposure on the interior surface of the core complex near the outer membrane (Fig. 6.5 A and B). This mutation, which consists of the introduction of a positive charge, may cause a conformational change that disrupts gating of the outer membrane pore leading to substrate leakage. Thus, while the G272R mutation appears to lock the channel into an open conformation, in wild-type cells additional checkpoints must be

Figure 6.5 Modeling of G272R in pKM101 crystal structures

A) Space-filling model of the pKM101 core complex comprised of homologs of VirB7 (TraN) in pink, VirB9 (TraO) in blue, and TraF (VirB10) in gray corresponding to the β -barrel/linker domains and yellow/green to the AP α -helices and intervening loop. VirB10 Gly272, corresponding to TraF Gly294, is indicated in red. B) Ribbon model of VirB10 (TraF) showing β -barrel, an α -helical lever arm extension, and antennae projection (AP). The G272R mutation sits in an unstructured linker domain between the β -barrel and AP. Modeled by Dr. Gabriel Waksman.



present to prevent the 'energy-activated' channel from translocating substrate until productive contact with target cells is established. In view of these observations, it is interesting to suggest that transenvelope VirB10 may also function as a transducer of a cell-contact-mediated signal(s) to activate substrate transfer through the T4SS. Such a transducer function could be required for propagation of the 'mating' signal, an unspecified recipient-produced signal that was postulated to exist by early investigators of the F-plasmid transfer system (219-221). The G272R mutation might bypass this signal rendering cells transfer competent even in the absence of a target cell.

The proposed outer membrane gating mechanism likely requires energy; however, energy is not readily available at the outer membrane. The periplasm does not maintain a pool of ATP and the outer membrane is unable to sustain an electrochemical gradient. VirB10 sensing of ATP binding or hydrolysis by the inner membrane channel ATPases, likely results in structural changes necessary not only for productive complex formation but also dynamic opening and closing the outer membrane pore. A similar mechanism for energy transduction to the outer membrane is seen in the TonB system that uses the inner membrane proton motive force, as well as the aerolysin secretion system of *Aeromonas hydrophila*, which relies on ATPase ExeA and TonB-like protein ExeB (222, 223). VirB10 might differ from TonB in that a target cell contact might also serve to regulate channel gating. Another notable difference is that whereas TonB activates transport by inducing conformational changes in an outer membrane transporter, VirB10 likely regulates assembly or activity of its own outer membrane AP pore.

Finally, it is of considerable interest that the G272R mutant, similar to the Δ AP and Δ BD (see chapter 5), was also defective in T-pilus biogenesis (Fig. 6.3). The G272R mutation completely blocked extracellular release of VirB2 and pilus-associated protein VirB5, whereas the deletion mutants showed disrupted pilus production but still allowed for release of monomers or short oligomers of VirB2. The G272R mutation appears to block delivery of VirB2 and VirB5 across the outer membrane, either as monomers or polymers, while the deletion mutants specifically disrupt T-pilus polymerization. It is still unknown if the T-pilus initiates polymerization from the inner membrane, extending through the core complex, or at the outer membrane using, perhaps, VirB10 as a platform. Cysteine accessibility labeling of the VirB2 cellular-associated and T-pilus forms supports the latter model (see Chapter 1 and (130)). Together the predicted flexible nature of the VirB10 AP/BD region, its position at the outer membrane pore, and the genetic evidence from mutations provide support for a model in which VirB10 actively participate during T-pilus

polymerization. Although details of the T-pilus polymerization reaction(s) remain unknown, a possible mechanism of action of the AP is offered through studies of the chaperone-usher pathway of Pap pilus biogenesis. For these pili, which are phylogenetically unrelated to T4SS-encoded pili, subunit polymerization takes place by a 'donor-strand exchange' mechanism, wherein a chaperone provides a temporary β -strand for folding of the pilin subunit; the next incoming pilin subunit displaces the chaperone β -strand with one of its own, resulting in polymerization at the outer-membrane (207). Conceivably, the VirB10 AP functions as a donor strand to promote folding of VirB2 pilin monomers; during the polymerization process, a hydrophobic helix of one pilin subunit might replace the VirB10 AP. Further studies will test this model vs. an alternative in which the AP serves more passively as a gating domain to regulate pilus/pilin passage across the outer membrane.

In conclusion, the G272R mutation as well as the bridging domain and antennae projection deletions highlights the role of VirB10 in substrate trafficking across the outer membrane and assembly of T-pilus. It is curious to think how a single machine subassembly can remain 'open' for protein substrates but 'closed' for VirB2 release. VirB10 might differentially regulate assembly/function of the secretion channel and T-pilus by distinct mechanisms and possibly as a component of different VirB subassemblies.

Chapter 7: Summary, Future Studies, and Perspectives

NOTE: Electron microscope images presented in this chapter were taken by Dr. Angel Paredes (University of Texas Health Science Center – Medical School – Pathology Department – Houston, TX) and denoted in the figure legend. I performed all sample preparations for electron microscope experiments.

Summary

The focus of this work has been to further characterize *A. tumefaciens* VirB2 pilin with respect to assembly of the secretion channel and T-pilus. My work focused primarily on VirB2, VirB4, and VirB10 which are all essential components of the VirB/D4 type IV secretion system (T4SS) (25, 104, 128, 133). A primary goal of the research presented here was to gain a broader understanding of the energetic, structural, and molecular events underlying the contributions of VirB2 pilin in assembly of the T4SS. Currently, there is little structural information for the VirB2 pilin subunit except for basic *in silico* analysis (115, 116, 224). There is some biochemical data describing early processing of pro-pilin to mature pilin (25) and contributions of certain VirB subunits to T-pilus biogenesis (122). However, prior to my studies, the specific roles of the VirB ATPases or of VirB10 in promoting incorporation of the pilin into the secretion channel or T-pilus was fundamentally unknown. Studies summarized below bring to light new findings regarding intermediate steps in the T-pilus pathway and assign specific roles for ATPases VirB4 and VirB11 along with domain contributions of VirB10.

Studies presented in chapter 3 examine the detailed structure of VirB2 at the inner membrane, as part of the secretion channel, and within the T-pilus by use of scanning cysteine accessibility method. Past studies using sequence hydrophathy had established that VirB2 possessed two hydrophobic stretches that likely created two transmembrane domains at the inner membrane. VirB2 was predicted to move from the inner membrane allowing for T-pilus polymerization in the presence of the remaining T4SS VirB subunits. I predicted that VirB2 would likely undergo a structural transition in response to T4SS activation. I tested this hypothesis by inserting unique cysteine residues along the length of VirB2 and assessing for changes in Cys labeling in the presence and absence of the VirB proteins. Initial phenotypic studies showed i) Cys substitutions at the N and C termini disrupted protein stability or function and ii) a C-terminal mutation (G119C) selectively abolished secretion channel activity without affecting T-pilus production. I then defined the inner membrane topology of VirB2 - comprised of two transmembrane regions, a small cytoplasmic loop, and a long periplasmic loop containing the covalently linked N and C termini. Next, I showed the cellular-associated form of VirB2 demonstrated differences in labeling consistent with extraction of the pilin from the inner membrane when in the presence of the other VirB subunits. I also showed that the labeling patterns of Cys mutants produced in a Tra^+ , Pil^- uncoupling mutant strain matched the isogenic, phenotypically wild-type strain, but differed appreciably from labeling patterns of pilins assembled into T-pili. In

the isolated T-pilus, Cys residues at positions 64, 67, and 77 but not elsewhere in the pilin were labeled, indicating that only a short motif comprised of hydrophilic and hydrophobic residues is surface-exposed. These findings supplied the first information about the pilin structural organization when assembled as an inner membrane pilin pool, and when incorporated into the secretion channel and the T-pilus.

Chapter 4 focused on determining the role of energy during early steps in the T-pilus biogenesis pathway. I proposed that the extraction of VirB2 from the inner membrane for further machine assembly requires one or more of the VirB ATPases. I again used my collection of Cys-substituted pilins to monitor differences in the VirB2 structural state in different genetic contexts. I determined that Cys-substituted pilins produced in strains lacking or producing the VirB4 or VirB11 ATPases exhibited differences in MPB-labeling patterns. I further showed that VirB4 synthesis, but not the Walker A box binding motif mutant, was correlated with labeling of a VirB2 cytoplasmic residue Cys94 regardless of the presence of other VirB proteins. Additionally, co-synthesis of VirB4 and VirB11 was correlated with labeling of periplasmic Cys64. I also showed that VirB2 and VirB4 formed an immunoprecipitable complex. Finally, I determined that VirB2 was released from the inner membrane in cells producing VirB4, but not in a $\Delta virB4$ mutant strain or a $\Delta virB4$ strain producing a VirB4 Walker A motif mutant proteins but no other VirB proteins. Overall, my findings support a model in which the VirB4 ATPase catalyzes extraction of VirB2 pilin from the inner membrane. Although the VirB11 ATPase is not required for pilin dislocation, it does seem to participate in modulating the VirB2 structural state during or after dislocation.

In chapter 5, I presented work characterizing the contribution of individual VirB10 domains to T-pilus biogenesis and substrate transfer. VirB10 was previously shown by the Christie lab to sense ATP energy at the inner membrane resulting in a conformational change within VirB10 leading to complex formation (83). A series of mutations were generated, by V. Krishnamoorthy and I. Garza, to determine the function of specific regions within VirB10. Phenotypic studies identified Tra⁺ Pil⁻ “uncoupling”: mutations that mapped to the N-terminal cytoplasmic region and transmembrane domain and the C-terminal $\alpha 2, \alpha 3$ helix (AP) extending from the β -barrel domain. On the basis of the “uncoupling” phenotypes, I propose that the extreme N-terminus, TM α -helical registry, and β -barrel antennae projection, assisted by the bridging domain, form specific intermolecular interactions that are critical for biogenesis of the T-pilus but not for a functional secretion channel. Together the data imply that VirB proteins can alternatively assemble as a secretion channel or a platform for the T-pilus.

In chapter 6, I focused on further characterizing a mutant from the laboratory of Dr. Lois Banta, identified during a screen for 'leaky' substrate channels. VirB7, VirB9, and VirB10 subunits form a stabilizing core complex early during activation of the T4SS (2, 3, 30). A detailed crystal structure of the pKM101 outer membrane core complex, from the Waksman lab, has revealed that VirB10 forms the external most part of the outer membrane pore. These findings have led to our hypothesis that VirB10 regulates substrate passage through the distal portion of the translocation channel. The Banta lab screened for mutations that would confer release of a tagged protein substrate (FLAG-VirE2) to the surface in the absence of a target cell. The screen identified one mutation G272R that mediated VirE2 release and also rendered the mutant insensitive to cellular ATP depletion. Notably, G272R was blocked for T-pilus biogenesis but unaffected in substrate delivery to plant and bacterial recipient cells. Modeling of the mutation by Dr. Gabriel Waksman showed that the G272R mutant is located near the antennae projection (AP) within the bridging domain (BD) of VirB10 homologue TraF_{pKM101}. The AP and BD form the outer membrane pore and deletion of these regions phenotypically resembled the G272R mutation by allowing substrate transfer but blocking T-pilus assembly; however, these deletions did not permit leaking of FLAG-VirE2. I propose that i) the G272R mutation disrupts regulation of substrate trafficking by locking the secretion channel in an 'open' position resulting in substrate leakage, and ii) the G272R mutation as well as the partial AP and BD deletion mutations selectively disrupt pilus polymerization by preventing formation of an outer membrane assembly platform. How the G272R mutation can confer substrate leakage without affecting intercellular substrate transfer, while also blocking pilus biogenesis, are intriguing questions for further studies. A working model is that the VirB10 contributes to substrate transfer or pilus biogenesis by modulating the structural organization of its AP and BD as a function of energy transduction from the inner membrane ATPases and sensory recognition of an extracellular signal(s) derived from a productive target cell interaction.

This work highlights the intriguing yet complex nature of type IV secretion systems. My studies contributed novel information pertaining to i) the structural organization of the VirB2 pilin in the inner membrane, secretion channel, and T-pilus ii) the role of an ATPase in driving pilin dislocation, and iii) contributions of VirB10 domains to T-pilus biogenesis and substrate transfer across the outer membrane. While these findings significantly advance our understanding of the structural, energetic and molecular events underlying type IV secretion system assembly and function, clearly there are still many unanswered questions.

Future Studies

The following experiments are meant to extend the analyses of the studies presented here.

Test the model that VirB2 accumulates in the inner membrane as a prerequisite to its polymerization into the T-pilus and secretion channel

Although early processing of the VirB2 propilin involving cleavage of the signal sequence and cyclization proceed via integration into the inner membrane, there is little experimental support for the notion that the mature pilin accumulates a pool in the membrane (delayed incorporation) (175, 225). An alternative model is that upon processing the pilin is immediately dislocated for polymerization into the secretion channel or pilus. In chapter 3, I presented evidence that the VirB2 Cys51 mutant protein is labeled in the absence but not the presence of other VirB proteins. This labeling pattern is not consistent with the accumulation of a pilin pool, as it is unlikely that the synthesis of other VirB proteins would result in extraction of all pilin monomers. Thus, at least a subset of the Cys51-substituted pilins should still label even in wild-type cells. The one caveat to this line of reasoning, however, is that the Cys51 substitution is a loss-of-function mutation. This phenotype prevents firm conclusions about findings relating to the structural organization of this mutant.

Further studies evaluating the pilin 'pool' model would involve screening other Cys-substitutions that do not block protein function, but display the same MPB labeling pattern as the Cys51 mutant protein. Such a mutation would constitute compelling genetic evidence against the pilin pool model. Another line of study would involve use of different promoters to modulate the timing of VirB2 synthesis relative to the other VirB proteins. For example, *virB2* expression by a tightly-controlled promoter could be used to synthesize a pool of membrane-integrated pilin prior to synthesis of the remaining VirB proteins from the acetosyringone-inducible *virB* promoter. Two such promoters that function in *A. tumefaciens* include the salicylic acid inducible *nah* promoter (*Pseudomonas*) and arabinose-inducible BAD promoter (*Escherichia coli*) (226, 227). In addition, a new set of LacI-based expression vectors was created for *E. coli* that are inducible by addition of isopropyl β -D-1-thiogalactopyranoside (IPTG) (228). Temporal expression of *virB2* would be monitored by transcript and protein accumulation via RT-PCR and Western blot analyses, respectively. Cells would be induced for synthesis of VirB2, then the inducing signal would be removed by centrifugation of cells and resuspension in fresh media. The remaining *virB* genes would be induced from the native promoter and assayed over time for

accumulation of pilin at the cell surface, pilus production, protein stability, and substrate transfer. Variations on this temporal gene expression assay could include reversing the time course of *virB2* vs. other *virB* gene expression, and differential synthesis of VirB4 with other VirB proteins to monitor the kinetics of pilin dislocation from the membrane. These kinds of studies should allow for a rigorous test of the pilin 'pool' model.

It is also of central interest to define the kinetics of pilus assembly and where on the cell surface the pilus polymerizes. Other studies have used immunogold labeling and phage fluorescence (175, 225, 229, 230) to observe the movement of pilin subunits from a pre-formed pool and monitor pilus extension. A similar technique could be used in *A. tumefaciens*; however, this application is more difficult in *Agrobacterium* because of its smaller size and lack of T-pilus-binding phage. A potential fluorescence recognition site that could be used is Fluorescein Arsenical Hairpin binder (FIAsH) which is a tetra cysteine motif that strongly interacts with fluorophores. This application might allow for real-time monitoring of pilus biogenesis and perhaps movement of pilin monomers across the cell envelope (231). However, tagged versions of VirB2 have proven difficult to produce. I engineered seven FLAG and tetra-cysteine motifs in different locations along the length of VirB2 using mutagenic PCR or cloning. I designed an *SphI* flanked FIAsH tag Kanamycin resistance cassette to place the FIAsH tag into the *SphI* site created by some of the Cys substitution mutants within VirB2 (Fig. 7.1A). Two tags could be accommodated without loss of protein function: a FLAG tag placed directly after residue 85 and a tetra-cysteine motif (FIAsH) placed in the *SphI* site created by the Cys83 substitution resulting in Ala-Cys-Cys-Pro-Gly-Cys-Cys-Cys (Fig. 7.1B). It is interesting that residues 83 and 85 are in the domain II hydrophobic patch within VirB2, near the cytoplasmic loop. Even though the FLAG tag introduces a cluster of negative charges near this loop, the tagged protein is still functional. Since this would violate the 'positive-inside' rule of von Heijne (164), it is intrinsically interesting to explore the mechanism by which this FLAG-tagged variant inserts into the inner membrane. However, for the pilus assembly kinetics and positioning studies, unfortunately, neither the FLAG- or FLAsH-tagged variants could be detected with anti-FLAG or addition of the FLAsH reagent (J. Kerr, data not shown). Because both tags might be buried in the pilus lumen, I suggest that additional FLAG tags be inserted within the region of VirB2 that I showed to be surface-displayed in the isolated T-pilus, e.g., between residues 67-77. This collection of FLAG or FIAsH tagged variants could be used in fluorescence microscopy studies aimed at characterizing the timing and placement of pilus polymerization on the cell surface.

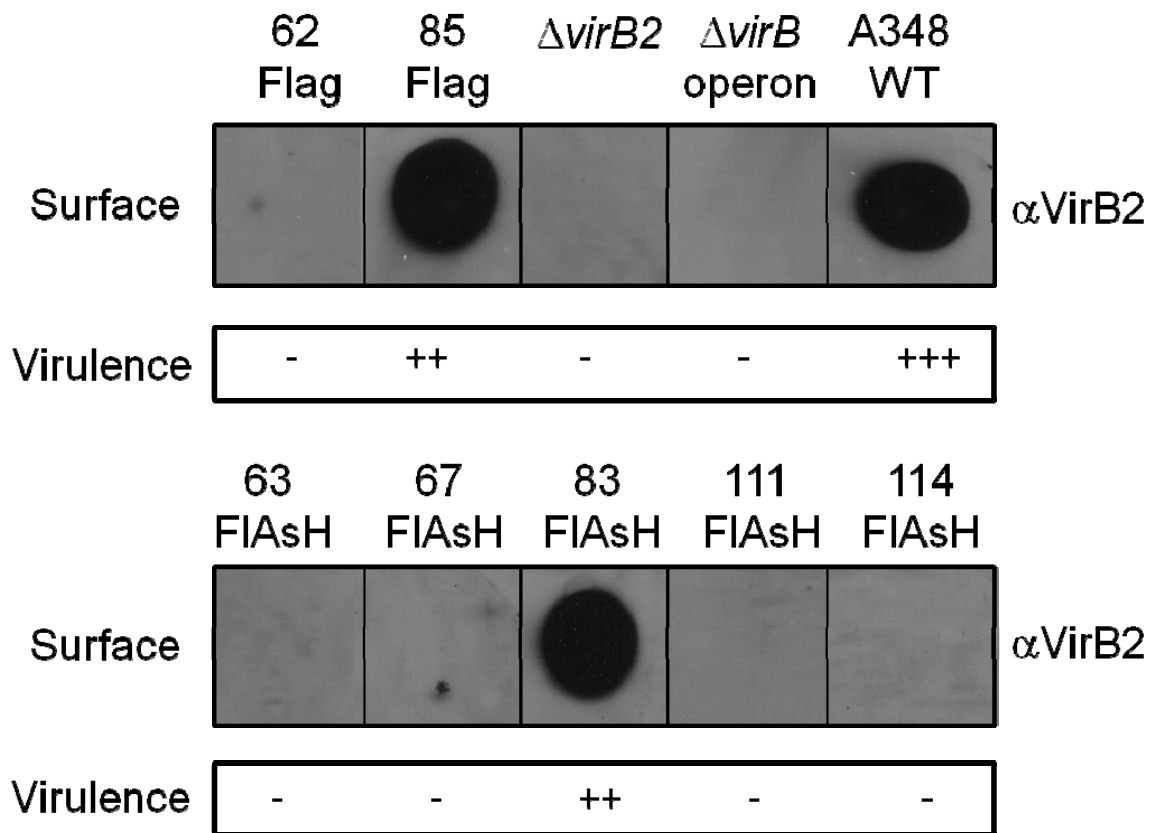
Figure 7.1 Schematic of FIAsh tag cassette and effects of tag introduction into VirB2 on surface display of VirB2 and virulence

A) Schematic of FIAsh tag cassette. Kanamycin resistance cassette (Kan^R) was PCR amplified from broad host range plasmid pXZ151 and flanked with a *Sma*I enzyme site and half of the FIAsh tag with an SphI site. Triangles represent enzyme sites. B) Extracellular blot (surface) assay of Flag and FIAsh tagged versions of VirB2. Negative controls $\Delta virB$ operon and $\Delta virB2$, and positive control WT: wild type strain A348. Mutagenic PCR was used for introduction of Flag 62, 85 and FlaSH 63, 114. FIAsh tag cassette in (A) was used for introduction of the tetra-cysteine motif at SphI sites created by Cys substitutions at residues 67, 83, and 111. Kanamycin cassette was removed following cloning by a *Sma*I digest. Virulence monitored by plants inoculation and scored on a scale of no virulence - to wild-type virulence +++.

A



B



Defining the Structure of the T-Pilus and Pilin Subunit Packing

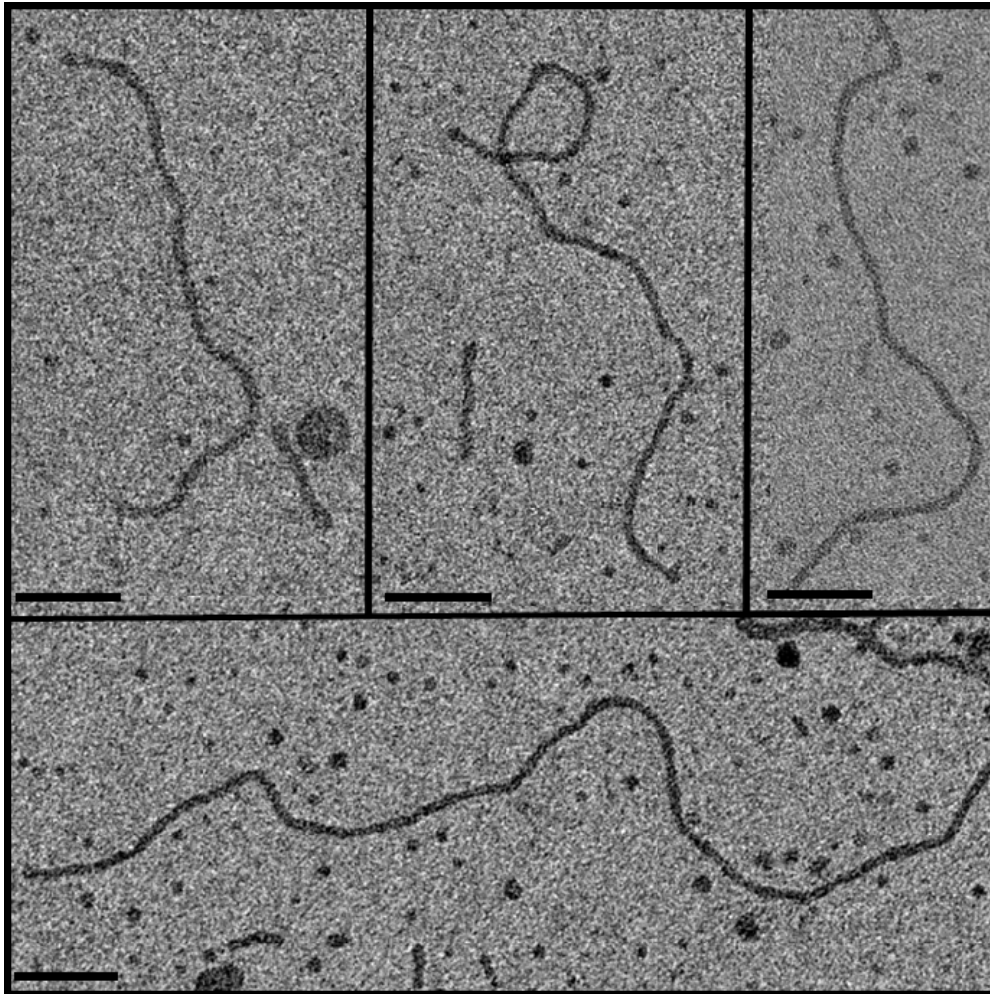
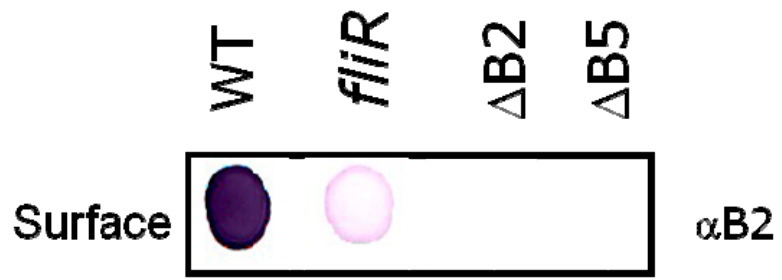
Studies presented in chapter 3 showed that VirB2 adopts different structural states in the inner membrane, secretion channel, and T-pilus. MPB-labeling further revealed that a patch of both hydrophilic and hydrophobic residues is exposed on the T-pilus surface. This presented the first structural information about the VirB2 pilin packing geometry within the T-pilus. Future studies aimed at defining the T-pilus structure are important because of another central, but unresolved question in the field of T4SSs: do substrates travel through the pilus? Although the isolation of Tra⁺, Pil⁻ "uncoupling" mutations establishes that the T-pili are not necessary for substrate transfer, other investigators suggest that T4SS-encoded pili function as conduits for substrate transfer (156, 232, 233). High-resolution structural information about the T-pilus would establish whether the T-pili have a lumen and, if so, whether it is of sufficient diameter to accommodate passage of secretion substrates.

I invested a large amount of time and effort attempting to purify the T-pilus for structural analysis. Purification proved challenging mainly due to contamination by the bacterial flagellum. I tested several purification protocols involving sequential density gradient centrifugation, e.g. sucrose and cesium chloride, and differential precipitation using excess magnesium chloride. These methods served to enrich the T-pilus, however, contaminating flagella were still present. We sent a highly enriched pilus sample to Dr. Joe Wall at Brookhaven National Labs for a mass per unit length measurement by scanning transmission electron microscope (STEM); this value was essential for use of iterative helical real-space reconstruction (IHRSR) software for generating a high resolution structure from pilus images collected by transmission electron microscopy. Results of the STEM analysis showed that the T-pilus filament appeared to vary in mass per unit length measurements. This may be due to an alternating structural arrangement along the length of the T-pilus, or to sample degradation or contamination with other fimbriae or flagella

I attempted to purify the T-pili from flagellar-minus mutant strains *nt1reB* (234) and *fliR* (235). However, the flagellar-minus mutant strains elaborate only very low levels of T-pili (Fig. 7.2). While exploring the underlying mechanism responsible for the apparent coordinated synthesis flagella and T-pili is of interest, the use of flagellar mutants complicates efforts to purify T-pili in sufficient amounts for image reconstructions. Future studies should explore the possibility of using other 'bald' strains or attempting to construct a tagged, functional VirB2 variant that could be used for pilus enrichment by affinity chromatography followed by other chromatography steps, e.g., gel filtration, to

Figure 7.2 Effects of flagella minus mutant on surface display of VirB2 and observed T-pili

Upper panel: *fliR* mutant displays reduction in extracellular VirB2 release. Extracellular blot (surface) assay of flagella minus strain, *fliR* and negative controls $\Delta virB2$ and $\Delta virB5$. WT: wild type strain A348. Lower panel: Electron micrographs of T-pili. Isolated T pili from a flagella minus strain *fliR* were stained with 1% Uranyl acetate. Samples were viewed using a Joel 1200 microscope. Black bar represents 50nm. Electron micrographs pictures were taken by Dr. Angel Paredes PhD from samples I prepared.



the purification protocol. With a completely pure sample, images could be collected by electron microscopy for IHRSR.

Another way to gain structural information about the T-pilus is to refine our knowledge of the pilin subunit packing geometry with a combination of SCAM and disulfide crosslinking studies with or without oxidative catalysts, e.g., copper phenanthroline or thiol-reactive chemical crosslinkers (236, 237). To date, I characterized a total of 16 Cys-substituted pilins. In addition to the studies reported earlier in this thesis, I assayed for the capacity of Cys-substitutions to form disulfide crosslinks in isolated T-pili. My initial findings support the idea that the hydrophobic residues in domain II of adjacent monomers form a packing interface. Those in the hydrophilic domains do not appear to form close contacts with the corresponding region of adjacent monomers. Those of hydrophobic domain IV also do not appear to pack against one another, but as noted in Chapter 3, this domain possesses a Gly zipper motif which could participate in packing of VirB2 monomers. Therefore, it is necessary to introduce additional Cys substitution mutations in this domain for a more complete analysis (Fig. 7 3). Ideally, all functional Cys-substituted pilins among the entire set of 74 replacements of native residues in the mature pilin would be subjected to the types of MPB labeling analyses I carried out thus far. Additionally, for the subunit-subunit packing studies by oxidative or chemical crosslinking, it would be necessary to combinatorially express pairs of Cys-substituted pilins. These studies would very accurately identify residues in the assembled T-pilus that are surface-exposed, exposed in the presumptive lumen, and buried in subunit – subunit interfaces.

Confirm the Dislocase Activity of VirB4 and Identify Regions Required for VirB2-VirB4 Interaction and Dislocase Activity

Scanning cysteine accessibility, immunoprecipitation, and osmotic shock experiments all provided evidence that VirB4 functions as a pilin dislocase (chapter 4). Future studies should rigorously test this model by i) assaying for dislocase activity *in vitro*, and ii) identifying regions of VirB2 and VirB4 required for dislocase activity. VirB4 dislocase activity can be tested further by using an *in vitro* reconstitution assay. Membrane vesicle fusion experiments have previously been used to demonstrate and characterize the *E. coli* FtsH dislocase activity (186, 238). Akiyama and Ito (238) showed that fusion of membrane vesicles carrying ATPase FtsH with vesicles containing an FtsH substrate resulted in translocation and FtsH-mediated degradation of the substrate. We do not think VirB4

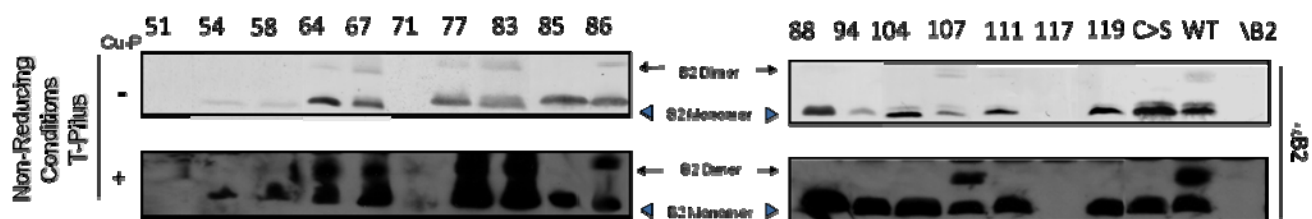
Figure 7.3 Disulfide crosslinking of Cys-substituted VirB2 in the T-pilus

Immunoblots of isolated T-pili developed with anti-VirB2 antibodies showing migration of native VirB2 and mutant proteins in A) reducing B) non-reducing Tricine SDS-polyacrylamide gels. Non-reducing conditions in the presence (+) or absence (-) of the oxidative crosslinker Copper phenanthroline (Cu-P).

A



B



functions as a protease, so the FtsH dislocase assay would need to be modified. Initial efforts could involve isolating membrane fractions from *A. tumefaciens* strains producing VirB2 alone or VirB4 alone and mixing them together in the presence of PEG to fuse the membranes. To assay for pilin release, one could attempt to use differential centrifugation to separate the membrane vesicles from the pilin. However, even when released the hydrophobic pilin might associate with or even re-integrate into the membrane. It could be possible to make use of cysteine labeling to define VirB4-mediated changes in the pilin structural state. Following membrane fusion, addition of MPB might identify exposed Cys residues that in the absence of VirB4 are buried from this thiol-reactive reagent.

VirB4-like ATPases have been found associated with all known T4SSs (15) and display similar physical properties such as size and the presence of conserved NTP-binding motifs. To examine whether dislocase activity is a common property of VirB4 homologs, approaches similar to the ones I used in my studies could be used. Interestingly, the lipid composition of the membrane appears to dramatically influence the functionality of several bacterial virulence systems (239, 240). *A. tumefaciens* mutants lacking the lipid phosphatidylcholine were shown to be unable to cause the formation of tumors on plants (239). Recently, the ATPase TrwB, a coupling protein from the R388 system and homolog of VirD4, was successfully purified and reconstituted into liposome bilayers (241). This ATPase was shown to only express specific NTP binding activity when in the presence of a membrane environment. These studies indicate that care must be taken when using reconstituted liposomes systems in order to maintain proper protein function.

Another line of study should focus on analyzing VirB2 and VirB4 mutants to define regions required for interaction and putative dislocase activity. Our lab has a large number of VirB4 truncation and substitution mutants and a growing collection of VirB2 mutants available to test for potential loss of interaction as monitored by immunoprecipitation and dislocation as monitored by osmotic shock. I predict that a region of VirB4 that spans the inner membrane is required for pilin dislocation via a direct protein-protein interaction. As shown in Chapter 4, I supplied evidence by MPB-labeling for the extramembraneous location of at least one VirB4 Cys residues. Further MPB-labeling studies of VirB4 Cys-modified proteins (lacking some or all of the existing Cys residues, or carrying other Cys replacements in putative periplasmic domain(s)) would further define the transmembrane domain(s) and potentially localize the pilin interaction domain. Additional mutations in this domain could be characterized for effects on the VirB4 - pilin interaction and on pilin dislocation.

Confirm the Role of the VirB10 AP/BD in T-Pilus Polymerization

Results from Chapter 5 and 6 showed that VirB10 has a large influence on the pilus biogenesis pathway. Most interestingly, the TM domain, the antennae projection (AP), and bridging domain (BD) all appear to selectively contribute to T-pilus formation. Future studies should test a model that the VirB10 AP forms the pore through which VirB2 pilin subunits exit and actively promotes the polymerization of the T-pilus through direct contact.

My data suggest that deletion of the VirB10 AP confers release of VirB2 as monomers, aggregates or short polymers. Follow-up studies should analyze the oligomeric state of pilin on the surface of these cells by electron microscopy to further define the function of the AP in pilus polymerization. A complementary approach would be to characterize the structural organization of pilin released by the Δ AP mutant by MPB labeling, and compare the labeling profile with that of pilins produced in the functionally wild-type strain. These studies would begin to test our hypothesis that the VirB10 AP participates in polymerization of the pilin subunits, perhaps by a strand-exchange method.

Further tests of this hypothesis would assay for a VirB2 interaction with VirB10, in particular, the AP/BD region. Such an interaction could be detected by coimmunoprecipitation (Co-IP) studies in the absence and presence of a protein crosslinker. If an interaction were observed, deletion constructs and point mutations would be tested in parallel to see if the interaction were disrupted and also, whether or not the interaction is dependent on the presence of other VirB proteins, e.g. other core components, ATPases, etc. Due to the potentially transient nature of the VirB2-VirB10 interaction, disulfide crosslinking experiments pairing cysteine substitutions within VirB2 (see chapter 3) and cysteine substitutions within VirB10 (69) may be more effective at trapping a VirB2-VirB10 interaction.

If the VirB10 AP region is found to interact with VirB2, future studies should focus on defining the requirements for this interaction. The AP region could be expressed as a tagged protein fragment and tested for potential interaction with VirB2 via Co-IP and protein-pull down assays. This fragment could then be overexpressed in the presence of native VirB10 and tested for negative dominance on T-pilus polymerization. Strains bearing mutations that permit substrate transfer but block pilus production (Tra⁺, Pil⁻ 'uncoupling mutations) could also be tested for a loss of VirB2-VirB10 interaction.

Determine if Deletion of the AP Domain Changes the Extracellular Localization VirB2 and VirB5

The T-pilus form a long thin (~10nm) filament that probably extends from the cell pole (104, 121). Immunogold labeling has shown that VirB5 primarily localizes to the tip of the T-pilus, while VirB2 extends the entire length of the pilus (121). In future studies, it will be important to determine if the AP contributes to the spatial positioning of the pilin or pilus at the cell surface. This could be achieved by analyzing the extracellular distribution of VirB2 and VirB5 at the cell surface of wild-type vs. AP mutant strains using a combination of immunofluorescence microscopy (IFM) and immunogold labeling paired with electron microscopy.

In previous studies, it was shown that each VirB protein is required for elaboration of the T-pilus (104). However, I observed that deletion of *virB1* reduces but does not completely abolish accumulation of extracellular VirB2, as monitored by the colony blot assay and T-pilus shear assay (Fig. 7.4). Interestingly, although in previous studies VirB5 routinely displayed the same requirements as VirB2 for surface display, I was not able to detect VirB5 in a $\Delta virB1$ mutant with the colony blot assay. I also was able to detect VirB2 but not VirB5 on the cell surface of the $\Delta virB1$ mutant by immunofluorescence microscopy, even though both VirB2 and VirB5 accumulated at abundant levels in these cells (Fig. 7.5). These findings raise the intriguing possibility that VirB1, a lytic transglycosylase (242), may participate in polymerization of the pilus. Since my studies highlighted the importance of VirB10 for pilus assembly, in future studies it will be interesting to determine whether VirB1 coordinates with VirB10 for pilus production. It is conceivable that the ΔAP mutant also selectively blocks surface localization of VirB5, or that the $\Delta virB1$ mutant also releases pilin monomers to the extracellular milieu. I could envision a model in which VirB1 interacts with VirB10 to promote delivery of the pilus-tip-associated VirB5 subunit to the VirB10 AP. This reaction would be required as a nucleation event for VirB2 recruitment and polymerization into the T-pilus. In the absence of VirB5-VirB10 AP complex formation, VirB2 pilin would not nucleate properly but in certain mutant strains, e.g., channel gating mutants, could still be released to the cell surface as monomers, aggregates or short polymers. In future studies, it will be intriguing to define the requirements at the outer membrane involving VirB1, VirB5, and the VirB10 AP for pilus polymerization.

Figure 7.4 Effects of *virB* deletion mutations on surface display of VirB2 and VirB5

A) total cellular material subjected to gel electrophoresis and blot development with anti-VirB2 or anti-VirB5 antibodies revealing total cellular levels of the protein (cellular); B) colony immunoblots developed with anti-VirB2 or anti-VirB5 antibodies showing presence of surface-exposed pilin protein (surface); C) extracellular shear fraction subjected to ultracentrifugation, gel electrophoresis and immunoblot development with anti-VirB2 or anti-VirB5 antibodies revealing presence of high-molecular-weight T pilus (shear).

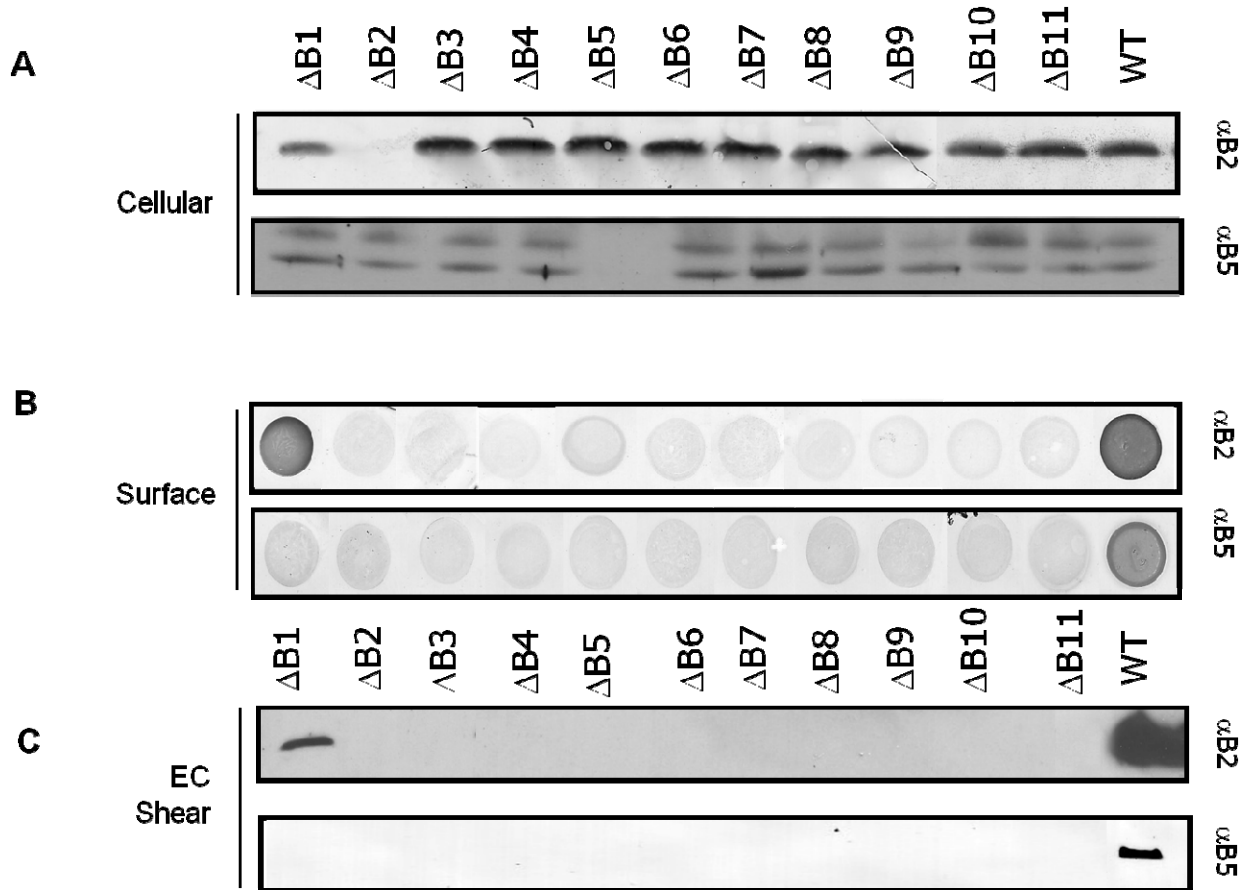
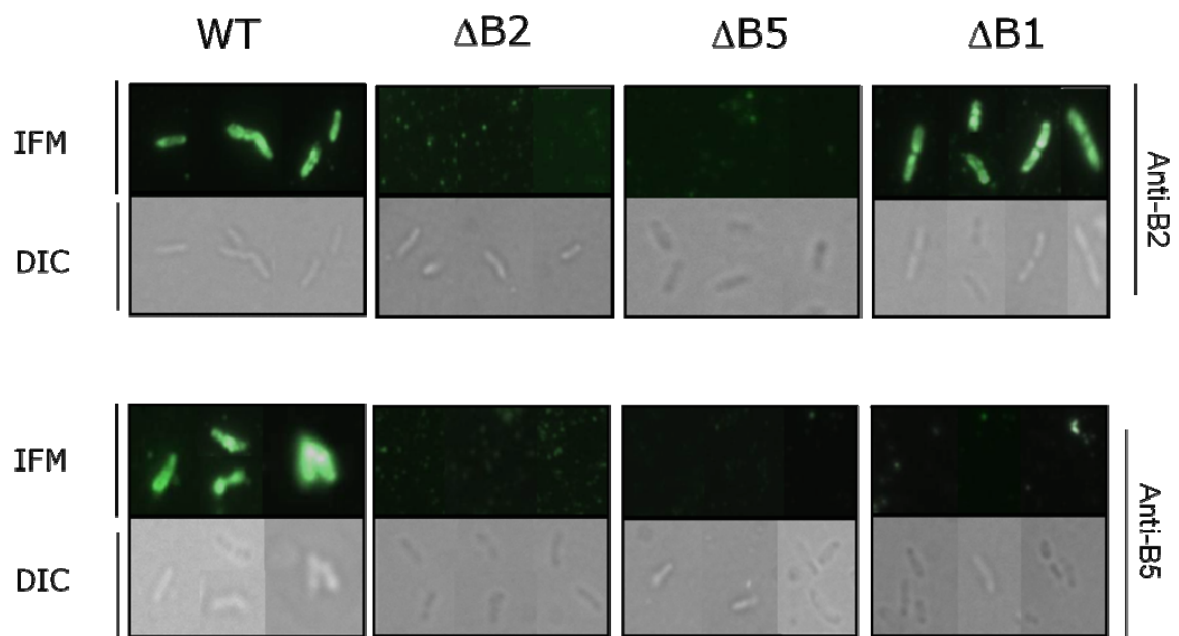


Figure 7.5 : Immunofluorescence assays showing localization VirB2 and VirB5 in the wild-type strain and nonpolar *virB1*, *virB2*, and *virB5* deletion mutants

VirB2 and VirB5 localization as monitored by immunofluorescence (IFM). AS-induced cells were examined by IFM for VirB2 or B5 localization with Alexa-488- goat anti-rabbit IgG probed with anti-VirB2 and anti-VirB5 antibodies. Corresponding DIC images by Nomarski microscopy shown below. VirB2 and VirB5 both display peripheral fluorescence in wild type cells, while only VirB2 shows fluorescence in the absence of VirB1.



Screen for Effectors From other T4SSs Using ‘Leaky’ Channel Mutant

The ‘leaky’ channel mutant identified during the screen by the Lois Banta’s lab presents a unique tool for identifying new, unknown substrates from related T4SSs. The G272R mutation could serve as the genetic context for the introduction of a DNA library containing tagged, unknown substrates that, like FLAG-VirE2, could be monitored for release to the cell surface using the colony blot assay. In the limited studies of substrate recognition signals, there is evidence that substrates from phylogenetically diverse species carry similar secretion motifs (15). If so, the *A. tumefaciens* VirB/VirD4 system might be a useful surrogate for identification of secretion substrates of T4SSs from bacterial species that are not genetically manipulable. For many human pathogens genetic tools and manipulations are not available. A simple translocation assay based on release of effectors to the *A. tumefaciens* cell surface could prove very useful for identification and characterization of T4SS effectors from medically-important pathogens

Perspectives

This is an exciting time for Type IV secretion systems (T4SS), as major structural breakthroughs are providing unprecedented detail about the architecture of these extraordinarily complex machines. The structures of the pKM101 outer membrane core complex provide excellent detail and allow our field the opportunity to rigorously test the structure/function relationship of these complexes and individual domains. Future advances in the field will need to continue to rely on a combination of *in vivo* biochemical analyses and *in vitro* isolation and structural resolution of larger machine subassemblies in order to answer difficult questions such as: i) Do T4SS assemble as one vs. two organelles, the secretion channel and T-pilus? ii) What is the physical relationship between the secretion channel and the T-pilus? iii) Does T-pilus polymerization initiate from the outer membrane or inner membrane? iv) What is the mechanism of action of VirB4 in dislocating pilin from the inner membrane, and v) What other steps in the biogenesis pathway direct the pilin to its final destination in the secretion channel or T-pilus?

T4SSs are intimately involved with a number of human and plant pathogens. A major, ongoing goal of T4SS research is to discover new ways of preventing these systems from contributing to disease progression (17). Many efforts have focused on identifying new effector proteins (243, 244), expanding vaccine development (245), and designing small molecule inhibitors (246). Intriguingly, outer membrane-associated and surface-localized components of T4SSs have been tested for their ability to induce an immunogenic response. In *Anaplasma*, for example, both VirB10-like and VirB2-like proteins were shown to induce an immune response (18, 245, 247). Determining the principal mechanisms responsible for T4SS biogenesis, channel gating, and intercellular translocation or release of these proteins to the cell surface or milieu is central to the development of prevention and treatment strategies for T4SS-associated diseases.

In recent years, significant progress has been made in deciphering underlying mechanisms and molecular architectures of paradigmatic T4SSs. However, the identification of new uncharacterized T4SSs through genomic sequencing and *in vivo* screens for virulence factors continues to raise more questions about the broad biological functions of these machines in environmental or clinical settings. Ultimately, structure – function studies of many different T4SS's will be necessary to suppress their action or exploit them for novel therapeutic or biotechnological applications.

REFERENCES

1. Cascales, E., and P. J. Christie. 2003. The versatile bacterial type IV secretion systems. *Nat. Rev. Microbiol.* 1:137-150.
2. Waksman, G., and R. Fronzes. 2010. Molecular architecture of bacterial type IV secretion systems. *Trends Biochem. Sci.* *In press.*
3. Wallden, K., A. Rivera-Calzada, and G. Waksman. Type IV secretion systems: versatility and diversity in function. *Cell. Microbiol.* 12:1203-1212.
4. Grohmann, E., Muth, G., Espinosa, M. 2003. Conjugative plasmid transfer in Gram-positive bacteria. *Microbiol. Mol. Biol. Rev.* 67:277-301.
5. Schroder, G., and E. Lanka. 2005. The mating pair formation system of conjugative plasmids - A versatile secretion machinery for transfer of proteins and DNA. *Plasmid* 54:1-25.
6. Ochman, H., J. G. Lawrence, and E. A. Groisman. 2000. Lateral gene transfer and the nature of bacterial innovation. *Nature.* 405:299-304.
7. Karnholz, A., C. Hoefler, S. Odenbreit, W. Fischer, D. Hofreuter, and R. Haas. 2006. Functional and topological characterization of novel components of the comB DNA transformation competence system in *Helicobacter pylori*. *J. Bacteriol.* 188:882-893.
8. Sexton, J. A., and J. P. Vogel. 2002. Type IVB secretion by intracellular pathogens. *Traffic.* 3:178-185.
9. Hamilton, H. L., N. M. Dominguez, K. J. Schwartz, K. T. Hackett, and J. P. Dillard. 2005. *Neisseria gonorrhoeae* secretes chromosomal DNA via a novel type IV secretion system. *Mol. Microbiol.* 55:1704-1721.
10. Bates, S., A. M. Cashmore, and B. M. Wilkins. 1998. IncP plasmids are unusually effective in mediating conjugation of *Escherichia coli* and *Saccharomyces cerevisiae*. *J. Bacteriol.* 180:6538-6543.
11. Bundock, P., D. R. A. den, A. Beijersbergen, and P. J. Hooykaas. 1995. Trans-kingdom T-DNA transfer from *Agrobacterium tumefaciens*. *EMBO J.* 14:3206-3214.
12. Schrammeijer, B., A. Dulk-Ras Ad, A. C. Vergunst, E. Jurado Jacome, and P. J. Hooykaas. 2003. Analysis of Vir protein translocation from *Agrobacterium tumefaciens* using *Saccharomyces cerevisiae* as a model: evidence for transport of a novel effector protein VirE3. *Nucl. Acids Res.* 31:860-868.
13. Waters, V. L. 2001. Conjugation between bacterial and mammalian cells. *Nat. Genet.* 29:375-376.

14. Zhu, J., P. M. Oger, B. Schrammeijer, P. J. Hooykaas, S. K. Farrand, and S. C. Winans. 2000. The bases of crown gall tumorigenesis. *J. Bacteriol.* 182:3885-3895.
15. Alvarez-Martinez, C. E., and P. J. Christie. 2009. Biological diversity of prokaryotic type IV secretion systems. *Microbiol. Mol. Biol. Rev.* 73:775-808.
16. Backert, S., and T. F. Meyer. 2006. Type IV secretion systems and their effectors in bacterial pathogenesis. *Curr. Opin. Microbiol.* 9:207-217.
17. Llosa, M., C. Roy, and C. Dehio. 2009. Bacterial type IV secretion systems in human disease. *Mol. Microbiol.* 73:141-151.
18. Lopez, J. E., G. H. Palmer, K. A. Brayton, M. J. Dark, S. E. Leach, and W. C. Brown. 2007. Immunogenicity of *Anaplasma marginale* type IV secretion system proteins in a protective outer membrane vaccine. *Infect. Immun.* 75:2333-2342.
19. Saenz, H. L., P. Engel, M. C. Stoeckli, C. Lanz, G. Raddatz, M. Vayssier-Taussat, R. Birtles, S. C. Schuster, and C. Dehio. 2007. Genomic analysis of *Bartonella* identifies type IV secretion systems as host adaptability factors. *Nat. Genet.* 39:1469-1476.
20. Cheng, Z., X. Wang, and Y. Rikihisa. 2008. Regulation of type IV secretion apparatus genes during *Ehrlichia chaffeensis* intracellular development by a previously unidentified protein. *J. Bacteriol.* 190:2096-2105.
21. Gillespie, J. J., N. C. Ammerman, S. M. Dreher-Lesnick, M. S. Rahman, M. J. Worley, J. C. Setubal, B. S. Sobral, and A. F. Azad. 2009. An anomalous type IV secretion system in *Rickettsia* is evolutionarily conserved. *PLoS ONE.* 4:e4833.
22. Ninio, S., J. Celli, and C. R. Roy. 2009. A *Legionella pneumophila* effector protein encoded in a region of genomic plasticity binds to Dot/Icm-modified vacuoles. *PLoS Pathog.* 5:e1000278.
23. Fischer, W., R. Haas, and S. Odenbreit. 2002. Type IV secretion systems in pathogenic bacteria. *Int. J. Med. Microbiol.* 292:159-168.
24. Ding, Z., K. Atmakuri, and P. J. Christie. 2003. The outs and ins of bacterial type IV secretion substrates. *Trends Microbiol.* 11:527-535.
25. Lai, E. M., and C. I. Kado. 1998. Processed VirB2 is the major subunit of the promiscuous pilus of *Agrobacterium tumefaciens*. *J. Bacteriol.* 180:2711-2717.
26. Rohde, M., J. Puls, R. Buhrdorf, W. Fischer, and R. Haas. 2003. A novel sheathed surface organelle of the *Helicobacter pylori* *cag* type IV secretion system. *Mol. Microbiol.* 49:219-234.

27. Tanaka, J., T. Suzuki, H. Mimuro, and C. Sasakawa. 2003. Structural definition on the surface of *Helicobacter pylori* type IV secretion apparatus. *Cell. Microbiol.* 5:395-404.
28. Watarai, M., I. Derre, J. Kirby, J. D. Gowney, W. F. Dietrich, and R. R. Isberg. 2001. *Legionella pneumophila* is internalized by a macropinocytotic uptake pathway controlled by the Dot/Icm system and the mouse Lgn1 locus. *J. Exp. Med.* 194:1081-1096.
29. Judd, P. K., R. B. Kumar, and A. Das. 2005. Spatial location and requirements for the assembly of the *Agrobacterium tumefaciens* type IV secretion apparatus. *Proc. Natl. Acad. Sci. U.S.A.* 102:11498-11503.
30. Fronzes, R., P. J. Christie, and G. Waksman. 2009. The structural biology of type IV secretion systems. *Nat. Rev. Microbiol.* 7:703-714.
31. Kalkum, M., R. Eisenbrandt, and E. Lanka. 2004. Protein circlets as sex pilus subunits. *Curr. Protein Pept. Sci.* 5:417-424.
32. Christie, P. J. 2004. Bacterial type IV secretion: The *Agrobacterium* VirB/D4 and related conjugation systems. *Biochem. Biophys. Acta.* 1694:219-234.
33. Douglas, C. J., W. Halperin, and E. W. Nester. 1982. *Agrobacterium tumefaciens* mutants affected in attachment to plant cells. *J. Bacteriol.* 152:1265-1275.
34. Lippincott, B. B., and J. A. Lippincott. 1969. Bacterial attachment to a specific wound site as an essential stage in tumor initiation by *Agrobacterium tumefaciens*. *J. Bacteriol.* 97:620-628.
35. Lai, E. M., H. W. Shih, S. R. Wen, M. W. Cheng, H. H. Hwang, and S. H. Chiu. 2006. Proteomic analysis of *Agrobacterium tumefaciens* response to the Vir gene inducer acetosyringone. *Proteomics.* 6:4130-4136.
36. Dehio, C. 2008. Infection-associated type IV secretion systems of *Bartonella* and their diverse roles in host cell interaction. *Cell. Microbiol.* 10:1591-1598.
37. Ninio, S., and C. R. Roy. 2007. Effector proteins translocated by *Legionella pneumophila*: strength in numbers. *Trends Microbiol.* 15:372-380.
38. Gao, R., A. Mukhopadhyay, F. Fang, and D. G. Lynn. 2006. Constitutive activation of two-component response regulators: characterization of VirG activation in *Agrobacterium tumefaciens*. *J. Bacteriol.* 188:5204-5211.
39. Christie, P. J., K. Atmakuri, V. Krishnamoorthy, S. Jakubowski, and E. Cascales. 2005. Biogenesis, architecture, and function of bacterial type IV secretion systems. *Annu. Rev. Microbiol.* 59:451-485.

40. Zhu, J., P. M. Oger, B. Schrammeijer, P. J. Hooykaas, S. K. Farrand, and S. C. Winans. 2000. The bases of crown gall tumorigenesis. *J. Bacteriol.* 182:3885-3895.
41. Christie, P. J. 2000. *Agrobacterium* and plant cell transformation. In *Encyclopedia of Microbiology*, Second ed. J. Lederberg, ed. Academic Press, San Diego, CA. 86-103.
42. Tzfira, T. 2006. On tracks and locomotives: the long route of DNA to the nucleus. *Trends Microbiol.* 14:61-63.
43. Tzfira, T., and V. Citovsky. 2006. *Agrobacterium*-mediated genetic transformation of plants: biology and biotechnology. *Curr. Opin. Biotech.* 17:147-154.
44. Tzfira, T., J. Li, B. Lacroix, and V. Citovsky. 2004. *Agrobacterium* T-DNA integration: molecules and models. *Trends Genet.* 20:375-383.
45. Atmakuri, K., E. Cascales, and P. J. Christie. 2004. Energetic components VirD4, VirB11 and VirB4 mediate early DNA transfer reactions required for bacterial type IV secretion. *Mol. Microbiol.* 54:1199-1211.
46. de Vos, G., and P. Zambryski. 1989. Expression of *Agrobacterium* nopaline-specific VirD1, VirD2, and VirC1 proteins and their requirement for T-strand production in *E. coli*. *Mol. Plant Microbe Inter.* 2:43-52.
47. Christie, P. J., J. E. Ward, S. C. Winans, and E. W. Nester. 1988. The *Agrobacterium tumefaciens virE2* gene product is a single-stranded-DNA-binding protein that associates with T-DNA. *J. Bacteriol.* 170:2659-2667.
48. Das, A. 1988. *Agrobacterium tumefaciens virE* operon encodes a single-stranded DNA-binding protein. *Proc. Natl. Acad. Sci. U.S.A.* 85:2909-2913.
49. Citovsky, V., D. Warnick, and P. Zambryski. 1994. Nuclear import of *Agrobacterium* VirD2 and VirE2 proteins in maize and tobacco. *Proc. Natl. Acad. Sci. U.S.A.* 91:3210-3214.
50. Citovsky, V., M. L. Wong, and P. Zambryski. 1989. Cooperative interaction of *Agrobacterium* VirE2 protein with single-stranded DNA: implications for the T-DNA transfer process. *Proc. Natl. Acad. Sci. U.S.A.* 86:1193-1197.
51. Citovsky, V., J. Zupan, D. Warnick, and P. Zambryski. 1992. Nuclear localization of *Agrobacterium* VirE2 protein in plant cells. *Science.* 256:1802-1805.
52. Lacroix, B., M. Vaidya, T. Tzfira, and V. Citovsky. 2004. The VirE3 protein of *Agrobacterium* mimics a host cell function required for plant genetic transformation. *EMBO J.* 24: 428-37.

53. Tzfira, T., M. Vaidya, and V. Citovsky. 2004. Involvement of targeted proteolysis in plant genetic transformation by *Agrobacterium*. *Nature*. 431:87-92.
54. McCullen, C. A., and A. N. Binns. 2006. *Agrobacterium tumefaciens* plant cell Interactions and activities required for interkingdom macromolecular transfer. *Annu Rev. Cell. Dev. Biol.* 22:101-127.
55. Sundberg, C., L. Meek, K. Carroll, A. Das, and W. Ream. 1996. VirE1 protein mediates export of the single-stranded DNA-binding protein VirE2 from *Agrobacterium tumefaciens* into plant cells. *J. Bacteriol.* 178:1207-1212.
56. Regensburg, T. A., and P. J. Hooykaas. 1993. Transgenic *N. glauca* plants expressing bacterial virulence gene *virF* are converted into hosts for nopaline strains of *A. tumefaciens*. *Nature*. 363:69-71.
57. Vergunst, A. C., M. C. van Lier, A. den Dulk-Ras, T. A. Grosse Stuve, A. Ouwehand, and P. J. Hooykaas. 2005. Positive charge is an important feature of the C-terminal transport signal of the VirB/D4-translocated proteins of *Agrobacterium*. *Proc. Natl. Acad. Sci. U.S.A.* 102:832-837.
58. Cascales, E., and P. J. Christie. 2004. Definition of a bacterial type IV secretion pathway for a DNA substrate. *Science*. 304:1170-1173.
59. Atmakuri, K., Z. Ding, and P. J. Christie. 2003. VirE2, a type IV secretion substrate, interacts with the VirD4 transfer protein at cell poles of *Agrobacterium tumefaciens*. *Mol. Microbiol.* 49:1699-1713.
60. Fullner, K. J. 1998. Role of *Agrobacterium virB* genes in transfer of T complexes and RSF1010. *J. Bacteriol.* 180:430-434.
61. Beijersbergen, A., A. D. Dulk-Ras, R. A. Schilperoort, and P. J. J. Hooykas. 1992. Conjugative transfer by the virulence system of *Agrobacterium tumefaciens*. *Science*. 256:1324-1327.
62. Cascales, E., K. Atmakuri, Z. Liu, A. N. Binns, and P. J. Christie. 2005. *Agrobacterium tumefaciens* oncogenic suppressors inhibit T-DNA and VirE2 protein substrate binding to the VirD4 coupling protein. *Mol. Microbiol.* 58:565-579.
63. Binns, A. N., C. E. Beaupre, and E. M. Dale. 1995. Inhibition of VirB-mediated transfer of diverse substrates from *Agrobacterium tumefaciens* by the IncQ plasmid RSF1010. *J. Bacteriol.* 177:4890-4899.
64. Buchanan-Wollaston, V., J. E. Passiatore, and F. Cannon. 1987. The *mob* and *oriT* mobilization functions of a bacterial plasmid promote its transfer to plants. *Nature*. 328:172-175.

65. Jakubowski, S. J., V. Krishnamoorthy, E. Cascales, and P. J. Christie. 2004. *Agrobacterium tumefaciens* VirB6 domains direct the ordered export of a DNA substrate through a type IV secretion system. *J. Molec. Biol.* 341:961-977.
66. Mossey, P., A. Hudacek, and A. Das. *Agrobacterium tumefaciens* type IV secretion protein VirB3 is an inner membrane protein and requires VirB4, VirB7, and VirB8 for stabilization. *J. Bacteriol.* 192:2830-2838.
67. Fronzes, R., E. Schafer, L. Wang, H. R. Saibil, E. V. Orlova, and G. Waksman. 2009. Structure of a type IV secretion system core complex. *Science.* 323:266-268.
68. Chandran, V., R. Fronzes, S. Duquerroy, N. Cronin, J. Navaza, and G. Waksman. 2009. Structure of the outer membrane complex of a type IV secretion system. *Nature.* 462:1011-1015.
69. Jakubowski, S. J., J. E. Kerr, I. Garza, V. Krishnamoorthy, R. Bayliss, G. Waksman, and P. J. Christie. 2009. *Agrobacterium* VirB10 domain requirements for type IV secretion and T pilus biogenesis. *Mol. Microbiol.* 71:779-794.
70. Saier, M. H., Jr. 2003. Tracing pathways of transport protein evolution. *Mol. Microbiol.* 48:1145-1156.
71. Das, A., and Y.-H. Xie. 2000. The *Agrobacterium* T-DNA transport pore proteins VirB8, VirB9, and VirB10 interact with one another. *J. Bacteriol.* 182:758-763.
72. Sivanesan, D., M. A. Hancock, A. M. Villamil Giraldo, and C. Baron. Quantitative analysis of VirB8-VirB9-VirB10 interactions provides a dynamic model of type IV secretion system core complex assembly. *Biochemistry.* 49:4483-4493.
73. Terradot, L., R. Bayliss, C. Oomen, Leonard., C. Baron, and G. Waksman. 2005. Structures of two core subunits of the bacterial type IV secretion system, VirB8 from *Brucella suis* and ComB10 from *Helicobacter pylori*. *Proc. Natl. Acad. Sci. U.S.A.* 102:4956-4961.
74. Spudich, G. M., D. Fernandez, X. R. Zhou, and P. J. Christie. 1996. Intermolecular disulfide bonds stabilize VirB7 homodimers and VirB7/VirB9 heterodimers during biogenesis of the *Agrobacterium tumefaciens* T-complex transport apparatus. *Proc. Natl. Acad. Sci. U. S. A.* 93:7512-7517.
75. Anderson, L. B., A. V. Hertzell, and A. Das. 1996. *Agrobacterium tumefaciens* VirB7 and VirB9 form a disulfide-linked protein complex. *Proc. Natl. Acad. Sci. U.S.A.* 93:8889-8894.

76. Bailey, S., D. Ward, R. Middleton, J. G. Grossmann, and P. C. Zambryski. 2006. *Agrobacterium tumefaciens* VirB8 structure reveals potential protein-protein interaction sites. *Proc. Natl. Acad. Sci. U.S.A.* 103:2582-2587.
77. Kumar, R. B., Y. H. Xie, and A. Das. 2000. Subcellular localization of the *Agrobacterium tumefaciens* T-DNA transport pore proteins: VirB8 is essential for the assembly of the transport pore. *Mol. Microbiol.* 36:608-617.
78. Cao, T. B., and M. H. Saier, Jr. 2001. Conjugal type IV macromolecular transfer systems of Gram-negative bacteria: organismal distribution, structural constraints and evolutionary conclusions. *Microbiology (Reading, England)* 147:3201-3214.
79. Chu, B. C., R. S. Peacock, and H. J. Vogel. 2007. Bioinformatic analysis of the TonB protein family. *Biometals* 20:467-483.
80. Fronzes, R., P. J. Christie, and G. Waksman. 2009. Structural biology of type IV secretion systems. *Nature Rev. Microbiol.* 7: 703-14.
81. Waksman, G., and R. Fronzes. 2010 Molecular architecture of bacterial type IV secretion systems. *Trends Biochem. Sci. In press.*
82. Jakubowski, S. J., V. Krishnamoorthy, and P. J. Christie. 2003. *Agrobacterium tumefaciens* VirB6 protein participates in formation of VirB7 and VirB9 complexes required for type IV secretion. *J. Bacteriol.* 185:2867-2878.
83. Cascales, E., and P. J. Christie. 2004. *Agrobacterium* VirB10, an ATP energy sensor required for type IV secretion. *Proc. Natl. Acad. Sci. U. S. A.* 101:17228-17233.
84. Rashkova, S., Zhou, X.-R., Christie, P. J. 2000. Self-assembly of the *Agrobacterium tumefaciens* VirB11 traffic ATPase. *J. Bacteriol.* 182:4137-4145.
85. Yeo, H. J., S. N. Savvides, A. B. Herr, E. Lanka, and G. Waksman. 2000. Crystal structure of the hexameric traffic ATPase of the *Helicobacter pylori* type IV secretion system. *Mol. Cell.* 6:1461-1472.
86. Hare, S., R. Bayliss, C. Baron, and G. Waksman. 2006. A large domain swap in the VirB11 ATPase of *Brucella suis* leaves the hexameric assembly intact. *J. Mol. Biol.* 360:56-66.
87. Sagulenko, Y., V. Sagulenko, J. Chen, and P. J. Christie. 2001. Role of *Agrobacterium* VirB11 ATPase in T-pilus assembly and substrate selection. *J. Bacteriol.* 183:5813-5825.

88. Sexton, J. A., J. S. Pinkner, R. Roth, J. E. Heuser, S. J. Hultgren, and J. P. Vogel. 2004. The *Legionella pneumophila* PilT homologue DotB exhibits ATPase activity that is critical for intracellular growth. *J. Bacteriol.* 186:1658-1666.
89. Stephens, K. M., C. Roush, and E. Nester. 1995. *Agrobacterium tumefaciens* VirB11 protein requires a consensus nucleotide-binding site for function in virulence. *J. Bacteriol.* 177:27-36.
90. Rashkova, S., G. M. Spudich, and P. J. Christie. 1997. Characterization of membrane and protein interaction determinants of the *Agrobacterium tumefaciens* VirB11 ATPase. *J. Bacteriol.* 179:583-591.
91. Turner, L. R., J. C. Lara, D. N. Nunn, and S. Lory. 1993. Mutations in the consensus ATP-binding sites of XcpR and PilB eliminate extracellular protein secretion and pilus biogenesis in *Pseudomonas aeruginosa*. *J. Bacteriol.* 175:4962-4969.
92. Rivas, S., S. Bolland, E. Cabezon, F. M. Goni, and F. de la Cruz. 1997. TrwD, a protein encoded by the IncW plasmid R388, displays an ATP hydrolase activity essential for bacterial conjugation. *J. Biol. Chem.* 272:25583-25590.
93. Schroder, G., S. Krause, E. L. Zechner, B. Traxler, H. J. Yeo, R. Lurz, G. Waksman, and E. Lanka. 2002. TraG-like proteins of DNA transfer systems and of the *Helicobacter pylori* type IV secretion system: inner membrane gate for exported substrates? *J. Bacteriol.* 184:2767-2779.
94. Schroder, G., and E. Lanka. 2003. TraG-like proteins of type IV secretion systems: functional dissection of the multiple activities of TraG (RP4) and TrwB (R388). *J. Bacteriol.* 185:4371-4381.
95. Gomis-Ruth, F. X., F. de la Cruz, and M. Coll. 2002. Structure and role of coupling proteins in conjugal DNA transfer. *Res. Microbiol.* 153:199-204.
96. Gomis-Ruth, F. X., M. Sola, F. de la Cruz, and M. Coll. 2004. Coupling factors in macromolecular type-IV secretion machineries. *Curr. Pharm. Des.* 10:1551-1565.
97. Gomis-Ruth, F. X., G. Moncalian, R. Perez-Luque, A. Gonzalez, E. Cabezon, F. de la Cruz, and M. Coll. 2001. The bacterial conjugation protein TrwB resembles ring helicases and F1-ATPase. *Nature.* 409:637-641.
98. Gomis-Ruth, F. X., G. Moncalian, F. de la Cruz, and M. Coll. 2002. Conjugative plasmid protein TrwB, an integral membrane type IV secretion system coupling protein. Detailed structural features and mapping of the active site cleft. *J. Biol. Chem.* 277:7556-7566.

99. Balzer, D., W. Pansegrau, and E. Lanka. 1994. Essential motifs of relaxase (Tral) and TraG proteins involved in conjugative transfer of plasmid RP4. *J. Bacteriol.* 176:4285-4295.
100. Lin, T. S., and C. I. Kado. 1993. The virD4 gene is required for virulence while virD3 and orf5 are not required for virulence of *Agrobacterium tumefaciens*. *Mol. Microbiol.* 9:803-812.
101. Gunton, J. E., M. W. Gilmour, G. Alonso, and D. E. Taylor. 2005. Subcellular localization and functional domains of the coupling protein, TraG, from IncHI1 plasmid R27. *Microbiology.* 151:3549-3561.
102. Matilla, I., C. Alfonso, G. Rivas, E. L. Bolt, F. de la Cruz, and E. Cabezon. The conjugative DNA translocase TrwB is a structure-specific DNA-binding protein. *The J. Biol Chem.* 285:17537-17544.
103. Atmakuri, K., E. Cascales, O. T. Burton, L. M. Banta, and P. J. Christie. 2007. *Agrobacterium* ParA/MinD-like VirC1 spatially coordinates early conjugative DNA transfer reactions. *EMBO J.* 26:2540-2551.
104. Lai, E. M., O. Chesnokova, L. M. Banta, and C. I. Kado. 2000. Genetic and environmental factors affecting T-pilin export and T-pilus biogenesis in relation to flagellation of *Agrobacterium tumefaciens*. *J. Bacteriol.* 182:3705-3716.
105. Dang, T. A., and P. J. Christie. 1997. The VirB4 ATPase of *Agrobacterium tumefaciens* is a cytoplasmic membrane protein exposed at the periplasmic surface. *J. Bacteriol.* 179:453-462.
106. Dang, T. A., X. R. Zhou, B. Graf, and P. J. Christie. 1999. Dimerization of the *Agrobacterium tumefaciens* VirB4 ATPase and the effect of ATP-binding cassette mutations on the assembly and function of the T-DNA transporter. *Mol. Microbiol.* 32:1239-1253.
107. Draper, O., R. Middleton, M. Doucleff, and P. C. Zambryski. 2006. Topology of the VirB4 C-terminus in the *agrobacterium tumefaciens* VirB/D4 type IV secretion system. *J. Biol. Chem.* 281:37628-37635.
108. Middleton, R., K. Sjolander, N. Krishamurthy, J. Foley, and P. Zambryski. 2005. Predicted hexameric structure of the *Agrobacterium* VirB4 C-terminus suggests VirB4 acts as a docking site during type IV secretion. *Proc. Natl. Acad. Sci U. S. A.* 102:1685-1690.
109. Arechaga, I., A. Pena, S. Zunzunegui, M. del Carmen Fernandez-Alonso, G. Rivas, and F. de la Cruz. 2008. ATPase activity and oligomeric state of TrwK, the VirB4

- homologue of the plasmid R388 type IV secretion system. *J. Bacteriol.* 190:5472-5479.
110. Durand, E., C. Oomen, and G. Waksman. Biochemical dissection of the ATPase TraB, the VirB4 homologue of the Escherichia coli pKM101 conjugation machinery. *J. Bacteriol.* 192:2315-2323.
 111. Rabel, C., A. M. Grahn, R. Lurz, and E. Lanka. 2003. The VirB4 family of proposed traffic nucleoside triphosphatases: common motifs in plasmid RP4 TrbE are essential for conjugation and phage adsorption. *J. Bacteriol.* 185:1045-1058.
 112. Fullner, K. J., K. M. Stephens, and E. W. Nester. 1994. An essential virulence protein of *Agrobacterium tumefaciens*, VirB4, requires an intact mononucleotide binding domain to function in transfer of T-DNA. *Molec. Gen. Genetics.* 245:704-715.
 113. Shirasu, K., N. Z. Koukolikova, B. Hohn, and C. I. Kado. 1994. An inner-membrane-associated virulence protein essential for T-DNA transfer from *Agrobacterium tumefaciens* to plants exhibits ATPase activity and similarities to conjugative transfer genes. *Mol. Microbiol.* 11:581-588.
 114. Schmidt-Eisenlohr, H., D. N., A. C., G. Wanner, P. C. Zambryski, and C. Baron. 1999. Vir proteins stabilize VirB5 and mediate its association with the T pilus of *Agrobacterium tumefaciens*. *J. Bacteriol.* 181:7485-7492.
 115. Eisenbrandt, R., M. Kalkum, E. M. Lai, R. Lurz, C. I. Kado, and E. Lanka. 1999. Conjugative pili of IncP plasmids, and the Ti plasmid T pilus are composed of cyclic subunits. *J. Biol. Chem.* 274:22548-22555.
 116. Lai, E. M., and C. I. Kado. 2000. The T-pilus of *Agrobacterium tumefaciens*. *Trends Microbiol.* 8:361-369.
 117. Lai, E. M., R. Eisenbrandt, M. Kalkum, E. Lanka, and C. I. Kado. 2002. Biogenesis of T pili in *Agrobacterium tumefaciens* requires precise VirB2 propilin cleavage and cyclization. *J. Bacteriol.* 184:327-330.
 118. Jones, A. L., E.-M. Lai, K. Shirasu, and C. I. Kado. 1996. VirB2 is a processed pilin-like protein encoded by the *Agrobacterium tumefaciens* Ti plasmid. *J. Bacteriol.* 178:5706-5711.
 119. Matthyse, A. G. 1987. Characterization of nonattaching mutants of *Agrobacterium*. *J. Bacteriol.* 169:313-323.

120. Hwang, H. H., and S. B. Gelvin. 2004. Plant proteins that interact with VirB2, the *Agrobacterium tumefaciens* pilin protein, mediate plant transformation. *Plant Cell*. 16:3148-3167.
121. Aly, K. A., and C. Baron. 2007. The VirB5 protein localizes to the T-pilus tips in *Agrobacterium tumefaciens*. *Microbiology*. 153:3766-3775.
122. Yuan, Q., A. Carle, C. Gao, D. Sivanesan, K. A. Aly, C. Hoppner, L. Krall, N. Domke, and C. Baron. 2005. Identification of the VirB4-VirB8-VirB5-VirB2 pilus assembly sequence of type IV secretion systems. *J. Biol. Chem.* 280:26349-26359.
123. Jakubowski, S. J., E. Cascales, V. Krishnamoorthy, and P. J. Christie. 2005. *Agrobacterium tumefaciens* VirB9, an outer-membrane-associated component of a type IV secretion system, regulates substrate selection and T-pilus biogenesis. *J. Bacteriol.* 187:3486-3495.
124. Baron, C., M. Llosa, S. Zhou, and Patricia C. Zambrysk. 1997. VirB1, a component of the T-complex transfer machinery of *Agrobacterium tumefaciens*, is processed to a C-terminal secreted product, VirB1*. *J. Bacteriol.* 179: 1203-1210.
125. Hoppner, C., Z. Liu, N. Domke, A. N. Binns, and C. Baron. 2004. VirB1 orthologs from *Brucella suis* and pKM101 complement defects of the lytic transglycosylase required for efficient type IV secretion from *Agrobacterium tumefaciens*. *J. Bacteriol.* 186:1415-1422.
126. Zupan, J., C. A. Hackworth, J. Aguilar, D. Ward, and P. Zambryski. 2007. VirB1* promotes T-pilus formation in the vir-Type IV secretion system of *Agrobacterium tumefaciens*. *J. Bacteriol.* 189:6551-6563.
127. Fullner, K. J., J. C. Lara, and E. W. Nester. 1996. Pilus assembly by *Agrobacterium* T-DNA transfer genes. *Science*. 273:1107-1109.
128. Berger, B. R., and P. J. Christie. 1994. Genetic complementation analysis of the *Agrobacterium tumefaciens virB* operon: *virB2* through *virB11* are essential virulence genes. *J. Bacteriol.* 176:3646-3660.
129. Jayaraman, K., S. A. Fingar, J. Shah, and J. Fyles. 1991. Polymerase chain reaction-mediated gene synthesis: synthesis of a gene coding for isozyme c of horseradish peroxidase. *Proc. Natl. Acad. Sci. U.S.A.* 88:4084-4088.
130. Kerr, J. E., and P. J. Christie. 2010. Evidence for VirB4-mediated dislocation of membrane-integrated VirB2 pilin during biogenesis of the *Agrobacterium* VirB/VirD4 type IV secretion system. *J. Bacteriol.* 192:4923-4934.

131. Garfinkel, D. J., R. B. Simpson, L. W. Ream, F. F. White, M. P. Gordon, and E. W. Nester. 1981. Genetic analysis of crown gall: fine structure map of the T-DNA by site-directed mutagenesis. *Cell*. 27:143-153.
132. Fernandez, D., G. M. Spudich, X. R. Zhou, and P. J. Christie. 1996. The *Agrobacterium tumefaciens* VirB7 lipoprotein is required for stabilization of VirB proteins during assembly of the T-complex transport apparatus. *J. Bacteriol.* 178:3168-3176.
133. Berger, B. R., and P. J. Christie. 1993. The *Agrobacterium tumefaciens* virB4 gene product is an essential virulence protein requiring an intact nucleoside triphosphate-binding domain. *J. Bacteriol.* 175:1723-1734.
134. Zhou, X.-R., and P. J. Christie. 1999. Mutagenesis of *Agrobacterium* VirE2 single-stranded DNA-binding protein identifies regions required for self-association and interaction with VirE1 and a permissive site for hybrid protein construction. *J. Bacteriol.* 181:4342-4352.
135. Kovach, M. E., R. W. Phillips, P. H. Elzer, R. M. Roop, 2nd, and K. M. Peterson. 1994. pBBR1MCS: a broad-host-range cloning vector. *Biotechniques*. 16:800-802.
136. Zhou, X.-R., and P. J. Christie. 1997. Suppression of mutant phenotypes of the *Agrobacterium tumefaciens* VirB11 ATPase by overproduction of VirB proteins. *J. Bacteriol.* 179:5835-5842.
137. Fernandez, D., T. A. Dang, G. M. Spudich, X. R. Zhou, B. R. Berger, and P. J. Christie. 1996. The *Agrobacterium tumefaciens* virB7 gene product, a proposed component of the T-complex transport apparatus, is a membrane-associated lipoprotein exposed at the periplasmic surface. *J. Bacteriol.* 178:3156-3167.
138. Sagulenko, V., E. Sagulenko, S. Jakubowski, E. Spudich, and P. J. Christie. 2001. VirB7 lipoprotein is exocellular and associates with the *Agrobacterium tumefaciens* T pilus. *J. Bacteriol.* 183:3642-3651.
139. Lazzaroni, J. C., and R. C. Portalier. 1981. Genetic and biochemical characterization of periplasmic-leaky mutants of *Escherichia coli* K-12. *J. Bacteriol.* 145:1351-1358.
140. Chen, J., K. S. de Felipe, M. Clarke, H. Lu, O. R. Anderson, G. Segal, and H. A. Shuman. 2004. Legionella effectors that promote nonlytic release from protozoa. *Science*. 303:1358-1361.

141. Schmidt-Eisenlohr, H., N. Domke, and C. Baron. 1999. TraC of IncN plasmid pKM101 associates with membranes and extracellular high-molecular-weight structures in *Escherichia coli*. *J. Bacteriol.* 181:5563-5571.
142. Haase, J., and E. Lanka. 1997. A specific protease encoded by the conjugative DNA transfer systems of IncP and Ti plasmids is essential for pilus synthesis. *J. Bacteriol.* 179:5728-5735.
143. Kalkum, M., R. Eisenbrandt, R. Lurz, and E. Lanka. 2002. Tying rings for sex. *Trends Microbiol.* 10:382-387.
144. Moore, D., C. M. Hamilton, K. Maneewannakul, Y. Mintz, L. S. Frost, and K. Ippen-Ihler. 1993. The *Escherichia coli* K-12 F plasmid gene traX is required for acetylation of F pilin. *J. Bacteriol.* 175:1375-1383.
145. Wang, Y. A., X. Yu, P. M. Silverman, R. L. Harris, and E. H. Egelman. 2009. The structure of F-pili. *J. Molec Biol.* 385:22-29.
146. Bogdanov, M., W. Zhang, J. Xie, and W. Dowhan. 2005. Transmembrane protein topology mapping by the substituted cysteine accessibility method (SCAM(TM)): application to lipid-specific membrane protein topogenesis. *Methods.* 36:148-171.
147. Ott, C. M., and V. R. Lingappa. 2002. Integral membrane protein biosynthesis: why topology is hard to predict. *J. Cell Sci.* 115:2003-2009.
148. Persson, B., and P. Argos. 1997. Prediction of membrane protein topology utilizing multiple sequence alignments. *J. Prot. Chem.* 16:453-457.
149. van Geest, M., and J. S. Lolkema. 2000. Membrane topology and insertion of membrane proteins: search for topogenic signals. *Microbiol. Mol. Biol. Rev.* 64:13-33.
150. Baron, C., N. Domke, M. Beinhofer, and S. Hapfelmeier. 2001. Elevated Temperature Differentially Affects Virulence, VirB Protein Accumulation, and T-Pilus Formation in Different *Agrobacterium tumefaciens* and *Agrobacterium vitis* Strains. *J. Bacteriol.* 183:6852-6861.
151. Kado, C. I. 1994. Promiscuous DNA transfer system of *Agrobacterium tumefaciens* : role of the *virB* operon in sex pilus assembly and synthesis. *Mol. Microbiol.* 12:17-22.
152. Paiva, W. D., T. Grossman, and P. M. Silverman. 1992. Characterization of F-pilin as an inner membrane component of *Escherichia coli* K12. *J. Biol. Chem.* 267:26191-26197.

153. Long, J. C., S. Wang, and S. B. Vik. 1998. Membrane topology of subunit a of the F1F0 ATP synthase as determined by labeling of unique cysteine residues. *J. Biol. Chem.* 273:16235-16240.
154. Loo, T. W., and D. M. Clarke. 1995. Membrane topology of a cysteine-less mutant of human P-glycoprotein. *J. Biol. Chem.* 270:843-848.
155. Bogdanov, M., J. Xie, P. Heacock, and W. Dowhan. 2008. To flip or not to flip: lipid-protein charge interactions are a determinant of final membrane protein topology. *J. Cell Biol.* 182:925-935.
156. Lai, E. M., and C. I. Kado. 2002. The *Agrobacterium tumefaciens* T pilus composed of cyclic T pilin is highly resilient to extreme environments. *FEMS Microbiol. Lett.* 210:111-114.
157. von Heijne, G., and C. Manoil. 1990. Membrane proteins: from sequence to structure. *Protein Eng.* 4:109-112.
158. Beijersbergen, A., S. J. Smith, and P. J. Hooykaas. 1994. Localization and topology of VirB proteins of *Agrobacterium tumefaciens*. *Plasmid.* 32:212-218.
159. Das, A., and Y. H. Xie. 1998. Construction of transposon Tn3phoA: its application in defining the membrane topology of the *Agrobacterium tumefaciens* DNA transfer proteins. *Mol. Microbiol.* 27:405-414.
160. Eisenbrandt, R., M. Kalkum, R. Lurz, and E. Lanka. 2000. Maturation of IncP pilin precursors resembles the catalytic Dyad-like mechanism of leader peptidases. *J. Bacteriol.* 182:6751-6761.
161. Manchak, J., K. G. Anthony, and L. S. Frost. 2002. Mutational analysis of F-pilin reveals domains for pilus assembly, phage infection and DNA transfer. *Mol. Microbiol.* 43:195-205.
162. Culham, D. E., A. Hillar, J. Henderson, A. Ly, Y. I. Vernikovska, K. I. Racher, J. M. Boggs, and J. M. Wood. 2003. Creation of a fully functional cysteine-less variant of osmosensor and proton-osmoprotectant symporter ProP from *Escherichia coli* and its application to assess the transporter's membrane orientation. *Biochemistry.* 42:11815-11823.
163. Bogdanov, M., J. Xie, and W. Dowhan. 2009. Lipid-protein interactions drive membrane protein topogenesis in accordance with the positive inside rule. *J. Biol. Chem.* 284:9637-9641.
164. von Heijne, G., and Y. Gavel. 1988. Topogenic signals in integral membrane proteins. *Eurp. J Biochem. FEBS.* 174:671-678.

165. Rondot, S., K. G. Anthony, S. Dubel, N. Ida, S. Wiemann, K. Beyreuther, L. S. Frost, M. Little, and F. Breitling. 1998. Epitopes fused to F-pilin are incorporated into functional recombinant pili. *J. Mol. Biol.* 279:589-603.
166. Frost, L. S., and W. Paranchych. 1988. DNA sequence analysis of point mutations in traA, the F pilin gene, reveal two domains involved in F-specific bacteriophage attachment. *Mol. Gen. Genet.* 213:134-139.
167. Russ, W. P., and D. M. Engelman. 2000. The GxxxG motif: a framework for transmembrane helix-helix association. *J. Mol. Biol.* 296:911-919.
168. Senes, A., M. Gerstein, and D. M. Engelman. 2000. Statistical analysis of amino acid patterns in transmembrane helices: the GxxxG motif occurs frequently and in association with beta-branched residues at neighboring positions. *J. Mol. Biol.* 296:921-936.
169. Bass, R. B., P. Strop, M. Barclay, and D. C. Rees. 2002. Crystal structure of Escherichia coli MscS, a voltage-modulated and mechanosensitive channel. *Science.* 298:1582-1587.
170. Chang, G., R. H. Spencer, A. T. Lee, M. T. Barclay, and D. C. Rees. 1998. Structure of the MscL homolog from Mycobacterium tuberculosis: a gated mechanosensitive ion channel. *Science.* 282:2220-2226.
171. Fu, D., A. Libson, L. J. Miercke, C. Weitzman, P. Nollert, J. Krucinski, and R. M. Stroud. 2000. Structure of a glycerol-conducting channel and the basis for its selectivity. *Science.* 290:481-486.
172. Fu, D., A. Libson, and R. Stroud. 2002. The structure of GlpF, a glycerol conducting channel. *Novartis Foundation symposium* 245:51-61; discussion 61-55, 165-168.
173. Kleiger, G., R. Grothe, P. Mallick, and D. Eisenberg. 2002. GXXXG and AXXXA: common alpha-helical interaction motifs in proteins, particularly in extremophiles. *Biochemistry.* 41:5990-5997.
174. Kim, S., T. J. Jeon, A. Oberai, D. Yang, J. J. Schmidt, and J. U. Bowie. 2005. Transmembrane glycine zippers: physiological and pathological roles in membrane proteins. *Proc. Natl. Acad. Sci. U.S.A.* 102:14278-14283.
175. Grossman, T. H., L. S. Frost, and P. M. Silverman. 1990. Structure and function of conjugative pili: monoclonal antibodies as probes for structural variants of F pili. *J. Bacteriol.* 172:1174-1179.

176. Wang, X., M. Bogdanov, and W. Dowhan. 2002. Topology of polytopic membrane protein subdomains is dictated by membrane phospholipid composition. *EMBO J.* 21:5673-5681.
177. Geibel, S., J. H. Kaplan, E. Bamberg, and T. Friedrich. 2003. Conformational dynamics of the Na⁺/K⁺-ATPase probed by voltage clamp fluorometry. *Proc. Natl. Acad. Sci. U.S.A.* 100:964-969.
178. Hu, J., M. Kornacker, and A. Hochschild. 2000. *Escherichia coli* one- and two-hybrid systems for the analysis and identification of protein-protein interactions. *Methods.* 20:80-94.
179. Bogdanov, M., P. N. Heacock, and W. Dowhan. 2002. A polytopic membrane protein displays a reversible topology dependent on membrane lipid composition. *EMBO J.* 21:2107-2116.
180. Dang TA, Zhou XR, Graf B, Christie PJ. 1999. Dimerization of the *Agrobacterium tumefaciens* VirB4 ATPase and the effect of ATP-binding cassette mutation on the assembly and function of the T-DNA transporter. *Mol. Microbiol.* 32: 1239-53.
181. Chen, L., C. M. Li, and E. W. Nester. 2000. Transferred DNA (T-DNA)-associated proteins of *Agrobacterium tumefaciens* are exported independently of virB. *Proc. Natl. Acad. Sci. U.S.A.* 97:7545-7550.
182. Schandel, K. A., M. M. Muller, and R. E. Webster. 1992. Localization of TraC, a protein involved in assembly of the F conjugative pilus. *J. Bacteriol.* 174:3800-3806.
183. Schandel, K. A., S. Maneewannakul, R. A. Vonder Haar, K. Ippen-Ihler, and R. E. Webster. 1990. Nucleotide sequence of the F plasmid gene, traC, and identification of its product. *Gene.* 96:137-140.
184. Maneewannakul, S., P. Kathir, D. Moore, L. A. Le, J. H. Wu, and K. Ippen-Ihler. 1987. Location of F plasmid transfer operon genes traC and traW and identification of the traW product. *J. Bacteriol.* 169:5119-5124.
185. Schandel, K. A., S. Maneewannakul, K. Ippen-Ihler, and R. E. Webster. 1987. A traC mutant that retains sensitivity to f1 bacteriophage but lacks F pili. *J. Bacteriol.* 169:3151-3159.
186. Ito, K., and Y. Akiyama. 2005. Cellular functions, mechanism of action, and regulation of FtsH protease. *Annu. Rev. Microbiol.* 59:211-231.
187. Savvides, S. N. 2007. Secretion superfamily ATPases swing big. *Structure.* 15:255-257.

188. Haas, J. M. k., and E. Lanka. 1996. TrbK, a small cytoplasmic membrane lipoprotein, functions in entry exclusion of the IncP alpha plasmid RP4. *J. Bacteriol.* 178:6720-6729.
189. Jones, A. L., K. Shirasu, and C. I. Kado. 1994. The product of the *virB4* gene of *Agrobacterium tumefaciens* promotes accumulation of VirB3 protein. *J. Bacteriol.* 176:5255-5261.
190. Paschos, A., G. Patey, D. Sivanesan, C. Gao, R. Bayliss, G. Waksman, D. O'Callaghan, and C. Baron. 2006. Dimerization and interactions of Brucella suis VirB8 with VirB4 and VirB10 are required for its biological activity. *Proc. Natl. Acad. Sci. U.S.A.* 103:7252-7257.
191. Yamagata, A., and J. A. Tainer. 2007. Hexameric structures of the archaeal secretion ATPase GspE and implications for a universal secretion mechanism. *EMBO J.* 26:878-890.
192. Craig, L., and J. Li. 2008. Type IV pili: paradoxes in form and function. *Curr. Opin. Struc. Biol.* 18:267-277.
193. Beaupre, C. E., J. Bohne, E. M. Dale, and A. N. Binns. 1997. Interactions between VirB9 and VirB10 membrane proteins involved in movement of DNA from *Agrobacterium tumefaciens* into plant cells. *J. Bacteriol.* 179:78-89.
194. Llosa, M., S. Zunzunegui, and F. de la Cruz. 2003. Conjugative coupling proteins interact with cognate and heterologous VirB10-like proteins while exhibiting specificity for cognate relaxosomes. *Proc. Natl. Acad. Sci. U. S. A.* 100:10465-10470.
195. Gilmour, M. W., J. E. Gunton, T. D. Lawley, and D. E. Taylor. 2003. Interaction between the IncHI1 plasmid R27 coupling protein and type IV secretion system: TraG associates with the coiled-coil mating pair formation protein TrhB. *Mol. Microbiol.* 49:105-116.
196. Ward, D. V., O. Draper, J. R. Zupan, and P. C. Zambryski. 2002. Peptide linkage mapping of the *Agrobacterium tumefaciens* *vir*-encoded type IV secretion system reveals protein subassemblies. *Proc. Natl. Acad. Sci. U. S. A.* 99:11493-11500.
197. Baron, C., Y. R. Thorstenson, and P. C. Zambryski. 1997. The lipoprotein VirB7 interacts with VirB9 in the membranes of *Agrobacterium tumefaciens*. *J. Bacteriol.* 179:1211-1218.

198. Das, A., L. B. Anderson, and Y. H. Xie. 1997. Delineation of the interaction domains of *Agrobacterium tumefaciens* VirB7 and VirB9 by use of the yeast two-hybrid assay. *J. Bacteriol.* 179:3404-3409.
199. Postle, K., and R. J. Kadner. 2003. Touch and go: tying TonB to transport. *Mol. Microbiol.* 49:869-882.
200. Postle, K. 2007. TonB system, in vivo assays and characterization. *Methods Enzymol.* 422:245-269.
201. Postle, K., and R. A. Larsen. 2007. TonB-dependent energy transduction between outer and cytoplasmic membranes. *Biomaterials.* 20:453-465.
202. Christie, P. J., and E. Cascales. 2005. Structural and dynamic properties of bacterial type IV secretion systems (review). *Mol. Membr. Biol.* 22:51-61.
203. Larsen, R. A., T. E. Letain, and K. Postle. 2003. In vivo evidence of TonB shuttling between the cytoplasmic and outer membrane in *Escherichia coli*. *Mol. Microbiol.* 49:211-218.
204. Terradot, L., N. Durnell, M. Li, D. Li, J. Ory, A. Labigne, P. Legrain, F. Colland, and G. Waksman. 2004. Biochemical characterization of protein complexes from the *Helicobacter pylori* protein interaction map: strategies for complex formation and evidence for novel interactions within type IV secretion systems. *Mol. Cell. Proteomics.* 3:809-819.
205. Williamson, M. P. 1994. The structure and function of proline-rich regions in proteins. *Biochem. J.* 297 (Pt 2):249-260.
206. Ruan, W., E. Lindner, and D. Langosch. 2004. The interface of a membrane-spanning leucine zipper mapped by asparagine-scanning mutagenesis. *Protein Sci.* 13:555-559.
207. Rego, A. T., V. Chandran, and G. Waksman. Two-step and one-step secretion mechanisms in Gram-negative bacteria: contrasting the type IV secretion system and the chaperone-usher pathway of pilus biogenesis. *Biochem. J.* 425:475-488.
208. Tomlinson, A. D., and C. Fuqua. 2009. Mechanisms and regulation of polar surface attachment in *Agrobacterium tumefaciens*. *Curr. Opin. Microbiol.* 12:708-714.
209. Pitzschke, A., and H. Hirt. New insights into an old story: *Agrobacterium*-induced tumour formation in plants by plant transformation. *EMBO J.* 29:1021-1032.
210. Benz, R., and K. Bauer. 1988. Permeation of hydrophilic molecules through the outer membrane of gram-negative bacteria. Review on bacterial porins. *Eurp. J. Biochem. FEBS.* 176:1-19.

211. Nikaido, H. 1992. Porins and specific channels of bacterial outer membranes. *Mol. Microbiol.* 6:435-442.
212. Nikaido, H. 1994. Porins and specific diffusion channels in bacterial outer membranes. *J. Biol. Chem.* 269:3905-3908.
213. Allen, N. E., and T. I. Nicas. 2003. Mechanism of action of oritavancin and related glycopeptide antibiotics. *FEMS Microbiol. Rev.* 26:511-532.
214. Reynolds, P. E. 1989. Structure, biochemistry and mechanism of action of glycopeptide antibiotics. *Eurp. J. Clin. Microbiol. Infect. Dis.* 8:943-950.
215. Rida, S., J. Caillet, and J. H. Alix. 1996. Amplification of a novel gene, *sanA*, abolishes a vancomycin-sensitive defect in *Escherichia coli*. *J. Bacteriol.* 178:94-102.
216. Rajagopal, S., N. Sudarsan, and K. W. Nickerson. 2002. Sodium dodecyl sulfate hypersensitivity of *clpP* and *clpB* mutants of *Escherichia coli*. *App. Envir. Microbiol.* 68:4117-4121.
217. Shimoda, N., A. Toyoda-Yamamoto, S. Aoki, and Y. Machida. 1993. Genetic evidence for an interaction between the *VirA* sensor protein and the *ChvE* sugar-binding protein of *Agrobacterium*. *J. Biol. Chem.* 268:26552-26558.
218. Pettersson, J., R. Nordfelth, E. Dubinina, T. Bergman, M. Gustafsson, K. E. Magnusson, and H. Wolf-Watz. 1996. Modulation of virulence factor expression by pathogen target cell contact. *Science.* 273:1231-1233.
219. Andrup, L., and K. Andersen. 1999. A comparison of the kinetics of plasmid transfer in the conjugation systems encoded by the *F* plasmid from *Escherichia coli* and plasmid *pCF10* from *Enterococcus faecalis*. *Microbiology.* 145 (Pt 8):2001-2009.
220. Maneewannakul, S., P. Kathir, and K. Ippen-Ihler. 1992. Characterization of the *F* plasmid mating aggregation gene *traN* and of a new *F* transfer region locus *trbE*. *J. Mol. Biol.* 225:299-311.
221. Willetts, N., and B. Wilkins. 1984. Processing of plasmid DNA during bacterial conjugation. *Microbiol. Rev.* 48:24-41.
222. Higgs, P. I., P. S. Myers, and K. Postle. 1998. Interactions in the *TonB*-dependent energy transduction complex: *ExbB* and *ExbD* form homomultimers. *J. Bacteriol.* 180:6031-6038.
223. Howard, S. P., H. G. Meiklejohn, D. Shivak, and R. Jahagirdar. 1996. A *TonB*-like protein and a novel membrane protein containing an ATP-binding cassette function together in exotoxin secretion. *Mol. Microbiol.* 22:595-604.

224. Andrzejewska, J., S. K. Lee, P. Olbermann, N. Lotzing, E. Katzowitsch, B. Linz, M. Achtman, C. I. Kado, S. Suerbaum, and C. Josenhans. 2006. Characterization of the pilin ortholog of the *Helicobacter pylori* type IV cag pathogenicity apparatus, a surface-associated protein expressed during infection. *J. Bacteriol.* 188:5865-5877.
225. Smit, J. 1987. Localizing the subunit pool for the temporally regulated polar pili of *Caulobacter crescentus*. *J. Cell Biol.*105:1821-1828.
226. Newman, J. R., and C. Fuqua. 1999. Broad-host-range expression vectors that carry the L-arabinose-inducible *Escherichia coli* araBAD promoter and the araC regulator. *Gene.* 227:197-203.
227. Yen, K. M. 1991. Construction of cloning cartridges for development of expression vectors in gram-negative bacteria. *J. Bacteriol.* 173:5328-5335.
228. Khan, S. R., J. Gaines, R. M. Roop, 2nd, and S. K. Farrand. 2008. Broad-host-range expression vectors with tightly regulated promoters and their use to examine the influence of TraR and TraM expression on Ti plasmid quorum sensing. *Appl. Envir. Microbiol.* 74:5053-5062.
229. Daehnel, K., R. Harris, L. Maddera, and P. Silverman. 2005. Fluorescence assays for F-pili and their application. *Microbiology.* 151:3541-3548.
230. Clarke, M., L. Maddera, R. L. Harris, and P. M. Silverman. 2008. F-pili dynamics by live-cell imaging. *Proc. Natl. Acad. Sci. U.S.A.*105:17978-17981.
231. Machleidt, T., M. Robers, and G. T. Hanson. 2007. Protein labeling with FIAsH and ReAsH. *Methods in molecular biology (Clifton, N.J)* 356:209-220.
232. Arencibia, A., ed. 2000. *In Plant Genetic Engineering: Towards the Third Millennium.* Elsevier Science BV, Amsterdam.
233. Kado, C. I. 2000. The role of the T-pilus in horizontal gene transfer and tumorigenesis. *Curr. Opin. Microbiol.* 3:643-648.
234. Chesnokova, O., J. B. Coutinho, I. H. Khan, M. S. Mikhail, and C. I. Kado. 1997. Characterization of flagella genes of *Agrobacterium tumefaciens*, and the effect of a bald strain on virulence. *Mol. Microbiol.* 23:579-590.
235. Fuqua, C., Indiana University. *Agrobacterium tumefaciens* C58 strain *fliR* deletion. In *unpublished lab strain*, Bloomington,IN.
236. Chan, C. S., M. R. Zlomislic, D. P. Tieleman, and R. J. Turner. 2007. The TatA subunit of *Escherichia coli* twin-arginine translocase has an N-in topology. *Biochemistry.* 46:7396-7404.

237. Wu, J., and H. R. Kaback. 1996. A general method for determining helix packing in membrane proteins in situ: helices I and II are close to helix VII in the lactose permease of *Escherichia coli*. *Proc. Natl. Acad. Sci. U.S.A.*93:14498-14502.
238. Akiyama, Y., T. Yoshihisa, and K. Ito. 1995. FtsH, a membrane-bound ATPase, forms a complex in the cytoplasmic membrane of *Escherichia coli*. *J. Biol. Chem.* 270:23485-23490.
239. Wessel, M., S. Klusener, J. Godeke, C. Fritz, S. Hacker, and F. Narberhaus. 2006. Virulence of *Agrobacterium tumefaciens* requires phosphatidylcholine in the bacterial membrane. *Mol. Microbiol.* 62:906-915.
240. Aktas, M., M. Wessel, S. Hacker, S. Klusener, J. Gleichenhagen, and F. Narberhaus. Phosphatidylcholine biosynthesis and its significance in bacteria interacting with eukaryotic cells. *Eur. J. Cell Biol.* 89(12):888-94.
241. Vecino, A. J., R. L. Segura, B. Ugarte-Urbe, S. Aguila, I. Hormaeche, F. la Cruz, F. M. Goni, and I. Alkorta. Reconstitution in liposome bilayers enhances nucleotide binding affinity and ATP-specificity of TrwB conjugative coupling protein. *Biochim. Biophys. Acta.* 1798:2160-2169.
242. Llosa, M., J. Zupan, C. Baron, and P. Zambryski. 2000. The N- and C-terminal portions of the *Agrobacterium* VirB1 protein independently enhance tumorigenesis. *J. Bacteriol.* 182:3437-3445.
243. Hubber, A., A. C. Vergunst, J. T. Sullivan, P. J. Hooykaas, and C. W. Ronson. 2004. Symbiotic phenotypes and translocated effector proteins of the *Mesorhizobium loti* strain R7A VirB/D4 type IV secretion system. *Mol. Microbiol.* 54:561-574.
244. Schroder, G., and C. Dehio. 2005. Virulence-associated type IV secretion systems of *Bartonella*. *Trends Microbiol.* 13:336-342.
245. Suttén, E. L., J. Norimine, P. A. Beare, R. A. Heinzen, J. E. Lopez, K. Morse, K. A. Brayton, J. J. Gillespie, and W. C. Brown. *Anaplasma marginale* type IV secretion system proteins VirB2, VirB7, VirB11, and VirD4 are immunogenic components of a protective bacterial membrane vaccine. *Infect. Immun.* 78:1314-1325.
246. Hilleringmann, M., W. Pansegrau, M. Doyle, S. Kaufman, M. L. MacKichan, C. Gianfaldoni, P. Ruggiero, and A. Covacci. 2006. Inhibitors of *Helicobacter pylori* ATPase Cagalpha block CagA transport and cag virulence. *Microbiology.* 152:2919-2930.
247. Araujo, F. R., C. M. Costa, C. A. Ramos, T. A. Farias, Souza, II, E. S. Melo, C. Elisei, G. M. Rosinha, C. O. Soares, S. P. Fragoso, and A. H. Fonseca. 2008. IgG

and IgG2 antibodies from cattle naturally infected with *Anaplasma marginale* recognize the recombinant vaccine candidate antigens VirB9, VirB10, and elongation factor-Tu. *Memor. Instit. Oswaldo Cruz.* 103:186-190.

VITA

Jennifer Evangeline Kerr was born in Atlanta, GA on March 2, 1982 the daughter of Mary Brock Kerr and William Henry Kerr. After completing her work at Druid Hills High School, Atlanta, Georgia in 2000, she entered Wesleyan College in Macon, Georgia. She received the degree of Bachelor of Arts with majors in biology and chemistry and minors of neuroscience and studio art from Wesleyan in May, 2004. In August of 2004, she entered The University of Texas Health Science Center at Houston, Graduate School of Biomedical Sciences.

Permanent address:

1780 Ridgewood Drive

Atlanta, GA 30307